Palaeontologia Electronica
palaeo-electronica.org

Miocene and Pliocene amphibians from Hambach (Germany): New evidence for a late Neogene refuge in northwestern Europe

Andrea Villa, Loredana Macaluso, and Thomas Mörs

ABSTRACT

The Hambach lignite mine in northwestern Germany is a renowned fossil locality, which has yielded remains of several vertebrates dated back to the Middle Miocene and the Late Pliocene. Among these is a recently-described and peculiar proteid urodele, *Euronecturus grogu,* currently known only from the Middle Miocene level in Hambach. Here, we provide detailed descriptions and identifications of the remaining fossil amphibians (both urodeles and anurans) from the Hambach mine, in total identifying at least 12 Middle Miocene taxa (Cryptobranchidae indet., *Palaeoproteus* cf. *miocenicus*, *E. grogu, Chelotriton* sp., *Lissotriton* sp., *Triturus* sp., *Latonia* sp., ?Palaeobatrachidae indet., Pelobatidae indet., *Hyla* sp., *Pelophylax* sp., *Rana* sp.) and at least nine Late Pliocene ones (*Palaeoproteus* cf. *miocenicus, Mioproteus* cf. *wezei, Lissotriton* sp., *Latonia* sp., *Palaeobatrachus eurydices*, cf. *Eopelobates* sp., *Hyla* sp., *Bufo* gr. *bufo*, Ranidae indet.). The high diversity of amphibians in both Miocene and Pliocene levels at Hambach supports a very humid climate persisting in the area for most of the Neogene, possibly originating a refugium for these animals in northwestern Europe that persisted until the Late Pliocene (and possibly even the Early Pleistocene). Urodeles such as *Palaeoproteus* and *Mioproteus* and anurans such as *Latonia*, the palaeobatrachids, and possibly *Eopelobates* are all significant occurrences in such a northern latitude at the end of the Pliocene, a period when southward withdrawal of thermophilic animals as well as the first effects of a deteriorizing climate ultimately leading to the Quaternary glaciation had already started in the European continent.

Andrea Villa. Institut Català de Paleontologia Miquel Crusafont (ICP-CERCA), Universitat Autònoma de Barcelona, Edifici ICTA-ICP, c/ Columnes s/n, Campus de la UAB, 08193 Cerdanyola del Vallès, Barcelona, Spain. andrea.villa@icp.cat
Loredana Macaluso. Natural Sciences Collections, Martin Luther University Halle-Wittenberg, Domplatz 4, 06108 Halle (Saale), Germany. loredana.macaluso@zns.uni-halle.de
Thomas Mörs. Department of Palaeobiology, Swedish Museum of Natural History, PO Box 50007, SE 10405, Stockholm, Sweden; Bolin Centre for Climate Research, Department of Environmental Science, Stockholm University, Geovetenskapens hus, Svante Arrhenius väg 8, Stockholm, Sweden. thomas.moers@nrm.se

Final citation: Villa, Andrea, Macaluso, Loredana, and Mörs, Thomas. 2024. Miocene and Pliocene amphibians from Hambach (Germany): New evidence for a late Neogene refuge in northwestern Europe. Palaeontologia Electronica, 27(1):a3. https://doi.org/10.26879/1323
palaeo-electronica.org/content/2024/5077-fossil-amphibians-from-hambach

Copyright: January 2024 Palaeontological Association.
This is an open access article distributed under the terms of Attribution-NonCommercial-ShareAlike 4.0 International (CC BY-NC-SA 4.0), which permits users to copy and redistribute the material in any medium or format, provided it is not used for commercial purposes and the original author and source are credited, with indications if any changes are made.
creativecommons.org/licenses/by-nc-sa/4.0/

Keywords: Urodela; Anura; Middle Miocene; Late Pliocene; Lower Rhine Embayment; Rhine-Meuse system

Submission: 18 July 2023. Acceptance: 24 November 2023.

INTRODUCTION

The current diversity of amphibian populations in Europe is the highest in the southern portion of the continent (Sillero et al., 2014; Speybroeck et al., 2016), with the three European Mediterranean peninsulae acting as current biodiversity hotspots and past refuges for these animals (e.g., Médail and Diadema, 2009; Blondel et al., 2010, and references therein). Northern areas, however, were also inhabited by a more diverse amphibian fauna throughout the Cenozoic (for reviews, see e.g., Estes, 1981; Roček, 1994a; Sanchiz, 1998; Rage and Roček, 2003), and particularly warm and humid periods supported the presence of taxa that are currently completely absent from even the closest vicinity of Europe like cryptobranchid salamanders as far north as central Germany and northwestern Ukraine (Böhme et al., 2012; Vasilyan et al., 2013). With the onset of the Quaternary glacial cycles, amphibians, together with the rest of the European herpetofauna, started to face unsuitable conditions in the areas most influenced by glaciers, thus retreating towards more appropriate environments in the South. The Italian Peninsula, in particular, seems to have acted as a better refuge for at least some groups of amphibians during these times (Macaluso et al., 2021, 2023a), possibly due to a less arid climate compared to the other northern Mediterranean peninsulae. In any case, the Pleistocene witnessed the extirpation or extinction of amphibians that were previously very widespread throughout Europe, such as the alytid frog *Latonia* von Meyer, 1843 (Szentesi, 2019; Sorbelli et al., 2021) and the whole anuran family Palaeobatrachidae Cope, 1865 (Wuttke et al., 2012; Villa et al., 2016; Roček et al., 2021). Allocaudates also had their last global occurrence in the Pleistocene of the Italian Alps, at the northern margin of the Italian Peninsula (Delfino and Sala, 2007; Villa et al., 2018b). Some reptiles also faced a similar fate of extirpation, such as varanid lizards (Georgalis et al., 2017; Villa et al., 2018a; Villa and Delfino, 2019) and trionychid turtles (Georgalis and Joyce, 2017).

Adding to the important role that Mediterranean Europe played for the herpetofauna in the late Neogene and Quaternary, recent discoveries from The Netherlands highlighted the survival of taxa that were previously thought to be absent from such a northern distribution in Pleistocene times, like palaeobatrachid anurans, turtles of the genus *Mauremys* Gray, 1869, and possibly large anguids of the genus *Pseudopus* Merrem, 1820 (van den Hoek Ostende and de Vos, 2006; Schouten, 2016, 2019, 2020; Villa et al., 2016, 2018c). *Pseudopus* was also found in Late Pliocene deposits in the German locality of Hambach (Čerňanský et al., 2017), not far from the Dutch border. This suggests the presence of some kind of late Neogene/early Quaternary refugial area for more thermophilic and water-related amphibians and reptiles in northwestern Europe as well, potentially corresponding with the Rhine-Meuse delta system. In a preliminary faunal list of the Late Pliocene Hambach vertebrate assemblage published by Mörs (2002), further taxa were mentioned that could be considered somehow unexpected for such a northwestern European locality, including cryptobranchids, palaeobatrachids, and a snapping turtle of the genus *Chelydropsis* Peters, 1868. This, together with the reported diversity of the microvertebrate assemblage, hints at the Hambach fauna being an interesting tile to better understand the herpetofaunal dynamics in this part of northwestern Europe and its possible suitability for the survival of certain taxa. The availability of a Miocene record from the same locality further allows to make a direct comparison between two different time periods in the same place, as well as with younger assemblages from nearby areas such as the one from Tegelen in The Netherlands (Villa et al., 2016, 2018c).

With this purpose, we here present the amphibians (urodeles and anurans) from the Middle Miocene and Late Pliocene of the Hambach mine. We further discuss their significance in terms of: 1) palaeobiogeography; 2) palaeoenvironment; and 3) the possible interpretation of the Lower Rhine Embayment and the Rhine-Meuse delta system as a late Neogene/early Quaternary refuge for amphibians (and reptiles) in northwestern Europe.

GEOLOGICAL SETTING

The material described and discussed in this work derives from fossiliferous channel fills in the

Middle Miocene Frimmersdorf lignite seam (stratum 6 = site Hambach 6C) and in the Upper Pliocene Reuver Clay (Öbel beds sensu Kemna, 2005; stratum 11 = sites Hambach 11 and 11C) exposed in the Hambach open cast lignite mine (Mörs, 2002). The mine conducted by the RWE Power mining company is situated 35 km west of Cologne in the southern part of the Lower Rhine Embayment, northwestern Germany (50° 54' 44'' N, 6° 29' 51'' E; Figure 1). The tectonic framework of the mine is the Erft block within the Lower Rhine graben that cuts into the Palaeozoic Rhenish Massif since the Oligocene (Schäfer et al., 2004).

The Miocene Ville Formation contains the paralic Rhenish Main Seam that is interlocked with beach sands of the transgressing North Sea and fluvial deposits of the Palaeo-Rhine and Meuse rivers system (Boenigk, 2002; Schäfer et al., 2004). The fossils derived from channel fill and floodplain deposits, stratum 6C according to the RWE stratigraphic framework (Mörs et al., 2000; Schäfer et al., 2004). An estuarine environment with extensive paralic coal swamps and a large fluviatile system is documented by sedimentological, palaeobotanical and palaeontological evidence (Mörs, 2002; Utescher et al., 2002; Schäfer et al., 2004). Hambach 6C has produced many aquatic and semiaquatic vertebrates such as freshwater fishes (cyprinids), the urodeles and anurans described in this work, turtles (trionychids, carettochelyids, chelydrids, emydids), an alligator, lizards (chamaeleonids, lacertids, anguids), snakes ("aniliids", constrictors, tropidophiids, colubrids, elapids, viperids), birds (anhingids, anatids, rallids), insectivores (metacodontids, desmanines, dimylids, soricids), carnivorans (mustelids), beavers (castorids), and deers (tragulids) (Mörs et al., 2000; Ziegler and Mörs, 2000; Mörs, 2002; Hierholzer and Mörs, 2003; Klein and Mörs, 2003; Joyce et al., 2004; Dalsätt et al., 2006; Stefen and Mörs, 2008; Mörs and Stefen, 2010; Čerňanský et al., 2017; Macaluso et al., 2022b). The rich Orleanian mammal fauna with 70 taxa, including about 30 rodent species (sciurids, petauristines, glirids, eomyids, cricetids, castorids), allows to correlate Hambach 6C with the upper part of Mammalian Neogene unit MN 5, indicating an early Middle Miocene age (16.0-15.2 Ma; Mörs et al., 2000; Mörs, 2002; Mörs and Kalthoff, 2004). Age and high vertebrate diversity with "tropical" elements fit well with the ~2 Myr greenhouse interval, the Miocene Climatic Optimum (Steinthorsdottir et al., 2021). The palaeoflora of the Ville Formation indicates paratropical (humid, warm, and with distinct seasonality) climate conditions. Mean Annual Precipitation (MAP) for Hambach 6C is between 897 and 996 mm, Mean Annual Temperature (MAT) between 15.76 and 18.0°C, coldest month mean between 9.6 and 11.72°C, and warmest month mean between 25.2 and 28.3°C (Utescher et al., 2000, 2002).

FIGURE 1. Location of the Hambach opencast lignite mine in northwestern Germany (from Mörs and Stefen, 2010).

Both Pliocene sites (Hambach 11 and 11C) produced less diverse vertebrate faunas compared with Hambach 6C, but as well aquatic and semiaquatic taxa such as freshwater fishes (esocids, cyprinids), salamanders, frogs, a turtle (an emydid), lizards (lacertids, anguids), snakes (colubrids), birds (anatids), insectivores (desmanines, soricids), and beavers (castorids) (Mörs et al., 1998; Mörs, 2002; Hierholzer and Mörs, 2003; Dalsätt et al., 2006; Čerňanský et al., 2017; Van Laere and Mörs, 2023). The evolutionary stage of the arvicoline rodents from Hambach 11 indicates an early Villanyian age, correlative with the Mammalian Neogene unit MN 16a (Mörs et al., 1998). Hambach 11C resembles Hambach 11 in the faunal content, indicating a more or less contemporaneous age (Mörs, 2002). Palynological data place Hambach 11C into the Reuverian B that still contains Tertiary floral elements such as Cupressa-

ceae*, Nyssa, Pterocarya, Sequoia, Sciadopitys,* and *Taxodium* (Heumann and Litt, 2002). Regarding the lithostratigraphic and magnetostratigraphic framework, stratum 11 belongs to the Öbel beds ("upper Reuver clay") with normal polarity; unstable heavy mineral and smectite contents indicate that this unit was deposited by the "Palaeo-Rhine" river that had an Alpine origin for the first time (Kemna, 2005). The overlying stratum 13 represents a local deposit ("Hambach beds") of a small river that had its origin in the Mechernich ore deposit in the Eifel mountains, based on high amounts of Pb and a smectite-free clay mineralogy according to Kemna (2005). The Gauss-Matuyama boundary (2.58 Ma) has been identified in stratum 13, 10 m above the top of the Öbel beds (Kemna, 2005). Material from Hambach 11C has been published before as Hambach 13 because the site has been considered to belong to stratum 13 (Heumann and Litt, 2002; Dalsätt et al., 2006; Lacombat and Mörs, 2008; Čerňanský et al., 2017).

MATERIAL AND METHODS

This study is based on fossil material stored at the Steinmann Institute of the Rheinische Friedrich-Wilhelms-Universität Bonn, Germany. The isolated vertebrae IPB-HaH 2011 (referred to *Chelotriton* Pomel, 1853) and IPB-HaH 2189 (a cryptobranchid vertebra) were not available for direct study, but they are included here on the basis of detailed photographs (also figured by Mörs et al., 2000). Selected specimens were photographed using a Leica M205 microscope equipped with the Leica Application Suite (LAS) 4.10 and a Leica M165 FC microscope equipped with a DFC450 camera and LAS 4.5. The anatomical terminology used in the description follows: Vater (2003), Villa et al. (2014), Vasilyan and Yanenko (2020), and Ratnikov and Litvinchuk (2007, 2009) for urodeles; Roček (1994b), Sanchiz (1998), and Gómez and Turazzini (2016) for anurans. Specimens of extant taxa used for comparisons are listed by Macaluso et al. (2023b), plus *Cryptobranchus alleganiensis* Sonnini de Manoncourt and Latreille, 1801 uf:herp:10881 and uf:herp:88726 and *Necturus beyeri* Viosca, 1937 uf:herp:177187 (all available on MorphoSource).

Institutional Abbreviations. IPB, Institute of Palaeontology Bonn, Germany; HaH, Hambach Hauptflöz (or main seam) = Hambach 6C; HaR, Hambach Reuverton (or Reuver clay) = Hambach 11 and 11C; RGM, Naturalis Biodiversity Center, Leiden, The Netherlands.

SYSTEMATIC PALAEONTOLOGY

AMPHIBIA Linnaeus, 1758
URODELA Duméril, 1806
CRYPTOBRANCHIDAE Fitzinger, 1826
Cryptobranchidae indet.
Figure 2

Material. Hambach 6C: two trunk vertebrae (IPB-HaH 2009, IPB-HaH 2189); two fragments of vertebra (IPB-HaH 2191, IPB-HaH 2388); one humerus (IPB-HaH 2395).

Description. IPB-HaH 2009 (Figure 2A-D) is a very large-sized, robust, and fragmentary trunk vertebra, the total length of which reaches 18 mm. Only the anterior half of the very large vertebral centrum is preserved. It has a very large anterior cotyle, with a notochordal pit in the middle. No foramen is visible on the preserved portion of the ventral surface of the centrum. The right transverse process is missing, but the basis of the left one is preserved. The latter is robust, and there is a large pit anteriorly to it. There are no anterior zygapophyseal crests, whereas the anterior ventral crests are present but poorly developed. The neural canal is narrow and slightly dorsoventrally compressed. The neural arch, the posterior portion of which is broken off, is low. As far as the zygapophyses are concerned, only the left anterior one is preserved. It is suboval and subhorizontal in anterior view. The neural spine is low in the preserved portion of the neural arch. IPB-HaH 2191 (Figure 2E) is a broken vertebral fragment including the dorsal surface of the vertebral centrum and part of the neural arch with the prezygapophyses. It is very large-sized and robust. The length of the fragment is 7 mm, but it represents only a portion of the original vertebra (probably the anterior half). The prezygapophyses are elliptical and tilted dorsally of 30°. IPB-HaH 2388 only preserves one of the cotyles. It is very large, with a size comparable to IPB-HaH 2009. The cotyle is subcircular and has a notochordal pit. IPB-HaH 2189 is also very large and robust, with a centrum length of roughly 20 mm. The amphicoelous centrum is very large, whereas the neural arch is very low. The posterior half of the latter is missing, but it was slightly rising posteriorly.

A very large humerus (Figure 2F-G) is represented only by the proximal half. The preserved fragment is 25 mm long. The bone strongly expands by the proximal end. The proximal epiphysis is poorly ossified distally and has an asymmetrical appearance, with a slightly higher expansion towards the ventral side.

Remarks. These vertebrae from Hambach 6C can be referred to Pancryptobrancha Vasilyan, Böhme,

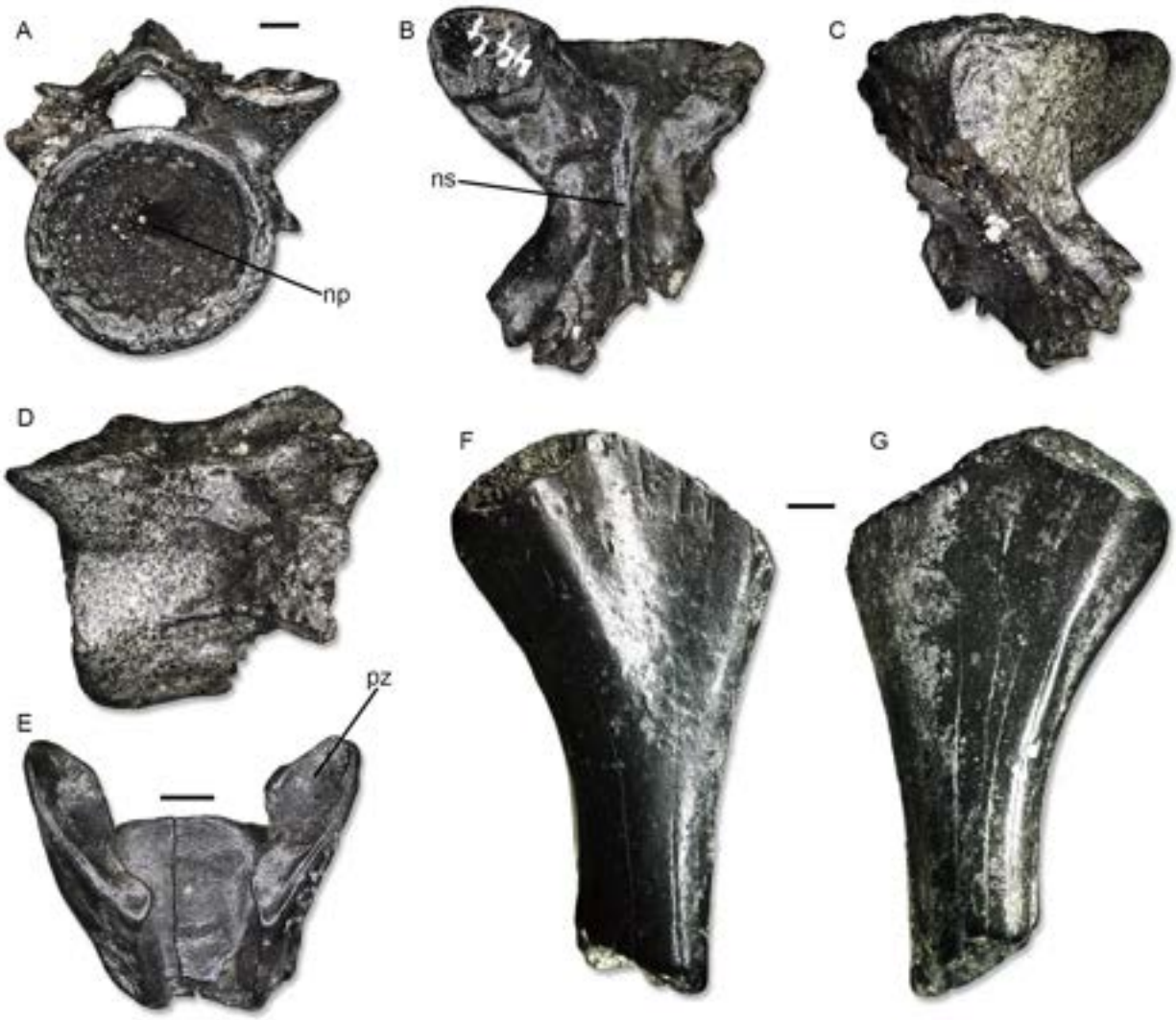

FIGURE 2. Cryptobranchidae indet. from Hambach: trunk vertebra (IPB-HaH 2009) in anterior (A), dorsal (B), ventral (C) and left lateral (D) views; fragment of trunk vertebra (IPB-HaH 2191) in dorsal view (E); left humerus (IPB-HaH 2395) in posterior (F) and anterior (G) view. Scale bars equal 2 mm. Abbreviations: np, notochordal pit; ns, neural spine; pz, prezygapophysis.

Chkhikvadze, Semenov, and Joyce, 2013, because of the large size and overall morphology similar to representatives of this group of salamanders (e.g., *Ukrainurus* Vasilyan, Böhme, Chkhikvadze, Semenov, and Joyce, 2013). The not-strongly-elongated articular facets of the zygapophyses support referral to the Cryptobranchidae. The humerus is also similar in both size and morphology to members of Cryptobranchidae, and it is thus attributed to this taxon as well here. In particular, this attribution is suggested by the poor ossification of the epiphysis and the very large size, which is matched only by cryptobranchid vertebrae among Hambach urodeles.

BATRACHOSAUROIDIDAE Auffenberg, 1958
PALAEOPROTEUS Herre, 1935
PALAEOPROTEUS MIOCENICUS Vasilyan and Yanenko, 2020
Palaeoproteus cf. *miocenicus*
Figures 3–4

Material. Hambach 6C: three atlases (IPB-HaH 2117, IPB-HaH 2175, IPB-HaH 2164); one trunk vertebra (IPB-HaH 2162). Hambach 11: two dentaries (IPB-HaR 2043, IPB-HaR 2071); one anterior trunk vertebra (IPB-HaR 2183); one trunk vertebra (IPB-HaR 2008). Hambach 11C: five trunk vertebrae (IPB-HaR 2404/2408).

Description. IPB-HaR 2071 (Figure 3) represents part of the posterior end of a very large dentary. It

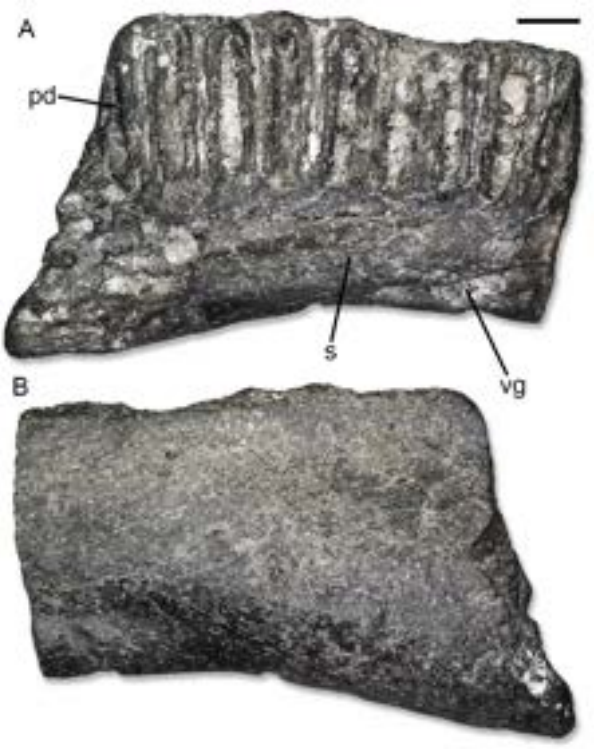

FIGURE 3. Skull elements of *Palaeoproteus* cf. *miocenicus* from Hambach: left dentary (IPB-HaR 2043) in medial (A) and lateral (B) views. Scale bar equals 1 mm. Abbreviations: pd, pars dentalis; s, shelf; vg, ventral groove.

is very fragmentary. IPB-HaR 2043 is also very large and robust. It represents a portion originally located somewhere in the middle of the dentary. The pars dentalis of the dentary is composed by a very high dental lamina and a very low subdental lamina. On the medial side, nine tooth positions are visible, hosting the poorly-preserved remains of pleurodont, very high, rather narrow and closely spaced teeth provided with thick walls. Ventral to the pars dentalis, there is a robust shelf, which is not strongly developed medially. The preservation of this shelf is rather poor, but a narrow and shallow groove is visible ventrally. The groove moves towards the medial surface near the anterior end of the fragment. The lateral surface is smooth. In lateral/medial view, the ventral margin is somehow concave, suggesting ventral development of the posterior part of the dentary.

IPB-HaH 2164 is a very small atlas, but the other ones are larger. The length of the largest atlas, IPB-HaH 2175 (Figure 4F-I), is 6 mm. All atlases miss almost completely the neural arch, preserving only the centrum. Anteriorly, the occipital joints are wide and mediolaterally elongated, with a suboval/subelliptical shape (i.e., slightly dorsoventrally compressed) in anterior view. They are very shallowly concave and do not coalesce in the middle, being separated by a thin and long processus odontoideus. The processus is slightly slenderer in IPB-HaH 2175 than in the other two specimens. It has a flat dorsal surface and an anteroventrally-directed and strip-like articular surface that is not separated into two distinct lateral areas. There is no postodontoideus foramen at the base of the process. The posterior end of the centrum is represented by a posterior cotyle with a notochordal pit in the middle. The cotyle is circular in IPB-HaH 2175 (Figure 4I) and more mediolaterally compressed in IPB-HaH 2117 (Figure 4D). In both specimens, it is larger than the processus odontoideus. This feature cannot be evaluated in IPB-HaH 2164 because the area is damaged. In IPB-HaH 2715, the ventral surface of the centrum shows a concave area with a number of large foramina (Figure 4G). On the other hand, IPB-HaH 2117 bears a very deep fossa in the middle of the centrum, which is flanked by two smaller symmetrical foramina by the sides and by other even smaller foramina posteriorly (Figure 4B). The ventral surface of IPB-HaH 2164 displays a depressed area by each side of the centrum. Foramina also cover the lateral surface of each processus lateralis in all specimens.

Both IPB-HaR 2008 (Figure 4O-T) and IPB-HaR 2408 (Figure 4U-Z) are amphicoelous and large sized (the centrum length reaches 6.5 mm and 9.5 mm, respectively). A notochordal pit is present in the middle of the large and hourglass-shaped centrum. The cotyles are circular in both anterior and posterior views. The ventral surface of the centrum bears two high and sharp longitudinal basapophyses, which run parallel along the entire length of the vertebra. Only in IPB-HaR 2408, the basapophyses contact in the middle at about one third of the centrum length (Figure 4V). Between the basapophyses, various central foramina are present. At least three large ones are visible on IPB-HaR 2008 (Figure 4P), surrounded by other smaller ones, whereas only a number of small ones are visible on IPB-HaR 2408 (Figure 4V). The neural arch is robust and dorsally flattened, being better preserved in IPB-HaR 2408. A neurapophysis is present. It is low anteriorly, but rises to a moderate degree posteriorly. A robust spine is present at the posterior end of the arch, strongly projecting posterodorsally beyond the postzygapophyses. The posterior end of the spine is truncated. A wide and deep, U-shaped anterior notch

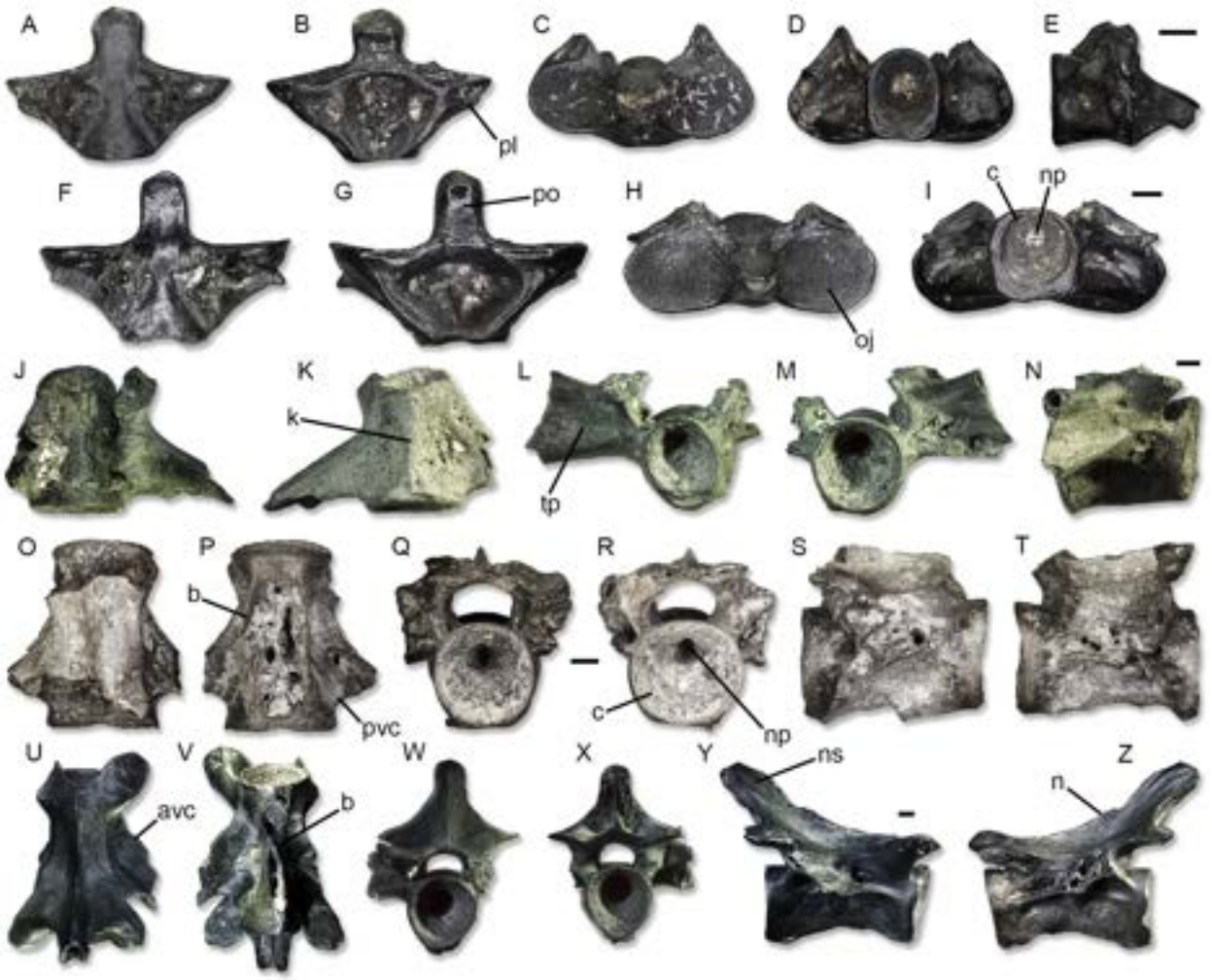

FIGURE 4. Vertebrae of *Palaeoproteus* cf. *miocenicus* from Hambach: atlas (IPB-HaH 2117) in dorsal (A), ventral (B), anterior (C), posterior (D) and right lateral (E) views; atlas (IPB-HaH 2175) in dorsal (F), ventral (G), anterior (H) and posterior (I) views; anterior trunk vertebra (IPB-HaR 2183) in dorsal (J), ventral (K), anterior (L), posterior (M) and right lateral (N) views; trunk vertebra (IPB-HaR 2008) in dorsal (O), ventral (P), anterior (Q), posterior (R), right lateral (S) and left lateral (T) views; trunk vertebra (IPB-HaR 2408) in dorsal (U), ventral (V), anterior (W), posterior (X), right lateral (Y) and left lateral (Z) views. Scale bars equal 1 mm. Abbreviations: avc, anterior ventral crest; b, basapophyses; c, cotyle; k, keel; n, neurapophysis; np, notochordal pit; ns, neural spine; oj, occipital joint; pl, processus lateralis; po, processus odontoideus; pvc, posterior ventral crest; tp, transverse process.

on the neural arch is visible on IPB-HaR 2408 (Figure 4U), allowing the anterior cotyle to be visible in dorsal view. The deepest part of the notch reaches the posterior margin of the prezygapophyses. The zygapophyses are more or less horizontal in both anterior and posterior view. The zygapophyseal facets are suboval. In posterior view, two shallow depressions are visible on the posteroventral surface of the neural arch, flanking a low longitudinal ridge running along the ventral side of the neural spine. The transverse processes are moderately developed and posterolaterally directed. Ventrally, they are connected to the centrum by moderately-(IPB-HaR 2008) or well-developed (IPB-HaR 2408) anterior ventral crests (anterior alar process in Vasilyan and Yanenko, 2020) and little-developed posterior ventral crests. On the other hand, the zygapophyseal crests are not developed. The other vertebrae only preserve isolated centra or fragments of centra, some of them being much smaller than the two previously described (IPB-HaR 2406 is about 4 mm long). Nevertheless, they share the same morphology.

IPB-HaR 2183 (Figure 4J-N) is the only trunk vertebra displaying some differences from the other ones. This large vertebra has a very massive,

almost 6 mm long centrum, which is amphicoelous, hour-glass-shaped and notochordal. The overall aspect is relatively shorter compared to the trunk vertebra IPB-HaR 2008, coming from the same level. The anterior cotyle is moderately mediolaterally compressed, appearing subelliptical in anterior view. The posterior cotyle, on the other hand, is subcircular in posterior view. The ventral surface of the centrum bears a narrow keel and no basapophyses. A number of small foramina are present by the ventrolateral sides of the centrum, in place of real subcentral foramina. Most of the neural arch is missing, preserving only the right lateral wall and the base of the left one. The transverse processes are long and moderately robust; they are directed posterolaterally. The anterior ventral crest is very low, whereas the posterior one is slightly more developed. Zygapophyseal crests are not developed. The base of the right prezygapophysis is also preserved, but not the zygapophysis itself. The shortness of this vertebra, together with its ventral keel, identify it as an anterior trunk vertebra (Estes et al., 1967).

Remarks. The diagnostic features recently reported by Vasilyan and Yanenko (2020) allow a rather straightforward identification for these remains as a batrachosauroidid salamander. The dentaries of these urodeles have thick-walled teeth and a ventrally-projecting posterior part. Trunk vertebrae are amphicoelous, with subcircular cotyles, basapophyses, and a posterodorsally-projecting neural spine. The atlases are provided with both anterior and posterior cotyles with a rounded outline, among which the former are large and concave. The well-developed paired ventral basapophyses, as well as maybe the flat neural arch and developed anterior ventral crest, suggest that the batrachosauroidid from Hambach is a member of the European genus *Palaeoproteus* (Vasilyan and Yanenko, 2020). In particular, the following combination of features observed in the studied material is diagnostic of *P. miocenicus* following Vasilyan and Yanenko (2020): overall large size; poorly-developed subdental shelf of dentary; vertebrae with a long neural spine; weakly-concave and slightly dorsoventrally-compressed anterior cotyles of the atlas; external surface of the atlas pierced by foramina of different sizes; strongly pronounced, lip-shaped odontoid process of the atlas (Vasilyan and Yanenko, 2020: p. 8, stated that “In *P. miocenicus,* the odontoid process is very large in comparison to all known batrachosauroidids”). However, the atlases from Hambach 6C show no postodontoid foramen, in contrast with the type and referred material of *P. miocenicus* (Vasilyan and Yanenko, 2020). All four *P. miocenicus* atlases share the presence of this foramen, whereas it is absent in *Palaeoproteus klatti* Herre, 1935, and *Palaeoproteus gallicus* Estes et al., 1967. Despite this difference, we refrain to name a new species here and attribute the fossils from Hambach 6C to *Palaeoproteus* cf. *miocenicus*, due to the overall similarity between bones of *P. miocenicus* and the German taxon as well as the low sample of atlases that hinders a complete understanding of the real variation of this feature in these animals. Material coming from the youngest level in Hambach also shares the same attribution, given that atlases from this level are currently unknown, and so it is not possible to verify the presence or absence of a postodontoid foramen.

?*Palaeoproteus* cf. *miocenicus*
Figure 5

Material. Hambach 6C: one humerus (IPB-HaH 2390).

Description. This humerus is rather large and robust. It misses only most of the distal epiphysis. The length of the preserved portion is about 16 mm. The bone expands strongly towards the epiphyses. Based on the preserved portion, it appears rather short. The proximal epiphysis is poorly ossified. It has an asymmetrical shape, more expanded toward the ventral side. The posterior surface displays a distinct fossa.

FIGURE 5. Limb bones of possible *Palaeoproteus* cf. *miocenicus* from Hambach: humerus (IPB-HaH 2390) in anterior (A) and posterior (B) views. Scale bar equals 1 mm.

Remarks. The size of this humerus suggests that it belongs to one of the two largest caudate taxa recognised in Hambach (i.e., either cryptobranchids or batrachosauroidids). The bone appears rather short in general appearance, which hints against *Chelotriton*, cryptobranchids, and possibly also proteids. Its shortness rather recalls the shortened limbs of *P. klatti* (see Vasilyan and Yanenko, 2020). Furthermore, the general morphology of the bone differs from the fragment of humerus attributed to *Mioproteus gardneri* Venczel and Codrea, 2018, whereas the poorly ossified proximal end hints against *Chelotriton*. Therefore, IPB-HaH 2390 is here attributed with doubt to the batrachosauroidid taxon found in the Hambach assemblage, *Palaeoproteus* cf. *miocenicus*.

PROTEIDAE Bonaparte, 1831
EURONECTURUS
Macaluso, Villa, and Mörs, 2022
Euronecturus grogu
Macaluso, Villa, and Mörs, 2022

Material. Hambach 6C: five atlases (IPB-HaH 2119/2121, IPB-HaH 2150, IPB-HaH 2165).
Remarks. These atlases were recently described as types of a new proteid taxon, *E. grogu.* The reader is referred to Macaluso et al. (2022b) for further information.

MIOPROTEUS Estes and Darevsky, 1977
Mioproteus wezei Estes in Młynarski, Szyndlar, Estes, and Sanchiz, 1984
Mioproteus cf. *wezei*
Figure 6

Material. Hambach 11: nine trunk vertebrae (IPB-HaR 2000/2007, IPB-HaR 2013). Hambach 11C: six trunk vertebrae (IPB-HaR 2400/2403, IPB-HaR 2427/2428).
Description. These vertebrae (Figure 6) reach a large size and are robustly ossified. The largest one has a centrum length of about 6.5 mm. They display a range of different degree of preservational statuses, from very fragmentary to well preserved. The centrum is amphicoelous and pierced by a wide notochordal canal. Ventrally, the centrum bears a robust and high keel, which is more or less narrow (from sharp to slightly thicker). By the anterior and posterior ends, the keel expands into triangular and flat ventral surfaces. The keel is flanked by small subcentral foramina, sometimes more than one per side. Posteriorly, poorly-developed basapophyses are present. The neural arch is low, without a significant rising posteriorly, and dorsally flat. A neurapophysis is present, being either rather low or slightly higher. It runs almost entirely along the dorsal surface of the arch. The anterior margin of the arch appears straight in dorsal view, even though it is never completely preserved. It is located roughly at midlength of the prezygapophyses. The posterior margin is rather straight (but very slightly wavy, even though with no median notch) and ends well before the end of the postzygapophyses. By each side of the neurapophysis, the posterior end of the dorsal surface of the neural arch carries a well-developed spine, which projects well beyond the posterior margin, but not beyond the postzygapophyses. The spines are well spaced in dorsal view, not strongly extended anteriorly (they do not reach the level of the transverse processes) and not connected to the neurapophysis medially. The zygapophyses are suboval and almost horizontal. The ventral lamina has a subtrapezoidal shape, originated by very well-developed anterior ventral crests and less-developed posterior ones. The zygapophyseal crests are also well developed, but not as much as the anterior ventral crests. The posterior zygapophyseal crests are distinctly convex dorsally in lateral view. Due to the strong development of both the ventral lamina and the zygapophyseal crests, the vertebrae assume a wide appearance in both ventral and dorsal views. The transverse processes are reduced to a small single structure, which is slender and posterolaterally directed. Individualized para- and diapophyses are not clearly discernible. A more-or-less large foramen is visible anterior to the base of the transverse process.
Remarks. These vertebrae are referred to *Mioproteus* because of the following combination of features (Estes and Darevsky, 1977): robust and well-ossified aspect; well-spaced posterior spines; wide appearance in dorsal and ventral views (i.e., wide neural arch, wide ventral lamina); presence of basapophyses. Three species of *Mioproteus* are currently known: *Mioproteus caucasicus* Estes and Darevsky, 1977, *M. gardneri,* and *M. wezei*. The vertebrae from Hambach are concordant in size with both *M. caucasicus* and *M. wezei,* whereas they are larger than *M. gardneri.* Regarding their morphology, they differ from *M. gardneri* in the more developed zygapophyseal crests, the taller neurapophysis, and the more laterally-trending prezygapophyses (Venczel and Codrea, 2018). Most characters reported to be diagnostic for *M. wezei* are variable, but at least the consistent absence of a connection between the posterior spines and the neurapophysis seems to be sufficiently reliable (Syromyatnikova et al., 2021). This condition is shown by the Hambach material,

FIGURE 6. *Mioproteus* cf. *wezei* from Hambach: trunk vertebra (IPB-HaR 2000) in dorsal (A), ventral (B) and right lateral (C) views; trunk vertebra (IPB-HaR 2006) in dorsal (D), ventral (E) and right lateral (F) views; trunk vertebra (IPB-HaR 2007) in dorsal (G), ventral (H) and left lateral (I) views; trunk vertebra (IPB-HaR 2403) in dorsal (J) and ventral (K) views. Scale bars equal 1 mm. Abbreviations: b, basapophysis; k, keel; n, neurapophysis; ps, posterior spine; tp, transverse process; vl, ventral lamina.

whereas *M. caucasicus* either has posterior spine that connect or not to the neurapophysis medially. Strongly dorsally-convex posterior zygapophyseal crests may also be typical for *M. wezei* (Młynarski et al., 1984; Bailon, 1995; even though Syromyatnikova et al., 2021, mentioned some variation of this feature in *Mioproteus* vertebrae). Considering this, we here tentatively attribute the Hambach *Mioproteus* vertebrae to *M. wezei,* even though pointing out uncertainty over this identification pending a clarification of the diagnostic features within Neogene *Mioproteus*.

SALAMANDRIDAE Goldfuss, 1820
CHELOTRITON Pomel, 1853
Chelotriton sp.
Figures 7–8

Material. Hambach 6C: one premaxilla (IPB-HaH 2005); two maxillae (IPB-HaH 2007, IPB-HaH 2046); three frontals (IPB-HaH 2000, IPB-HaH 2001, IPB-HaH 2337); four dentaries (IPB-HaH 2004, IPB-HaH 2039; IPB-HaH 2231/2232); one fragment of indeterminate tooth bearing bone (IPB-HaH 2008); one atlas (IPB-HaH 2022); 21 trunk vertebrae (IPB-HaH 2010/2011, IPB-HaH 2012/2021, IPB-HaH 2023, IPB-HaH 2038, IPB-HaH 2111/2112, IPB-HaH 2114, IPB-HaH 2177/2179; IPB-HaH 2386); one caudal vertebra (IPB-HaH 2113); 14 ribs (IPB-HaH 2024/2037); eight indeterminate bone fragments (IPB-HaH 2006, IPB-HaH 2041/2045, IPB-HaH 2048, IPB-HaH 2401).

Description. The premaxilla (Figure 7A-E) is small. It was most likely paired and preserves mainly the pars palatina and the pars dentale. The base of the pars faciale is also preserved, showing a dense sculpturing made up by pits and ridges anterodorsally. The sculpturing extends on the anterior surface of the low crista lateralis, but it is less developed here. In posterior view, a wide and deep concavity is visible by the base of the pars faciale. The pars palatina is very expanded, being mediolaterally wider than anteroposteriorly long. The tooth row seems almost complete, even though rather poorly preserved. At least 23/24 closely spaced tooth positions can be counted.

The maxilla IPB-HaH 2046 is represented only by a very small fragment. It displays a strongly sculptured lateral surface, with numerous distinct tubercles. On the medial surface, a well-developed lamina horizontalis is present. Ventral to this, poorly preserved tooth positions are visible. IPB-HaH 2007 (Figure 7F-G), on the other hand, preserves the posterior end of the maxilla. By the anterior breakage, it displays a medially-directed process, which most likely contacted the pterygoid in origin. This process is short and distally rounded. Ventral to the process, the posterior end of the tooth row is visible, showing at least seven closely spaced tooth positions. The tooth row does not extend posterior to the process and it is followed by a long toothless portion of the ventral margin. The lateral surface of the bone is covered by a dense

FIGURE 7. Skull elements of *Chelotriton* sp. from Hambach: left premaxilla (IPB-HaH 2005) in anterior (A), posterior (B), dorsal (C), ventral (D) and lateral (E) views; right maxilla (IPB-HaH 2007) in lateral (F) and medial (G) views; left frontal (IPB-HaH 2000) in ventral (H) and dorsal (I) views; right frontal (IPB-HaH 2001) in ventral (J) and dorsal (K) views; left frontal (IPB-HaH 2337) in ventral (L) and dorsal (M) views; right dentary (IPB-HaH 2004) in lateral (N) and medial (O) views; left dentary (IPB-HaH 2039) in lateral (P) and medial (Q) views. Scale bars equal 1 mm. Abbreviations: pa, pars palatina; pf, pars faciale; po, processus postorbitalis.

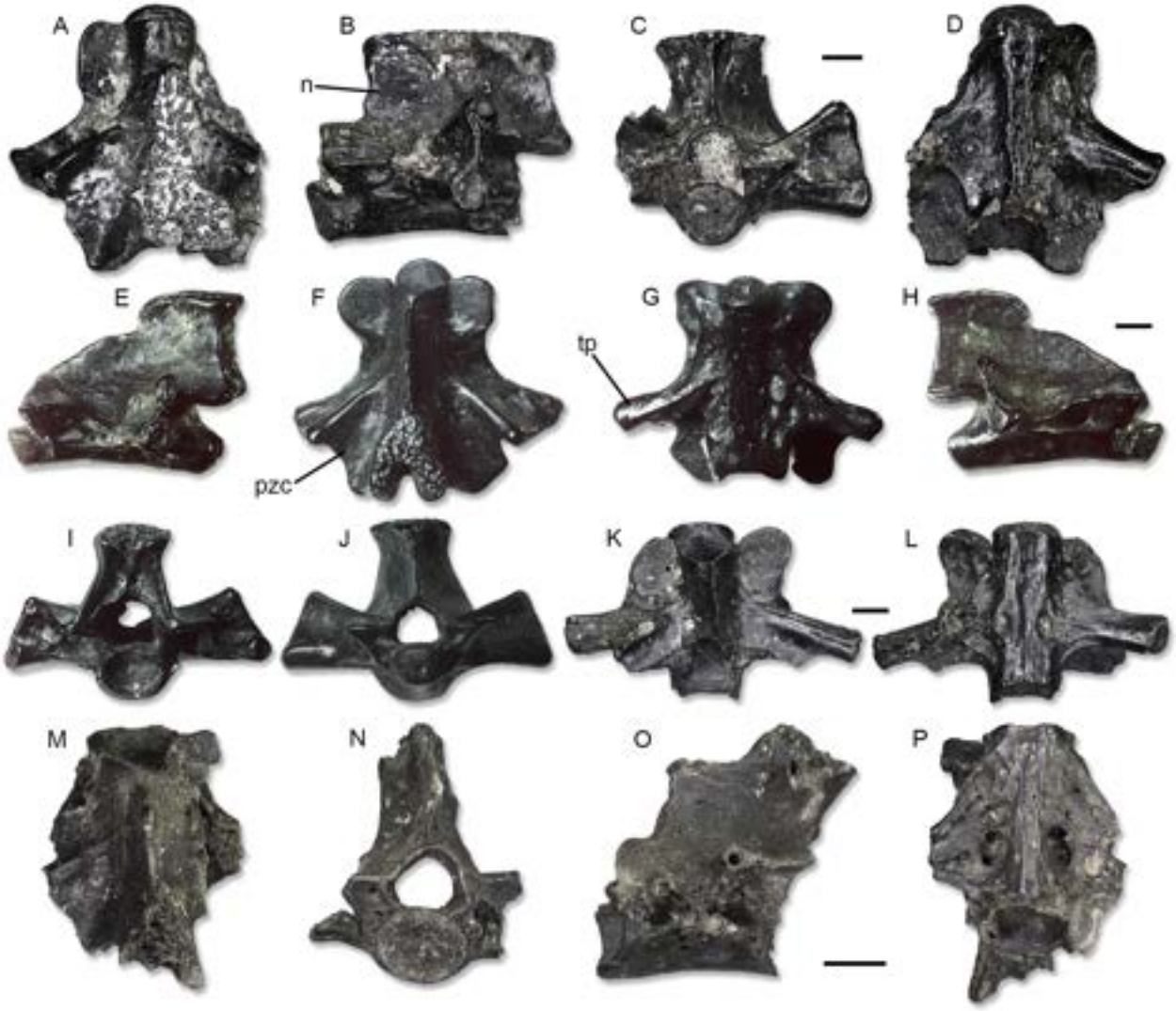

FIGURE 8. Vertebrae of *Chelotriton* sp. from Hambach: trunk vertebra (IPB-HaH 2010) in dorsal (A), left lateral (B), anterior (C) and ventral (D) views; trunk vertebra (IPB-HaH 2038) in left lateral (E), dorsal (F), ventral (G), right lateral (H), posterior (I) and anterior (J) views; trunk vertebra (IPB-HaH 2177) in dorsal (K) and ventral (L) views; trunk vertebra (IPB-HaH 2114) in dorsal (M), anterior (N), left lateral (O) and ventral (P) views. Scale bars equal 1 mm. Abbreviations: n, neurapophysis; pzc, posterior zygapophyseal crest; tp, transverse process.

dermal sculpturing made up by pits, ridges, and tubercles. The dorsal margin bends in medial direction and the sculpturing does not extend onto the bent part. The posterior end of the specimen expands into a robust structure for a strong contact with the quadratojugal, but its distal end is broken.

The frontals are moderately large and rather robustly built. IPB-HaH 2000 (Figure 7H-I) and IPB-HaH 2337 (Figure 7L-M) only preserve part of the lateral margin, whereas IPB-HaH 2001 (Figure 7J-K) is relatively complete, preserving also the posterior margin of the orbital cavity. A wide and long processus postorbitalis is present in all of them, representing the posterolateral projection participating in the anterior part of the fronto-squamosal arch. Ventrally, part of the sharp crista orbitosphenoideum is visible in IPB-HaH 2000 (Figure 7H) and IPB-HaH 2001 (Figure 7J). The dorsal surface is covered by a very dense dermal sculpturing made up by isolated tubercles.

Dentaries (Figure 7N-Q) are fragmentary, but they clearly show a well-developed dermal sculpturing made by pits, tubercles, and ridges on the lateral surface. IPB-HaH 2004 (Figure 7N-O) preserves the anterior end of the bone, with the symphyseal region. The latter is high and roughly teardrop shaped, but with a straight lateral margin. On the medial surface, the sutura incisura dentalis is

closed far posterior to the foramen alveolaris, which is located between the thirteenth and fourteenth tooth positions. Moreover, starting just posterior to the same foramen, a sharp ridge runs on the medial surface of the bone, defining a distinct sulcus dentalis. The sulcus is present anteriorly also, but it is shallower here.

The poorly preserved fragment of tooth bearing bone shows a dermal sculpturing made up by large pits and tubercles connected by sharp ridges.

The atlas has a posterior cotyle and is moderately large-sized, with a centrum length of 3.9 mm. It has large and roughly subelliptical occipital joints and a small and wedge-shaped odontoid process. The neural canal is drop-shaped in anterior view. The dorsal margin of the neural arch forms a dorsally flattened surface, which is triangular in dorsal view. This surface is dorsally eroded, and therefore the presence of sculpturing cannot be established.

Trunk vertebrae (Figure 8) are robust and large-sized (centrum length goes from 3 mm to 6 mm), provided with strong transverse processes. The vertebral centrum is opisthocoelous and has a flattened and very slightly anteroventrally inclined anterior condyle. There is no neck. On the ventral surface, the subcentral foramina are replaced by few smaller foramina. Anterior ventral and anterior zygapophyseal crests are lacking or poorly developed, whereas posterior ventral ones are moderately developed and posterior zygapophyseal ones are very well developed. Only in IPB-HaH 2114 (Figure 8M-P), both ventral crests are well developed, clearly defining a triangular ventral lamina. Both pre- and postzygapophyses are subcircular to subelliptical; the latter extend behind the posterior margin of the neural arch. The neural arch is low and defines a small and subcircular neural canal; its anterior margin is straight in dorsal view and reaches the anterior margin of the prezygapophyses. There is no zygosphene/zyganthrum complex. The neurapophysis is very high and robust. In dorsal view, it forms a triangular and flattened surface provided with a dense sculpturing made by pits, tubercles, and ridges. This triangular surface can be notched posteriorly, as in e.g., IPB-HaH 2038 (Figure 8F). In such case, the notch is deep and narrow.

The caudal vertebra has similar morphology and proportions to the trunk vertebrae. However, the neurapophysis is mostly missing.

Ribs have a robust aspect and a moderately large size. All of them narrow distally. The proximal end is expanded and bears the articulation surfaces with the transverse process of the related vertebra. At least some of them clearly display a small spiny process.

The indeterminate bone fragments are characterized by the presence of a very dense sculpturing made by pits, ridges, and tubercles on their external surface.

Remarks. The vertebrae are clearly referrable to *Chelotriton* because of the large size and the tall neurapophysis with a large, triangular, and sculptured area at the apex (Colombero et al., 2017). Other elements agree with *Chelotriton* as well because of similar size, robustness, and sculpturing. The taxonomy of *Chelotriton* is currently not well understood. Schoch et al. (2015) only included *Chelotriton paradoxus* Pomel, 1853, within the genus, but few other species were described in the past. Due to these uncertainties, we here refer the Hambach material only to *Chelotriton* sp. pending a thorough revision and clarification of the *Chelotriton* taxonomy. Nevertheless, these fossils agree with the diagnosis of *C. paradoxus* given by Schoch et al. (2015) at least in the robustly-built elements and the extensive tubercular dermal sculpturing. Moreover, they differ from *Chelotriton pliocenicus* Bailon, 1989, because of the absence of zygosphene/zyganthrum.

?*Chelotriton* sp.
Figure 9

Material. Hambach 6C: two humeri (IPB-HaH 2389, IPB-HaH 2393).

Description. These humeri are moderately large and well ossified. IPB-HaH 2389 (Figure 9A-B) preserves only the proximal half, which is about 9.5 mm long. The humerus head is rather flat proximally. On the ventral side, the ventral crest of the humerus is well developed and robust. It has an almost horizontal distal margin and a rather steep proximal margin. The crest does not bear a distinct sulcus ventrally. On the other side of the bone, the dorsal crest of the humerus is present as a short and pointed process. IPB-HaH 2393 (Figure 9C-D), on the other hand, is represented only by the distal epiphysis, which is about 6.5 mm in length. It has deep cubital ventral and olecranon fossae. The distal portion of the epiphysis was not coossified with the rest of it.

Remarks. These humeri are tentatively assigned to *Chelotriton* because of the size and the strong ossification. Proteids and likely batrachosauroidids have poorly ossified long bones, and the two specimens are larger and more ossified than bones of other salamandrids identified in Hambach and not as large as those of adult cryptobranchids.

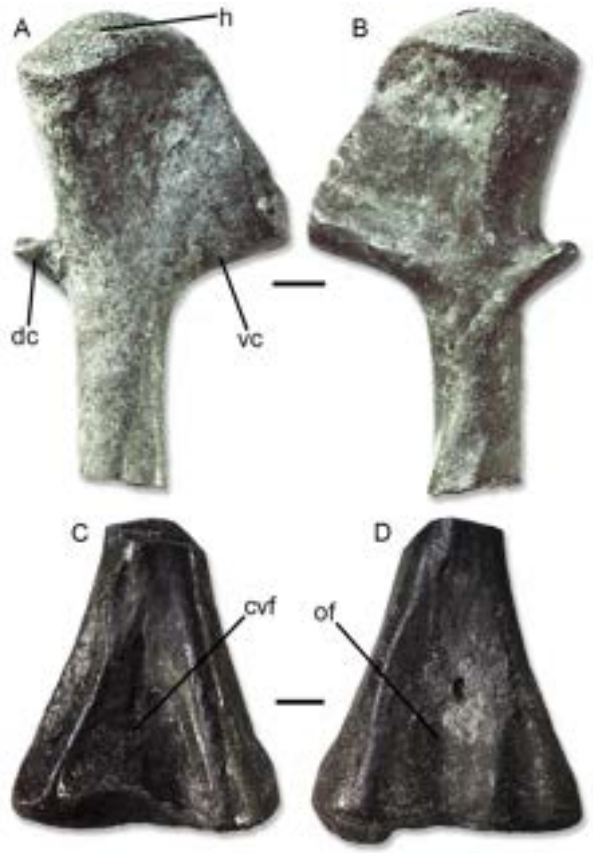

FIGURE 9. Limb bones of possible *Chelotriton* sp. from Hambach: left humerus (IPB-HaH 2389) in anterior (A) and posterior (B) views; right humerus (IPB-HaH 2393) in ventral (C) and dorsal (D) views. Scale bars equal 1 mm. Abbreviations: cvf, cubital ventral fossa; dc, dorsal crest of the humerus; h, humeral head; of, olecranon fossa; vc, ventral crest of the humerus.

LISSOTRITON Bell, 1839
Lissotriton sp.
Figures 10–11

Material. Hambach 6C: one atlas (IPB-HaH 2118); three trunk vertebrae (IPB-HaH 2110, IPB-HaH 2115/2116). Hambach 11: two trunk vertebrae (IPB-HaR 2009, IPB-HaR 2011); two caudal vertebrae (IPB-HaR 2010, IPB-HaR 2012).

Description. The small atlas (Figure 10A-E), missing most of the neural arch, has circular and flat occipital joints separated by a wide, thin and strongly gutter-like processus odontoideus. The articular surface of the latter is composed by two well-distinct separate areas facing ventrolaterally, medially contacting each other. The neural canal is roughly as wide as the processus odontoideus. The posterior cotyle is rather small and circular, being clearly narrower than the processus odontoideus. Ventrally, a longitudinal ridge runs in the middle of the centrum, flanked by two other ridges (one on each side). Some foramina are sparsely present on the ventral surface between the ridges. A lateral foramen is present on each processus lateralis, followed posteriorly by a ridge. These latter foramina are hosted in a concave area oriented anterolaterally, being visible on the lateral side of the occipital joints in anterior view. These concavities are defined by distinct lateral crests, which start from the occipital joints.

The trunk vertebrae from Hambach 6C are medium to very small sized. The centrum length is 3.5 mm in IPB-HaH 2115 (Figure 10J-M), at least 2.5 mm in IPB-HaH 2116 (Figure 10N-Q), and slightly less than 1.5 mm in IPB-HaH 2110 (Figure 10F-I). The centrum of IPB-HaH 2116 is slightly eroded and it was therefore slightly longer in origin. They have an opisthocoelous centrum, with a distinct neck. In lateral view, the anterior condyle is anteriorly rounded and either straight or lightly ventrally inclined. The ventral surface of the centrum displays a number of more or less small foramina. Both the ventral and the zygapophyseal crests are well developed. The former originate a subtriangular ventral lamina. The zygapophyseal crests contact the dorsal part of the diapophyses. The neural arch is high; its posterior part is flat (IPB-HaH 2110) or somehow concave (other vertebrae). In dorsal view, IPB-HaH 2110 (Figure 10F) has a straight anterior margin of the arch, which is on the other hand slightly concave in IPB-HaH 2115 (Figure 10J) and IPB-HaH 2116 (Figure 10N). The deepest point of the margin is located close to the anterior end of the prezygapophyses. The neural arch does not show a clear hourglass shape between the prezygapophyses in dorsal view. The posterior margin has a wide and moderately shallow notch. The zygapophyses are subelliptical and either almost subhorizontal or slightly dorsally inclined. The neurapophysis is high. Its straight dorsal margin is only preserved in IPB-HaH 2110, even though with a large notch on it due to damage. The anterior end of the spine is broken off. The neurapophysis starts either by the posterior end of the prezygapophyses in the smallest vertebra, therefore being far from the anterior margin of the neural arch, or immediately posterior to the latter margin in the other specimens. Posteriorly, it expands in a triangular area that contacts the posterior margin. The posterior end of the postzygapophyses and the posterior margin of the neural arch, both preserved only in IPB-HaH 2110, are roughly aligned. The transverse processes of the vertebrae are slender,

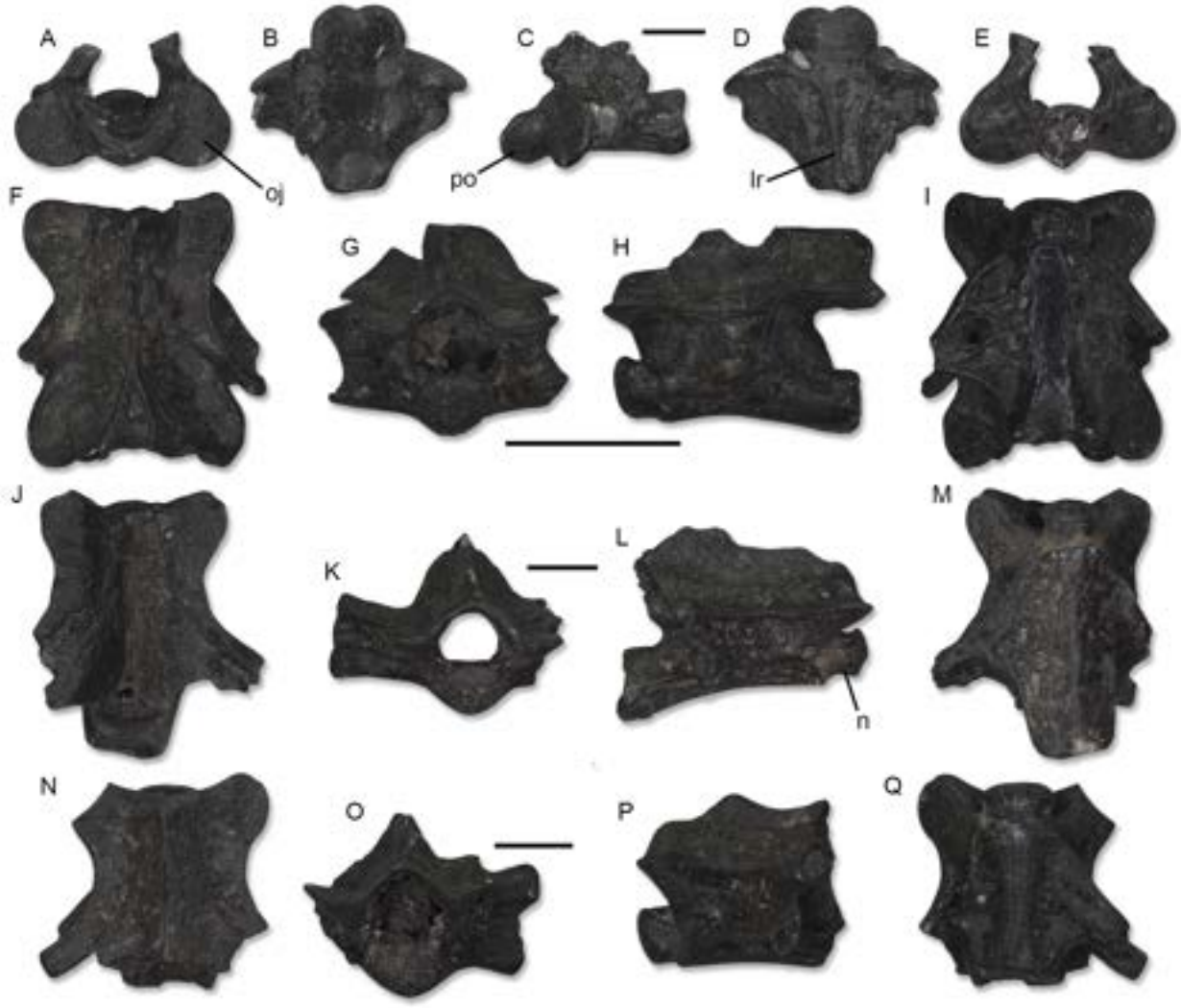

FIGURE 10. *Lissotriton* sp. from Hambach 6C: atlas (IPB-HaH 2118) in anterior (A), dorsal (B), left lateral (C), ventral (D) and posterior (E) views; trunk vertebra (IPB-HaH 2110) in dorsal (F), anterior (G), left lateral (H) and ventral (I) views; trunk vertebra (IPB-HaH 2115) in dorsal (J), anterior (K), right lateral (L) and ventral (M) views; trunk vertebra (IPB-HaH 2116) in dorsal (N), anterior (O), left lateral (P) and ventral (Q) views. Scale bars equal 1 mm. Abbreviations: lr, longitudinal ridge; n, neck; oj, occipital joint; po, processus odontoideus.

posterolaterally directed and provided with a foramen by their base.

The vertebrae from Hambach 11 (Figure 11) are opisthocoelous and very small (centrum length goes from 1.3 mm in IPB-HaR 2010 to 3 mm in IPB-HaR 2012). They have no developed neck. The anterior condyle of IPB-HaR 2009 is eroded, but it appears flattened in other specimens. It is vertical in IPB-HaR 2010 and IPB-HaR 2011 or slightly ventrally inclined in IPB-HaR 2012. Zygapophyseal crests are always well developed, whereas the ventral ones are moderately developed in IPB-HaR 2011 (Figure 11I) and IPB-HaR 2012 (Figure 11Q) or not developed in IPB-HaR 2009 (Figure 11E) and IPB-HaR 2010 (Figure 11N). The ventral surface is poorly preserved in all specimens, but the left side of IPB-HaR 2009 shows a moderately wide subcentral foramen and a number of small foramina are present ventrally in IPB-HaR 2011. Zygapophyses are narrow, almost horizontal and subelliptical. The neural arch is high and flattened posteriorly. The straight anterior margin of the neural arch reaches almost the anterior end of the prezygapophyses. Also in this case, the neural arch does not show a clear hourglass shape between the prezygapophyses in dorsal view. The neurapophysis is high and starts near the anterior margin of the arch; its dorsal half is broken in both specimens. A wide and deep V-shaped notch is present in the middle of the posterior end of the

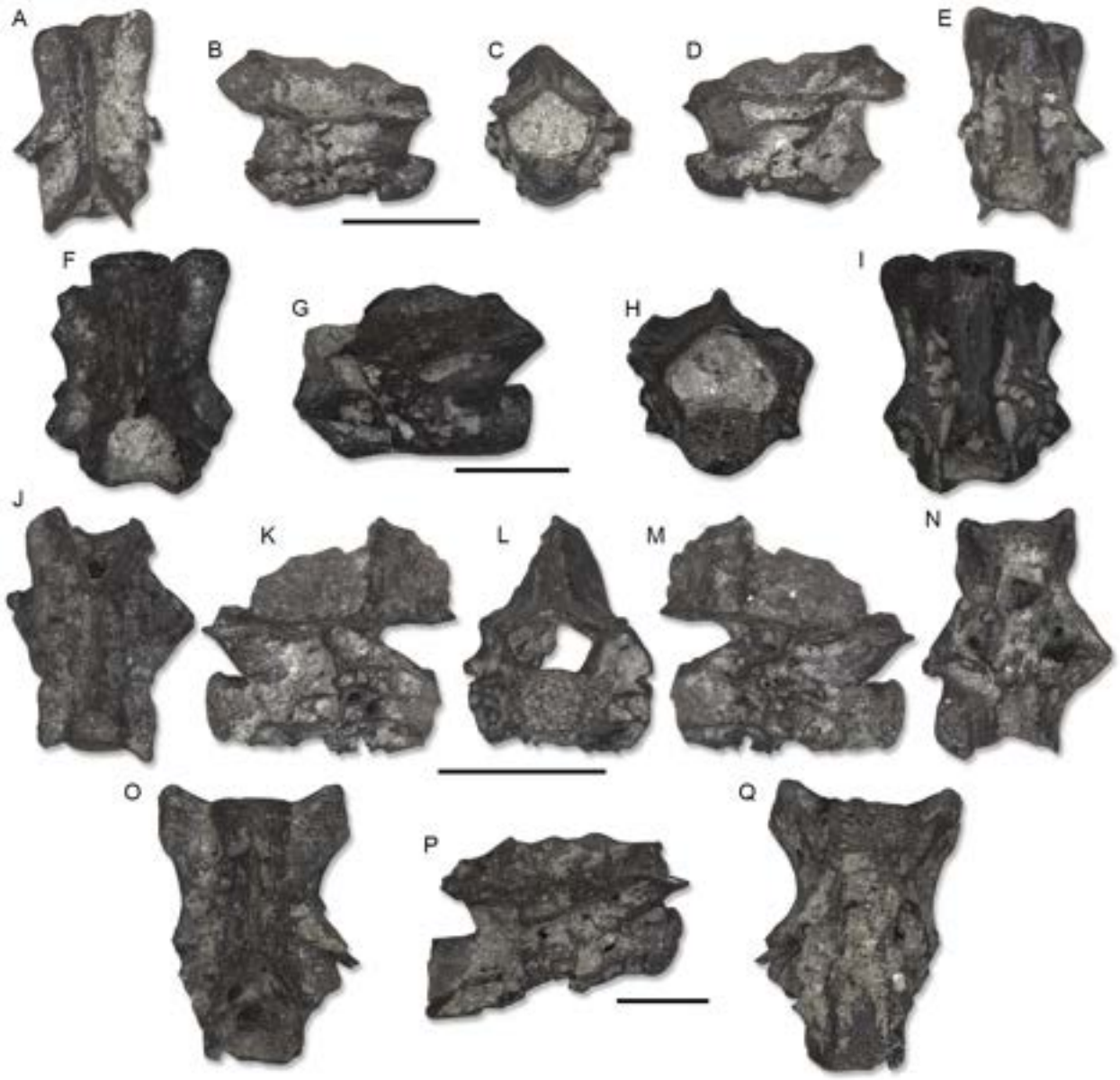

FIGURE 11. *Lissotriton* sp. from Hambach 11: trunk vertebra (IPB-HaR 2009) in dorsal (A), left lateral (B), anterior (C), right lateral (D) and ventral (E) views; trunk vertebra (IPB-HaR 2011) in dorsal (F), right lateral (G), anterior (H) and ventral (I) views; caudal vertebra (IPB-HaR 2010) in dorsal (J), left lateral (K), anterior (L), right lateral (M) and ventral (N) views; caudal vertebra (IPB-HaR 2012) in dorsal (O), right lateral (P) and ventral (Q) views. Scale bars equal 1 mm.

arch. The posterior margin of the neural arch does not extend posteriorly beyond the postzygapophyses. The latter are always broken off, but the base of the right one of IPB-HaR 2010 is preserved and extends beyond the margin. The portion of neural arch located by the sides of the posterior notch are almost vertically oriented.

Remarks. A small-sized salamandrid is also present in both Hambach 6C and 11. The atlas has sparse foramina on the ventral surface, a processus odontoideus that is wider than the posterior cotyle, and well-developed lateral crests (Ratnikov and Litvinchuk, 2009). The morphology of the vertebrae is generally alike that of both *Ichthyosaura* Sonnini de Manoncourt and Latreille, 1801, and *Lissotriton*, but few characters allow the attribution of the material to the latter. On the atlas, the articular facets of the processus odontoideus are in medial contact, thus differing from the condition showed by *Ichthyosaura* (whose surfaces are sep-

FIGURE 12. *Triturus* sp. from Hambach: atlas (IPB-HaH 2196) in dorsal (A), anterior (B), left lateral (C), posterior (D) and ventral (E) views; trunk vertebra (IPB-HaH 2101) in dorsal (F) and left lateral (G) views; trunk vertebra (IPB-HaH 2103) in dorsal (H), ventral (I) and left lateral (J) views; trunk vertebra (IPB-HaH 2224) in dorsal (K), anterior (L), right lateral (M), posterior (N) and ventral (O) views. Scale bars equal 1 mm. Abbreviations: avc, anterior ventral crest; azc, anterior zygapophyseal crest; n, neurapophysis; oj, occipital joint; op, odontoid process; sc, secondary dorsal crest.

arated by a large or, rarely, narrow groove) and consistent with the variability seen in the extant species of *Lissotriton*. The neural arch does not show a clear hourglass shape between the prezygapophyses in dorsal view, further supporting affinities between the Hambach remains and *Lissotriton*. Attribution to *Lissotriton boscai* (Lataste in Tourneville, 1879) can be excluded because this species shows small lateral eversions of the neurapophysis. Caudal vertebrae (only found in Hambach 11) allow the exclusion of *Lissotriton vulgaris* (Linnaeus, 1758) and *Lissotriton italicus* (Peracca, 1898): in caudal vertebrae of these species, the posterior end of the neural arch is higher than the centrum in lateral view (Macaluso et al., 2023b), which is not the case in the Hambach remains (this can be clearly evaluated in IPB-HaR 2010). We were unable to observe the longitudinal ridge on the ventral surface of the atlas in any of the specimens of extant *Lissotriton* available to us for comparison. This may suggest that the Hambach vertebrae belong to a still unknown species, but given the high variability shown by urodele species we consider more cautious to herein refer all of the remains from Hambach (both 6C and 11) only at genus level.

TRITURUS Rafinesque, 1815
Triturus sp.
Figure 12

Material. Hambach 6C: one atlas (IPB-HaH 2196); 10 trunk vertebrae (IPB-HaH 2101/2103, IPB-HaH 2155, IPB-HaH 2163, IPB-HaH 2166/2167, IPB-HaH 2172/2173, IPB-HaH 2224); one caudal vertebra (IPB-HaH 2168).

Description. IPB-HaH 2196 (Figure 12A-E) is a moderately small atlas (centrum length is 3 mm). The odontoid process is wide, gutter-shaped and bears two ventrolaterally directed articulation surfaces; it is roughly as large as the posterior cotyle and slightly narrower than the neural canal. The occipital joints, the posterior cotyle, and the neural

canal are subcircular. The ventral surface shows only very rare and small foramina, and evident inferior crests (sensu Macaluso et al., 2020). The lateral surface of each lateral process shows a well-developed and sharp lateral crest. A low and wide neurapophysis is visible on the dorsal surface of the neural arch; it widens posteriorly and it is flanked by a secondary dorsal crest by each side. The latter touch the former by its posterior third and anteriorly they split into two low ridges. The dorsal portion of the neural arch is strongly sloping anteriorly in lateral view and thick and subtrapezoidal in posterior view. The postzygapophyses are subelliptical and very slightly tilted dorsally; their posterior margin develops beyond the posterior margin of the neural arch, which is slightly wavy in dorsal view.

Trunk vertebrae (Figure 12F-O) are large in size (centrum length up to 7 mm). They are opisthocoelous and have a weakly developed neck and small subcentral foramina. Ventral and zygapophyseal crests are well developed. The transverse processes are moderately slender and posterolaterally directed (more laterally in IPB-HaH 2172 and IPB-HaH 2173). The neural arch is moderately low in its anterior portion, but tends to rise abruptly posteriorly. The anterior margin is straight or concave and reaches the anterior half of the prezygapophyses. The posterior margin is well preserved only in IPB-HaH 2103 and IPB-HaH 2224: it does not show a medial notch, but instead it has either a convex outline (IPB-HaH 2103; Figure 12H) or a small posteriorly directed point (IPB-HaH 2224; Figure 12K). The margin does not reach the posterior end of the postzygapophyses in IPB-HaH 2224, but it is roughly aligned with the latter in IPB-HaH 2103 (and in IPB-HaH 2101 and IPB-HaH 2102 as well). Absence of the posterior notch can be supposed for other vertebrae as well based on less preserved posterior margins. Zygapophyses are suboval and subhorizontal. The neurapophysis is low and is present along the entire preserved portion of the neural arch, but starting at some distance from the anterior margin in at least some vertebrae (e.g., IPB-HaH 2101 and IPB-HaH 2102). The morphology of the caudal vertebra is similar to that of the trunk vertebrae.

Remarks. The above-described large and opisthocoelous trunk vertebrae provided with subcentral foramina (Ratnikov and Litvinchuk, 2007) are evidence for the presence of another rather large-sized salamandrid in the fossil material from Hambach 6C. The small atlas can be assigned to the same urodele family due to the following combination of features (Ratnikov and Litvinchuk, 2009): processus odontoideus gutter-shaped, with two ventrolateral articular surfaces; dorsal part of neural arch thick in posterior view; dorsal margin of neural arch anteriorly sloping in lateral view; presence of neurapophysis and well-developed secondary and lateral crests; posterior margin of the postzygapophyses extending beyond the posterior margin of the neural arch in dorsal view. Furthermore, all these vertebrae share *Triturus* features. These are, for the atlas (Ratnikov and Litvinchuk, 2009): dorsal margin of neural arch inclined; posterior margin of neural arch slightly wavy; lateral crests well developed; neurapophysis large and low; and subcircular neural canal. As far as the trunk vertebrae are concerned, on the other hand, they are (Ratnikov and Litvinchuk, 2007): condyle neck weakly developed; low neural arch, which rises posteriorly; and anterior margin of the neural arch either straight or concave in dorsal view, located at midlength of the prezygapophyses. A specific identification of the fossils is hindered by the scant knowledge of the comparative osteology of the genus *Triturus*, as well as by a set of differences observed with the few species for which axial bone morphology is known (data mainly from Ratnikov and Litvinchuk, 2007, 2009). The atlas from Hambach differs from *Triturus cristatus* (Laurenti, 1768) in the strongly evident inferior crests, from *Triturus dobrogicus* (Kiritzescu, 1903) in the larger size and the neurapophysis not disappearing posteriorly, and from *Triturus karelinii* (Strauch, 1870) in the secondary dorsal crests not reaching the posterior margin, the neural arch not arched in posterior view, and the absence of accessory crests on the lateral processes. It shares with *T. karelinii* the neurapophysis expanded in a sort of subtriangular area posteriorly and with *T. dobrogicus* the secondary dorsal crest not reaching the posterior margin, the inclination and orientation of the articular facets of the processus odontoideus, and the already mentioned strongly evident inferior crests. It also shares with both species, as well as with *T. cristatus,* the processus odontoideus that is as wide as the cotyle but narrower than neural canal and the inclined neural arch that is thick and subtrapezoid in posterior view. The trunk vertebrae differ from all *T. cristatus, T. dobrogicus,* and *T. karelinii* in the larger size and the well development of all crests, and from *T. cristatus* and *T. dobrogicus* only in the neurapophysis devoid of an increased development in its middle part. *Triturus marmoratus* (Latreille, 1800) has a posterior margin of the neural arch ending well anterior to the

postzygapophyses (Holman, 1998), which is not always the case in the Hambach fossils. Moreover, the trunk vertebrae show some minor differences with all the known species of *Triturus*, as the shape of the postzygapophyses is narrow and drop-shaped in the Hambach fossils (L.M., pers. obs.). The caudal vertebra is here assigned to the same taxon as the rest of the material due to the morphological similarity shared with the trunk elements. Considering all of this, the Hambach *Triturus* may either be a new species or a member of a lineage the osteology of which is not deeply investigated (such as *T. marmoratus,* which currently reaches up to northwestern France in Western Europe; Sillero et al., 2014). Pending a more detailed comparison with other *Triturus*, both fossils and extant, the material is here only identified as *Triturus* sp.

Urodela indet.

Material. Hambach 6C: one dentary (IPB-HaH 2003); 27 trunk vertebrae (IPB-HaH 2075/2076, IPB-HaH 2107/2109, IPB-HaH 2122/2131, IPB-HaH 2143, IPB-HaH 2152/2154, IPB-HaH 2159/2160, IPB-HaH 2169, IPB-HaH 2176, IPB-HaH 2187/2188, IPB-HaH 2223); 28 caudal vertebrae (IPB-HaH 2077/2079, IPB-HaH 2104/2106, IPB-HaH 2132/2141, IPB-HaH 2146/2149, IPB-HaH 2161, IPB-HaH 2170/2171, IPB-HaH 2184/2186, IPB-HaH 2376/2377); two femurs (IPB-HaH 2047, IPB-HaH 2394); one tibia (IPB-HaH 2049); one indeterminate limb element (IPB-HaH 2040).

Remarks. The fossil material from Hambach 6C includes numerous urodele specimens that cannot be identified more precisely due to either poor preservational status or poor taxonomic significance.

ANURA Fischer, 1813

ALYTIDAE Fitzinger, 1843

LATONIA von Meyer, 1843

Latonia sp.

Figures 13–15

Material. Hambach 6C: three premaxillae (IPB-HaH 2050, IPB-HaH 2280/2281); 12 maxillae (IPB-HaH 2052/2053, IPB-HaH 2056/2060, IPB-HaH 2069/2070, IPB-HaH 2266/2267, IPB-HaH 2278); two frontoparietals (IPB-HaH 2002, IPB-HaH 2338); three angulars (IPB-HaH 2051, IPB-HaH 2396/2397); one atlas (IPB-HaH 2071); six trunk vertebrae (IPB-HaH 2072/2074, IPB-HaH 2221/2222, IPB-HaH 2229); one sacral vertebra (IPB-HaH 2219); two urostyles (IPB-HaH 2199/2200); three scapulae (IPB-HaH 2324/2325, IPB-HaH 2329); four humeri (IPB-HaH 2055, IPB-HaH 2061, IPB-HaH 2316, IPB-HaH 2336). Hambach 11: four maxillae (IPB-HaR 2016/2017, IPB-HaR 2041/2042); five angulars (IPB-HaR 2115/2117, IPB-HaR 2142/2143); four trunk vertebrae (IPB-HaR 2022/2023; IPB-HaR 2032/2033); one sacral vertebra (IPB-HaR 2014); one urostyle (IPB-HaR 2034); one humerus (IPB-HaR 2127); two ilia (IPB-HaR 2015, IPB-HaR 2083). Hambach 11C: two maxillae (IPB-HaR 2425/2426); one angular (IPB-HaR 2416); one ilium (IPB-HaR 2417).

Description. Premaxillae are moderately large in size and have a mediolaterally elongated pars dentalis, with a robust and short lamina horizontalis. The tooth row covers the entire length of the bone. In IPB-HaH 2050 (Figure 13A-B; the only specimen in which it is complete), the tooth row shows 13 tooth positions. None of the specimens preserve the complete pars facialis, but a deep recess is recognisable on the inner surface of its base. The external surface of the bone is smooth.

Maxillae (Figure 13C-H) are always fragmentary, but they can reach a very large size. The lamina horizontalis is robust and not strongly developed in medial direction; a moderately shallow groove for the palatoquadrate bar is present on the dorsal surface of its posterior portion. The processus palatinus is partially preserved only in IPB-HaH 2052, IPB-HaH 2056, IPB-HaH 2059 (Figure 13E-F), IPB-HaR 2042, and IPB-HaR 2426; a moderately developed and strongly anteriorly inclined edge provided with a groove on its posterodorsal surface is present on the medial side of the process. The processus pterygoideus is usually broken off, but a large posterior depression is still recognizable on the medial surface between it and the processus zygomaticomaxillaris. When preserved (IPB-HaH 2058, IPB-HaH 2060, IPB-HaH 2266, IPB-HaH 2267, IPB-HaR 2016, and IPB-HaR 2017), the processus pterygoideus is short, moderately robust and pointed. The anterior margin of the depression is marked by a moderately developed ridge. The tooth row continues posteriorly slightly beyond the lamina horizontalis. The lateral surface is covered by a dermal sculpturing made by tubercles and ridges, which concentrates mainly in the posterodorsal part of the bone. IPB-HaH 2056, IPB-HaH 2057, IPB-HaH 2059, IPB-HaH 2060, IPB-HaH 2266, IPB-HaH 2267, IPB-HaH 2278, IPB-HaR 2041, IPB-HaR 2042, IPB-HaR 2425, and IPB-HaR 2426 have a smooth lateral surface, but they represent only the anterior end (IPB-HaH 2059), the middle portion of the bone (IPB-HaH 2056, IPB-HaH 2057, IPB-HaR 2042, IPB-HaR 2425, and IPB-HaR 2426) or part of the posteroventral portion (IPB-HaH 2060, IPB-HaH 2266,

FIGURE 13. Skull elements of *Latonia* sp. from Hambach: premaxilla (IPB-HaH 2050) in anterior (A) and posterior (B) views; right maxilla (IPB-HaH 2053) in lateral (C) and medial (D) views; right maxilla (IPB-HaH 2059) in lateral (E) and medial (F) views; left maxilla (IPB-HaR 2016) in lateral (G) and medial (H) views; frontoparietal (IPB-HaH 2002) in dorsal (I) and ventral (J) views; left angular (IPB-HaH 2051) in lateral (K), medial (L) and dorsal (M) views; right angular (IPB-HaR 2117) in dorsal (N) and medial (O) views; left angular (IPB-HaR 2142) in lateral (P), medial (Q) and dorsal (R) views; right angular (IPB-HaR 2416) in dorsal view (S). Scale bars equal 1 mm. Abbreviations: cme, crista mandibulae externa; if, incrassatio frontoparietalis; lh, lamina horizontalis; pc, processus coronoideus; pd, posterior depression; pp, processus palatinus; pr, processus paracoronoideus.

IPB-HaH 2267, IPB-HaH 2278, and IPB-HaR 2041). Some of these smooth specimens can be very large in size (e.g., IPB-HaH 2059).

IPB-HaH 2002 (Figure 13I-J) is a moderately large fragment of frontoparietal, probably representing part of the left anterolateral portion of the bone. The ventral surface displays a narrow and elongated incrassatio frontoparietalis. The preserved portion of the incrassatio has a symmetrical appearance, thus suggesting that it was unpaired

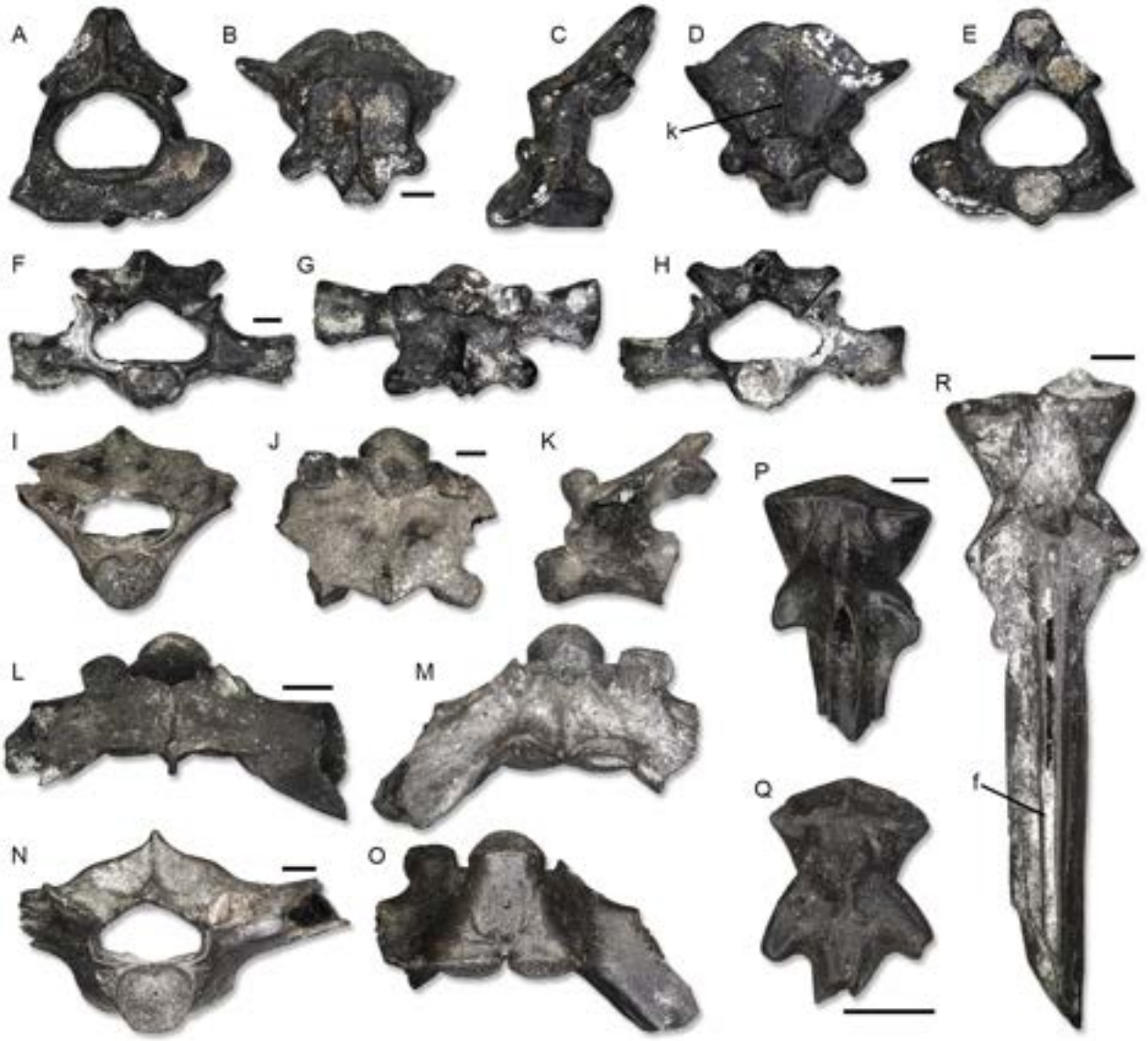

FIGURE 14. Axial elements of *Latonia* sp. from Hambach: atlas (IPB-HaH 2071) in anterior (A), dorsal (B), left lateral (C), ventral (D) and posterior (E) views; trunk vertebra (IPB-HaH 2073) in anterior (F), dorsal (G) and posterior (H) views; trunk vertebra (IPB-HaR 2032) in anterior (I), dorsal (J) and left lateral (K) views; sacral vertebra (IPB-HaH 2219) in dorsal view (L); sacral vertebra (IPB-HaR 2014) in dorsal (M), anterior (N) and ventral (O) views; urostyle (IPB-2199) in dorsal view (P); urostyle (IPB-HaH 2200) in dorsal view (Q); urostyle (IPB-HaR 2034) in dorsal view (R). Scale bars equal 1 mm. Abbreviations: f, fissure; k, keel.

and that a small part of the right lateral side of the bone is also represented. The foramen parietale is not present in the preserved portion of the frontoparietal. The pars contacta is laminar and rather well developed. The anterolateral corner of the fragment represents part of the left anterior horn. The dorsal surface of the specimen is almost completely covered by a well-developed dermal sculpturing, made up by tubercles. These are densely arranged and some of them fuse to origin short ridges. Part of the anterior horn is unsculptured. IPB-HaH 2338 is a fragment of the left posterolateral portion of a frontoparietal with a similar dermal sculpturing.

Angulars (Figure 13K-S) have a processus paracoronoideus anterior to the processus coronoideus. The two processes are similar in size. The former is horizontal, whereas the latter is almost vertical or slightly medially inclined. The processus coronoideus is well developed and does not extend posteriorly. By the processes, the sulcus cartilagine Meckeli is only a moderately shallow groove. A low

FIGURE 15. Appendicular elements of *Latonia* sp. from Hambach: left scapula (IPB-HaH 2324) in dorsal (A) and ventral (B) views; left scapula (IPB-HaH 2325) in dorsal (C) and ventral (D) views; left scapula (IPB-HaH 2329) in dorsal (E) and ventral (F) views; right humerus (IPB-HaH 2061) in ventral (G) and dorsal (H) views; left ilium (IPB-HaR 2015) in lateral (I) and medial (J) views; right ilium (IPB-HaR 2083) in lateral (K) and medial (L) views; right ilium (IPB-HaR 2417) in lateral (M) and medial (N) views. Scale bars equal 1 mm. Abbreviations: ca, crista anterior; dt, dorsal tubercle; ig, interiliac groove; pa, pars acromialis.

crista mandibulae externa is visible on the lateral surface of the bone; it defines the ventral margin of a very slightly depressed area. In IPB-HaH 2051, IPB-HaH 2396, and IPB-HaH 2397, which are very large specimens, both the crista and the depressed area are more developed.

Presacral vertebrae (Figure 14A-K) are opisthocoelous, robust and very large. The centrum is subcylindrical and the neural canal is subelliptical

(main axis directed horizontally) in anterior view. The anterior cotyles of the atlas (Figure 14A-E) are almost in contact medially. The same vertebra displays a sharp keel on its ventral surface. The transverse processes of the trunk vertebrae (Figure 14F-K) are robust and laterally directed. The dorsal surface of the neural arch is large and flattened, with a low, moderately- or well-developed carina neuralis. Zygapophyses are suboval and twisted dorsally of about 45°.

Sacral vertebrae (Figure 14L-O) have an anterior condyle and two posterior condyles. The dorsal surface of the neural arch shows a low carina neuralis developing a small posterior tip. Prezygapophyses are subelliptical and dorsally inclined of about 45°. Transverse processes are broken in both specimens, but in IPB-HaH 2219 they show a slight anteroposterior enlargement (Figure 14L). The anterior margin of these processes is clearly perpendicular to the vertebral centrum in IPB-HaH 2219 (Figure14L), but it seems posterolaterally inclined in IPB-HaR 2014 (Figure 14M). However, transverse processes of the latter sacral vertebra are less preserved and reconstruction of their original shape is somehow doubtful.

Urostyles (Figure 14P-R) preserve only the anterior end, showing two anterior cotyles. Except for IPB-HaH 2200 (Figure 14Q), which is rather small, they can reach a large size. A transverse process is present on each side of the neural arch, continuing posteriorly in a horizontal lamina in IPB-HaR 2034 (Figure 14R). The carina neuralis is not developed and, posteriorly to the transverse processes, the neural arch presents a narrow fissure in the middle of the dorsal surface.

Scapulae (Figure 15A-F) are very large and robust. They are short and wide and show a very well-developed crista anterior (though broken in IPB-HaH 2325 and completely missing in IPB-HaH 2329). The pars suprascapularis is very wide. The pars acromialis is missing in all specimens, whereas the robust pars glenoidalis is always poorly preserved.

Humeri are very robust and large-sized. IPB-HaH 2055, IPB-HaH 2336, and IPB-HaR 2127 preserve only the distal end, IPB-HaH 2061 (Figure 15G-H) misses the proximal half, whereas IPB-HaH 2316 lacks only the proximal portion. The eminentia capitata is spherical and distinctly shifted laterally compared to the axis of the diaphysis. A moderately deep fossa cubitalis ventralis is present, except for IPB-HaH 2061 and IPB-HaH 2336. The epicondylus ulnaris is more than twice as large as the radialis one. Cristae medialis and lateralis are well developed and sharp in IPB-HaH 2061 and IPB-HaH 2316 and moderately developed in IPB-HaH 2055, IPB-HaH 2336, and IPB-HaR 2127; the former bends in dorsal direction proximally. The olecranon scar is moderately large in most specimen (though it is poorly visible in IPB-HaH 2061 and IPB-HaR 2127), but small in IPB-HaH 2055.

Ilia (Figure 15I-N) are large. They display a dorsal crest, which merges posteriorly with the dorsal tubercle. The tubercle is low, elongated and rather poorly distinct. The posterior portion of the dorsal crest, anteroventral to the tubercle, hosts a shallow tubercular fossa with few foramina on its lateral surface. The acetabular fossa is moderately wide and somehow elongated. The supraacetabular fossa is present and shallow. The dorsal acetabular expansion is short. Together with the strongly anteriorly-inclined dorsal tubercle, it originates a very obtuse angle. The ventral acetabular expansion seems more developed, but it is never completely preserved. The medial side of the ilial body displays a deep interiliac groove and the base of a (broken) interiliac tubercle.

Remarks. A large *Latonia* is clearly present in Hambach, being identifiable based on the following combination of characters (Roček, 1994b, 2013): presence of both a coronoid and a paracoronoid process on the angular; posterior depression on the maxilla; ventral keel on the atlas; laterally-shifted eminentia capitata on the humeri; ilia with a thin dorsal crest and an obtuse angle between the tubercle and the dorsal acetabular expansion; and possibly also unpaired frontoparietal. Syromyatnikova and Roček (2019) recently summarized the most taxonomically-significant osteological features of the known species within this genus. The sculptured frontoparietal clearly exclude affinities with the extant *Latonia nigriventer* (Mendelssohn and Steinitz, 1943) (see also Biton et al., 2013, 2016), whereas the well-developed coronoid process is unlike the morphology seen in *Latonia vertaizoni* (Friant, 1944). Furthermore, the absence of a posterior extension of the latter process differs from at least some *Latonia ragei* Hossini, 1993. In the *Latonia* from Hambach, the maxillary tooth row exceeds posteriorly the extension of the lamina horizontalis, recalling in this *L. nigriventer, L. ragei,* and some *Latonia seyfriedi* von Meyer, 1843 (in the sense of Syromyatnikova et al., 2019, that is including *Latonia gigantea* (Lartet, 1851) as well) but differing from *Latonia caucasica* Syromyatnikova and Roček, 2019. The presence or absence of sculpturing on the maxillae was commonly used

in the past to distinguish two groups within *Latonia*: sculptured maxillae were generally referred to *L. gigantea,* in contrast with *L. ragei* and *L. vertaizoni* having unsculptured maxillae. This distinction was, however, complicated by the fact that the lateral surface of the maxillae of *L. seyfriedi* was not known for a long time. Only recently, Syromyatnikova et al. (2019) demonstrated that the latter species has sculptured maxillae as well, proposing *L. gigantea* as a junior synonym of it based on this and other features. Moreover, Syromyatnikova and Roček (2019) added *L. caucasica* to the list of the *Latonia* species with unsculptured maxillae. To add further complexity to the maxillary sculpturing character, these dermal ossifications originate in *Latonia* as a separate layer, which only contacts the surface of the bone through fragile trabeculae (Roček, 1994b; Syromyatnikova et al., 2019). Thus, separation of the sculptured layer from the bone due to breakage of these trabeculae is not unlikely, leading to the possible artifactual recognition of unsculptured maxillae in place of the original sculptured ones. What is more, maxillae referred to *Latonia* showing an overall smooth lateral surface, but with few rugosities usually concentrated on the posterodorsal corner, have been described lately (e.g., from the Early Miocene of Greece; Georgalis et al., 2019a). These may be interpreted as juveniles of sculptured forms when small, but the presence of some large elements presenting the same pattern (such as is the case with the Hambach fossils) hints towards the need of further scrutiny of this feature. Another important character for the identification of *Latonia* species is the direction of the sacral transverse processes. The possible presence of two different morphologies in the two sacral vertebrae from Hambach (i.e., clearly perpendicular versus possibly posterolaterally-inclined processes), furthermore coming from two different layers, may suggest the presence of two different taxa in the two different stratigraphic portions of the site. However, the uncertainty surrounding the observation of the second morphotype, together with the possible variation of this character apparent in at least *L. seyfriedi* (see Syromyatnikova and Roček, 2019) as well as the generally comparable morphology showed by all other *Latonia* remains from Hambach, suggest caution on this. It is evident that, based on the current state of knowledge, a specific identification of the *Latonia* from Hambach would be somehow ambiguous, and we thus refrain from proposing one, pending a detailed revision and clarification of the diagnostic characters of the species currently included in the genus.

PALAEOBATRACHIDAE Cope, 1865
PALAEOBATRACHUS Tschudi, 1838
Palaeobatrachus eurydices Villa, Roček, Tschopp, van den Hoek
Ostende, and Delfino, 2016
Figures 16–17

Material. Hambach 11: one sphenethmoid (IPB-HaR 2021); 11 angulars (IPB-HaR 2110/2113, IPB-HaR 2129/2132, IPB-HaR 2144/2146); one trunk vertebra (IPB-HaR 2030); five humeri (IPB-HaR 2148/2152); five ilia (IPB-HaR 2099/2102, IPB-HaR 2147). Hambach 11C: one maxilla (IPB-HaR 2429); one angular (IPB-HaR 2418); two humeri (IPB-HaR 2419/2420).

Description. IPB-HaR 2429 (Figure 16A-C) is a fragment of maxilla, measuring about 5.5 mm in length and preserving only the area of the processus palatinus. The bone is robustly built. On the medial side, part of the tooth row is preserved, even though in bad conditions. Four wide tooth positions are preserved, one of them still hosting the base of a tooth. The tooth positions are separated by knob-like structures. The lamina horizontalis is mostly broken, but it clearly extended medially with a toothless portion. No clear ridge is visible ventrally separating the toothed and toothless portion of the lamina. On its dorsal side, a deep recessus vaginiformis is present. The processus palatinus is represented in this specimen by a low, subtriangular structure with a truncated dorsal tip. In dorsal view, it is shifted medially, thus originating a concavity on the lateral surface of the maxilla. Both the anterior and posterior margins of the process are distinctly irregular, and its lateral surface displays few foramina.

IPB-HaR 2021 (Figure 16D-G) is a fragmentary sphenethmoid. It is anteroposteriorly elongated and large-sized. The lateral margins of the bone are rather eroded, but distinctly developed laminae supraorbitalis and trabecula seem not to be present. In dorsal view, a long and U-shaped fenestra frontoparietalis is recognizable, even if the left portion of the bone is lacking. Anteriorly to the fenestra, the dorsal surface of the bone is smooth. The contact surface with the parasphenoid is visible on the ventral surface: it is delimited laterally by two low ridges and widens anteriorly.

Angulars are robust and large-sized. They have a rather deep sulcus cartilagine Meckeli and an anteroposteriorly elongate, stocky and dorsoventrally compressed processus coronoideus. The dorsal surface of the latter is strongly irregular, with pits and/or ridges, and shows a certain degree of individual variation (Figure 17). A few angulars,

FIGURE 16. *Palaeobatrachus eurydices* from Hambach: right maxilla (IPB-HaR 2429) in dorsal (A), medial (B) and lateral (C) views; sphenethmoid (IPB-HaR 2021) in dorsal (D), ventral (E), anterior (F) and right lateral (G) views; left humerus (IPB-HaR 2148) in ventral (H) and dorsal (I) views; left humerus (IPB-HaR 2152) in ventral (J) and dorsal (K) views; left humerus (IPB-HaR 2420) in ventral (L) and dorsal (M) views, right ilium (IPB-HaR 2099) in lateral view (N); right ilium (IPB-HaR 2100) in lateral view (O); left ilium (IPB-HaR 2101) in lateral view (P); right ilium (IPB-HaR 2147) in lateral view (Q). Scale bars equal 1 mm. Abbreviations: dt, dorsal tubercle; pp, processus palatinus; ps, contact surface for the parasphenoid.

such as e.g., IPB-HaR 2111 (Figure 17A) and IPB-HaR 2418, bear a small tubercle on the lateral side, in correspondence with the anterior end of the processus coronoideus. The extremitas spatulata is short and broad.

IPB-HaR 2030 is a fragmentary trunk vertebra provided with a very dorsoventrally compressed centrum. The latter is procoelous, wide, and shows numerous small pits on the ventral surface.

Humeri (Figure 16H-M) are very large-sized and lack a fossa cubitalis ventralis. The eminentia capitata and the epicondyles are distally eroded and were probably partly cartilaginous in the living animal. The epicondylus ulnaris is only slightly larger than the epicondylus radialis. The olecranon scar is depressed, but the articular surface with the olecranon of the radioulna is small and poorly developed. All specimens but IPB-HaR 2420 preserve only the distal epiphysis and the distal part of the diaphysis. IPB-HaR 2420 is more preserved, but the proximal end of the bone is still missing. A hint of a robust crista ventralis is recognizable on the ventral surface of the humeri. This is particularly evident in IPB-HaR 2420, which also express the base of a crista paraventralis. Cristae medialis and lateralis are not developed.

FIGURE 17. Individual variation in the angulars of *Palaeobatrachus eurydices* from Hambach: left angular (IPB-HaR 2111) in dorsal view (A); left angular (IPB-HaR 2132) in dorsal view (B); left angular (IPB-HaR 2144) in dorsal view (C); right angular (IPB-HaR 2110), detail of the processus coronoideus in dorsal view (D); left angular (IPB-HaR 2112), detail of the processus coronoideus in dorsal view (E); left angular (IPB-HaR 2130), detail of the processus coronoideus in dorsal view (F); right angular (IPB-HaR 2131), detail of the processus coronoideus in dorsal view (G); right angular (IPB-HaR 2145), detail of the processus coronoideus in dorsal view (H); right angular (IPB-HaR 2146), detail of the processus coronoideus in dorsal view (I). Scale bars equal 1 mm. Abbreviations: pc, processus coronoideus; t, tubercle.

Ilia (Figure 16N-Q) show a well-developed and elongated dorsal tubercle, but no dorsal crest. The tubercle bends in lateral direction. The large acetabular fossa has a prominent anteroventral rim. The ventral acetabular expansion is not developed, whereas the dorsal one is moderately developed. A supraacetabular fossa is visible dorsally to the acetabulum. A wide and deep interiliac groove is visible on the medial surface of the body of the bone.

Remarks. Clear diagnostic features of palaeobatrachid anurans in the above-described material are the following (Wuttke et al., 2012; Roček, 2013; Roček et al., 2021): knob-like structures separating tooth positions in the maxilla; elongated spheneth-moid, provided with frontoparietal fenestra longer than half the total length of the bone and with two

parallel ridges delimiting the articulation area for the parasphenoid on the ventral surface; coronoid process of the angular either smooth or bearing muscle scars on dorsal surface; vertebral centrum strongly dorsoventrally compressed and with numerous pits on the ventral surface; humerus devoid of fossa cubitalis ventralis (different from Eocene palaeobatrachids, though) and provided with a comparatively small eminentia capitata that is located on or near the long axis of bone, as well as similar-sized epicondyles; ilium with massive dorsal acetabular expansion; large acetabular fossa extending anteroventrally beyond the margin of the ilial body, thus concealing the ventral expansion; dorsal tubercle protruding only slightly in dorsal direction, but more prominent laterally and bearing muscle scars on the lateral surface; distinct horizontal depression on the inner surface of the iliac shaft. Specific attribution to *P. eurydices* appears also justified, due to the following combination of features (Villa et al., 2016): the interorbital section of the processus cultriformis of the parasphenoid was narrow, but the process becomes wider towards the anterior (as suggested by the divergent longitudinal ridges on the ventral side of sphenethmoid, which delimit laterally the area of attachment of the parasphenoid); the sphenethmoid lacks articular facets for the nasals; the dorsal surface of the sphenethmoid shows no median ridge; the processus coronoideus of the angular extends parallel to most of the extremitas spatulata; the extremitas spatulata is short and broad; the fossa cubitalis ventralis of humerus is absent. Despite its very fragmentary status, the maxilla IPB-HaR 2429 is also very similar in morphology to maxillae of *P. eurydices.* In particular, it could be somehow representative of a sort of “intermediate” stage between the supposed juvenile maxilla reported by Villa et al. (2016) and the adult ones. Similar to the purported juvenile specimen, IPB-HaR 2429 has a subtriangular processus palatinus, which gives to the bone a concave lateral appearance in dorsal view due to a slight medial shifting. However, the size of the specimen, as well as the number of teeth in the processus palatinus area and the absence of a ridge separating the toothed and toothless portions of the ventral surface of the lamina horizontalis, seem to be more comparable with the adult holotype maxilla of *P. eurydices.*

?Palaeobatrachidae indet.
Figure 18

Material. Hambach 6C: one maxilla (IPB-HaH 2279).

Description. IPB-HaH 2279 is a fragmentary and robust maxilla, lacking the anterior and posterior portions. The lamina horizontalis is robust and moderately developed in medial direction. On the ventral surface of the lamina, a low longitudinal ridge separates a toothless medial half from the crista dentalis. Teeth were pleurodont, but no one is preserved; they were separated by small processes, which are now eroded. Nine tooth positions are recognizable. In the middle of the dorsal surface of the lamina, a deep and circular recess is visible. By the recess, the lateral wall of the maxilla bends medially. The processus palatinus should be located by this bending, but it is not clearly recognizable in this specimen; this could be either due to a real absence of the processus or, more likely, to preservational reasons. The lateral surface of the bone is smooth.

Remarks. This specimen from Hambach 6C is rather similar to the maxillae of *P. eurydices* in

FIGURE 18. Possible Palaeobatrachidae indet. from Hambach: fragment of maxilla (IPB-HaH 2279) in medial (A), lateral (B), dorsal (C) and ventral (D) views. Scale bar equals 1 mm.

(Villa et al., 2016): overall robustness; presence of the circular recess (recessus vaginiformis for the processus maxillaris anterior, which is the anterior termination of the subocular bar; Roček, 2003: 1941) on the lamina horizontalis; presence of processes separating the teeth (even though it is not possible to say if they were knob-like in origin). On the ventral surface of the lamina horizontalis, the low ridge delimitating medially the toothed area recalls the maxilla RGM 632039, possibly referred to a young *P. eurydices* by Villa et al. (2016). However, the Hambach 6C specimen has more teeth than the latter. IPB-HaH 2279 may thus represent a palaeobatrachid, maybe even related to *P. eurydices,* but in absence of further, better preserved and more taxonomically significant, material from the Miocene level of Hambach, it appears more confident to propose only a cautious identification.

PELOBATIDAE Bonaparte, 1850
EOPELOBATES Parker, 1929
cf. *Eopelobates* sp.
Figure 19A-J

Material. Hambach 11: one sacral vertebra (IPB-HaR 2179); one humerus (IPB-HaR 2154); two ilia (IPB-HaR 2084, IPB-HaR 2103).

Description. IPB-HaR 2179 (Figure 19A-D) is a moderately small sacral vertebra and has an amphicoelous and cylindrical centrum. The neural canal is circular and the dorsal surface of the neural arch is smooth. Both the prezygapophyses and the transverse processes are broken off. The latter are anteroposteriorly extended.

IPB-HaR 2154 (Figure 19E-F) is a poorly preserved humerus provided with a curved diaphysis (though it is broken and misses the proximal portion) and an eminentia capitata that is shifted laterally compared to the main axis of the bone. A deep fossa cubitalis ventralis is present; it opens on the lateral side. There are no cristae medialis and lateralis.

Ilia (Figure 19G-J) lack a dorsal tubercle and a dorsal crest. They have an acetabular fossa provided with a strong anteroventral rim. The dorsal acetabular expansion is rather short. No supraacetabular fossa, preacetabular fossa, interiliac groove, or interiliac tubercle are visible. The spiral groove is not distinct. The posterior end of the bone is slightly eroded in both specimens, but very light striae are visible on their posteromedial surface.

Remarks. Few elements from Hambach 11 are attributed to Pelobatidae because of the following combination of features (Bailon, 1999; Roček, 2013): curved diaphysis of the humerus; laterally-shifted eminentia capitata; deep fossa cubitalis ventralis, which is open laterally; ilia with no dorsal crest and no dorsal tubercle; no preacetabular and supracetabular fossae; striae on the medial side of the ilial body. Within pelobatids, the absence of a deep spiral (or oblique) groove is used to distinguish *Eopelobates* from *Pelobates* Wagler, 1830 (Böhme, 2010; Syromyatnikova, 2019), and thus these fossils are here assigned to the former genus. However, this identification is only considered tentative here, because not all authors deem isolated postcranial elements sufficient for genus level discrimination (Rage and Roček, 2003). Known *Eopelobates* species are all based on articulated material (Roček et al., 2014), making comparison with the disarticulated specimens from Hambach difficult. Furthermore, most of the diagnostic features of the species are on cranial elements. Nevertheless, at least *Eopelobates deani* Roček et al., 2014, and *Eopelobates grandis* Zweifel, 1956, seem to differ from the Hambach ilia in the low dorsal tubercle and the low dorsal crest in the anterior portion of the shaft respectively. The sacral vertebra IPB-HaR 2179 is also tentatively attributed to cf. *Eopelobates* sp. because of the cylindrical centrum and the extended transverse processes, as well as the presence of the spinal foramina. In pelobatids, sacral vertebrae not fused to the urostyle are present in both *Eopelobates* and *Pelobates* (Bailon, 1999; Roček et al., 2014; Syromyatnikova, 2017). However, vertebrae of pelobatids are usually procoelous. Amphicoelous vertebrae, followed by a cartilaginous disk, are known only in *E. grandis* (even though its referral to *Eopelobates* is called into question by some authors also because of this feature; Roček et al., 2014). The holotype and only known specimen of *E. grandis* does not preserve the sacral centrum or the anterior part of the urostyle, and so an amphicoelous condition of the former cannot be evaluated. Amphicoelous sacral centra are shown by *Ascaphus* Stejneger, 1899, and some extinct Mesozoic frogs (Reilly and Jorgensen, 2011), but accounting for the absence of any existing evidence supporting the possible presence of the North American ascaphids in Europe at any moment in time as well as the highly unlikely circumstance of a survival of an early-branching Mesozoic anuran lineage in the Pliocene of the continent, we here consider more probable that IPB-HaR 2179 could represent a pelobatid with either a peculiar vertebral morphology or an anomalous condition due to ontogenetic or pathologic circumstances.

FIGURE 19. Pelobatids from Hambach: sacral vertebra (IPB-HaR 2179) of cf. *Eopelobates* sp. in dorsal (A), anterior (B), posterior (C) and ventral (D) views; left humerus (IPB-HaR 2154) of cf. *Eopelobates* sp. in ventral (E) and dorsal (F) views; left ilium (IPB-HaR 2084) of cf. *Eopelobates* sp. in lateral (G) and medial (H) views; right ilium (IPB-HaR 2103) of cf. *Eopelobates* sp. in lateral (I) and medial (J) views; right humerus (IPB-HaR 2414) of ?*Eopelobates* sp. in ventral (K) and dorsal (L) views; left humerus (IPB-HaR 2415) of ?*Eopelobates* sp. in ventral view (M); right ilium (IPB-HaR 2421) of ?*Eopelobates* sp. in lateral (N) and medial (O) views; trunk vertebra (IPB-HaH 2220) of Pelobatidae indet. in right lateral (P), anterior (Q), dorsal (R) and posterior (S) views; left humerus (IPB-HaH 2399) of Pelobatidae indet. in ventral (T) and dorsal (U) views. Scale bars equal 1 mm. Abbreviations: dae, dorsal acetabular expansion; fcv, fossa cubitalis ventralis.

?*Eopelobates* sp.
Figure 19K-O

Material. Hambach 11C: two humeri (IPB-HaR 2414/2415); one ilium (IPB-HaR 2421).

Description. The two humeri (Figure 19K-M) are represented only by their distal epiphyses. They reach a moderately large size. A spherical eminentia capitata is present, as well as a fossa cubitalis ventralis. The latter is open on the lateral side. Both humeri have a well-developed epicondylus ulnaris and a less developed epicondylus radialis. On the dorsal surface, a wide and elongated olecranon scar is present. Based on the position of the scar, it seems that the eminentia capitata was laterally shifted, but this cannot be confidently evaluated given the absence of the diaphysis.

The ilium (Figure 19N-O) is very poorly preserved, with only the base of the shaft and the anterior portion of the body remaining. It clearly has no dorsal crest and no dorsal tubercle. The acetabular rim is slightly higher in its anteroventral part. There are no supraacetabular and preacetabular fossae and the spiral groove is not distinct. The dorsal acetabular expansion appears rather short, whereas the development of the ventral one cannot be evaluated due to breakage. The medial surface of the ilial body is flat in its preserved portion. The absence of its posterior part hinders an evaluation of the presence or absence of striae.

Remarks. These elements are here tentatively attributed to *Eopelobates* because of the overall morphological similarity with those from Hambach 11 referred to this genus, in particular in the indistinct spiral groove on the ilium. However, poor preservation hinders confidence in the attribution.

Pelobatidae indet.
Figure 19P-U

Material. Hambach 6C: one trunk vertebra (IPB-HaH 2220); one humerus (IPB-HaH 2399).

Discussion. IPB-HaH 2220 (Figure 19P-S) is a moderately large-sized and procoelous trunk vertebra. It has a cylindrical centrum and a long neural arch, with a low carina neuralis and a well-developed posterior point. Transverse processes are broken off, but they were located under the prezygapophyses.

The humerus (Figure 19T-U) is small, but preserves part of the diaphysis and part of the epiphysis. The eminentia capitata is shifted laterally. A shallow fossa cubitalis ventralis, which is open on the lateral side, is present. The epicondyles are missing. The cristae medialis and lateralis are not developed. On the dorsal side, the visible part of the olecranon scar is poorly marked.

Remarks. Following Bailon (1999), these two fossils can be assigned to pelobatids. This attribution is based on: vertebra procoelous, with a long neural arch, transverse processes located ventral to the prezygapophyses, a cylindrical centrum, and a well-developed posterior point; humerus with a laterally-open fossa cubitalis ventralis and maybe also lateral shift of the eminentia capitata. The absence of more taxonomically significant elements in the Miocene level of Hambach, however, hinders a discrimination of either *Eopelobates* or *Pelobates*.

HYLIDAE Rafinesque, 1815
HYLA Laurenti, 1768
Hyla sp.
Figure 20

Material. Hambach 6C: one sacral vertebra (IPB-HaH 2195). Hambach 11: one ilium (IPB-HaR 2088).

Description. The sacral vertebra (Figure 20A-D) is moderately small and has an anterior cotyle and two posterior condyles. The posterior condyles are well separated. The neural canal is elliptical and the dorsal surface of the neural arch does not present a distinct carina neuralis. The prezygapophyses are suboval and slightly tilted dorsally (about 30°). The transverse processes are broken off, but, judging from the preserved portion of the left one, they seem to have been anteroposteriorly extended.

IPB-HaR 2088 (Figure 20E) is a small ilium with a globular and laterally-bending dorsal tubercle. The dorsal crest is absent and the preacetabular zone is strongly expanded anteroventrally. The posterior portion of the ilial body is broken.

Remarks. Following the diagnostic criteria reported by Bailon (1999), these two fossils can be attributed to a tree frog. The combination of features that is diagnostic for the sacral vertebra is: anterior cotyle; two well-differentiated posterior condyles; extended transverse processes; and no carina neuralis. The diagnostic combination for the ilium is, on the other hand: no dorsal crest; expanded preacetabular zone; and globular and laterally-bending dorsal tubercle. A specific identification of European *Hyla* species based on isolated bones is considered impossible by most authors (e.g., Bailon, 1999; Sanchiz, 1981; Sanchiz and Młynarski, 1979a; Sanchiz and Sanz, 1980). Nevertheless, it is possible that at least the ilium coming from the most recent level in Hambach pertains to the *Hyla arborea* (Linnaeus, 1758) species com-

FIGURE 20. *Hyla* sp. from Hambach: sacral vertebra (IPB-HaH 2195) in dorsal (A), ventral (B), anterior (C) and posterior (D) views; left ilium (IPB-HaR 2088) in lateral view (E). Scale bars equal 1 mm. Abbreviations: dt, dorsal tubercle; pz, preacetabular zone.

plex, including the extant European species of the genus (Faivovich et al., 2005; Stöck et al., 2008).

BUFONIDAE Gray, 1825
BUFO Laurenti, 1768
BUFO BUFO (Linnaeus, 1758)
Bufo gr. *bufo*
Figure 21

Material. Hambach 11: one sacral vertebra (IPB-HaR 2020).

Description. IPB-HaR 2020 is a medium-sized sacral vertebra provided with an anterior cotyle and two posterior condyles. The neural canal is subelliptical. A low carina neuralis is present on the dorsal surface of the neural arch, whereas there are no fossettes. Transverse processes are broken and so it is not easy to evaluate their complete anteroposterior extension. Nevertheless, the preserved bases suggest that they were not cylindrical and also not strongly expanded.

Remarks. This sacral vertebra is here attributed to a representative of the common toad species group due to (Bailon, 1999): presence of an anterior cotyle; transverse processes not strongly extended; presence of a carina neuralis; and absence of fossettes on the dorsal surface of the neural arch.

FIGURE 21. *Bufo* gr. *bufo* from Hambach: sacral vertebra (IPB-HaR 2020) in dorsal (A) and ventral (B) views. Scale bar equals 1 mm.

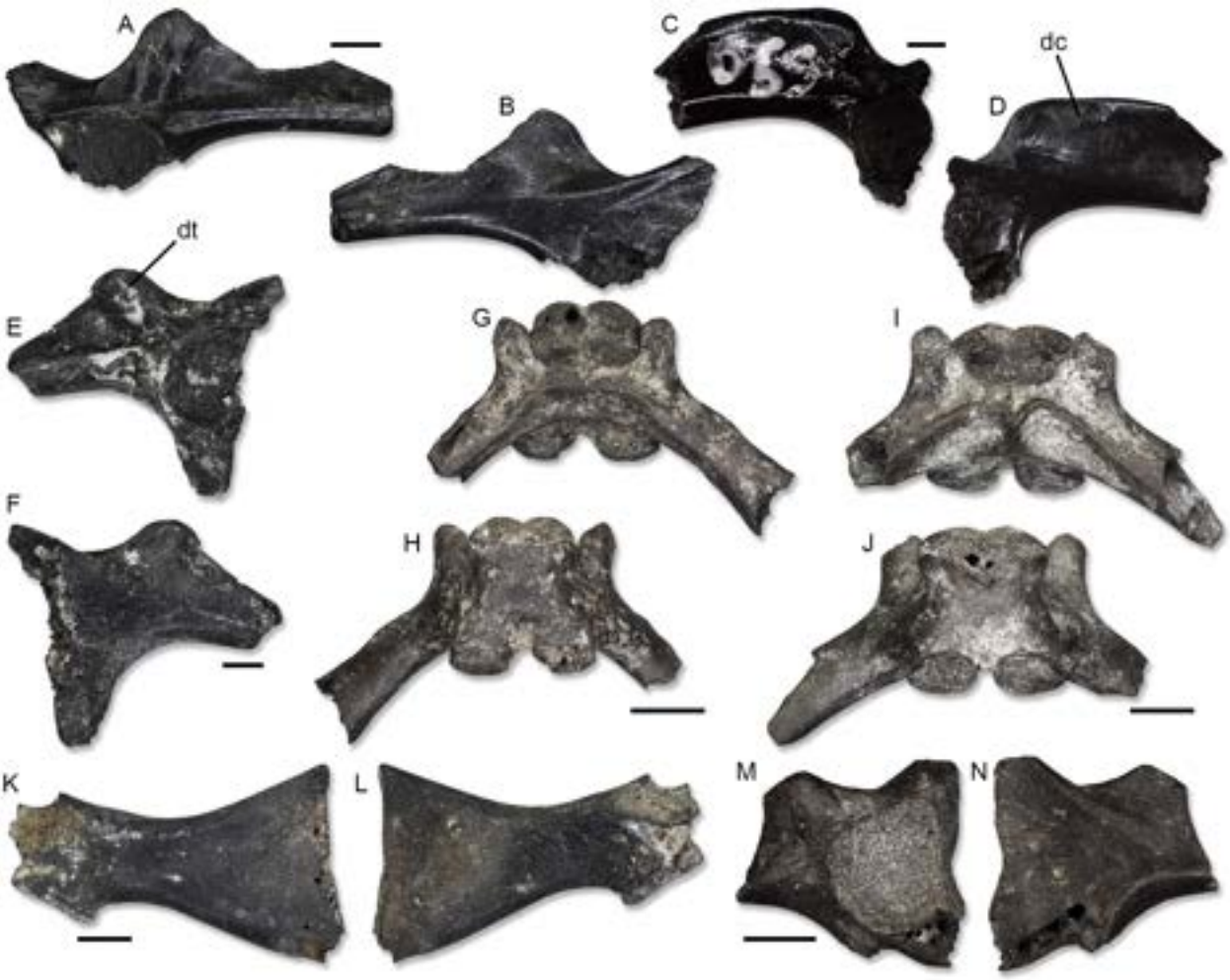

FIGURE 22. Ranids from Hambach: right ilium (IPB-HaH 2307) of *Pelophylax* sp. in lateral (A) and medial (B) views; left ilium (IPB-HaH 2387) of *Pelophylax* sp. in lateral (C) and medial (D) views; left ilium (IPB-HaH 2321) of *Rana* sp. in lateral (E) and medial (F) views; sacral vertebra (IPB-HaR 2018) of Ranidae indet. in dorsal (G) and ventral (H) views; sacral vertebra (IPB-HaR 2019) of Ranidae indet. in dorsal (I) and ventral (J) views; left scapula (IPB-HaH 2323) of Ranidae indet. in ventral (K) and dorsal (L) views; left ilium (IPB-HaR 2087) of Ranidae indet. in lateral (M) and medial (N) views. Scale bars equal 1 mm. Abbreviations: dc, dorsal crest; dt, dorsal tubercle.

RANIDAE Batsch, 1796
PELOPHYLAX Fitzinger, 1843
Pelophylax sp.
Figure 22A-D

Material. Hambach 6C: two ilia (IPB-HaH 2307, IPB-HaH 2387).

Description. These rather large and moderately preserved ilia have a well-developed and almost vertical dorsal tubercle, which is continued anteriorly by a high dorsal crest. The dorsal acetabular expansion is moderately short. The angle comprised between the latter and the tubercle approaches 90°. A shallow supraacetabular fossa is present. The medial surface of the ilial body is flat, without interiliac groove. The shape of the ilioischiatic juncture cannot be clearly described due to preservational reasons.

Remarks. Identification of these ilia as pertaining to green frogs is supported by (Bailon, 1999): high dorsal crest; well-developed dorsal tubercle; and angle comprised between the tubercle and the dorsal acetabular expansion equals 90°. Specific identification of green frogs is possible only with a population-sized amount of ilia (Blain et al., 2015).

RANA Linnaeus, 1758
Rana sp.
Figure 22E-F

Material. Hambach 6C: one ilium (IPB-HaH 2321).

Description. IPB-HaH 2321 is moderately preserved. Laterally, a wide and subcircular acetabu-

lar fossa is visible. Dorsal to it, there is a shallow supraacetabular fossa. The dorsal tubercle is moderately distinct, low, and anteriorly inclined. Its lateral surface is smooth. The dorsal crest is present, but almost completely broken off. Both dorsal and ventral acetabular expansions are preserved and well distinct, with the latter that is more developed than the former. The dorsal acetabular expansion and the dorsal tubercle define an obtuse angle. The flat medial surface has neither an interiliac tubercle nor a groove. The ilioischiatic juncture is high and narrow.

Remarks. The following combination of features allows referral of this ilium to a brown frog (Gleed-Owen, 1998; Bailon, 1999): presence of a dorsal crest; poorly distinct dorsal tubercle; angle between tubercle and dorsal acetabular expansion obtuse; and ilioischiatic juncture high and narrow.

Ranidae indet.
Figure 22G-N

Material. Hambach 6C: nine sacral vertebrae (IPB-HaH 2193/2194, IPB-HaH 2209/2215); one scapula (IPB-HaH 2323). Hambach 11: one trunk vertebra (IPB-HaR 2184); three sacral vertebrae (IPB-HaR 2018/2019; IPB-HaR 2031); one ilium (IPB-HaR 2087).

Description. IPB-HaR 2184 is a small and amphicoelous trunk vertebra, with a short neural arch and laterally directed transverse processes.

Sacral vertebrae (Figure 22G-J) are small and provided with one anterior and two posterior condyles. They have cylindrical transverse processes.

IPB-HaH 2323 (Figure 22K-L) is an elongated scapula. It has no ridges on the anterior margin, but it is provided with a ridge on the inner surface. The cavitas glenoidalis opens in posterior direction and is partially hidden by the pars acromialis in ventral view.

The ilium (Figure 22M-N) is small and poorly preserved, missing completely the shaft. It has a large and subcircular acetabular fossa. Dorsal to the latter, a deep supraacetabular fossa is present. The dorsal tubercle is also present, even though mostly broken away. Nevertheless, it appears moderately distinct. Anteriorly, it is in continuation with a dorsal crest. Both the dorsal and ventral acetabular expansions are broken, but the former appears well developed based on what is preserved. Medially, there is no interiliac groove or tubercle. The ilioischiatic juncture seems rather low and large, but it is not completely preserved.

Remarks. All these specimens present a combination of features supporting attribution to indeterminate ranids according to the criteria presented by Bailon (1999). For the trunk vertebra, this combination includes amphicoely, the short neural arch, and the laterally directed processes; this further suggests that it represents the eighth vertebra in the column (Bailon, 1999). In the sacral vertebra, the diagnostic combination consists of the anterior condyle, the two posterior condyles, and the cylindrical processes. For the scapula, significant are the elongation, the absence of crista anterior, the cavitas glenoidalis hidden in ventral view, as well as the presence of an inner ridge on scapula. The attribution of the ilium is supported by the presence of the dorsal crest and the absence of interiliac tubercles and grooves. The low and large juncture could hint at green frogs for the ilium (Gleed-Owen, 1998), but it is not clear how much this apparent morphology may be influenced by the preservation.

Anura indet.

Material. Hambach 6C: four premaxillae (IPB-HaH 2268/2270, IPB-HaH 2299); 51 fragments of maxilla (IPB-HaH 2233/2265, IPB-HaH 2282/2298, IPB-HaH 2300); 17 trunk vertebrae (IPB-HaH 2089/2097, IPB-HaH 2144/2145, IPB-HaH 2157/2158, IPB-HaH 2181/2183, IPB-HaH 2192); seven sacral vertebrae (IPB-HaH 2087, IPB-HaH 2206/2208, IPB-HaH 2217/2218, IPB-HaH 2225); 12 urostyles (IPB-HaH 2088, IPB-HaH 2197/2198, IPB-HaH 2201/2205, IPB-HaH 2216, IPB-HaH 2226/2227, IPB-HaH 2306); three coracoids (IPB-HaH 2313/2314, IPB-HaH 2378); nine humeri (IPB-HaH 2063, IPB-HaH 2303/2304, IPB-HaH 2311/2312, IPB-HaH 2317/2318, IPB-HaH 2331); five radioulnae (IPB-HaH 2301/2302, IPB-HaH 2309, IPB-HaH 2330, IPB-HaH 2335); two ilia (IPB-HaH 2319/2320); one ischium (IPB-HaH 2322); one femur (IPB-HaH 2326); 14 tibiofibulae (IPB-HaH 2054, IPB-HaH 2062, IPB-HaH 2064/2068, IPB-HaH 2305, IPB-HaH 2310, IPB-HaH 2327, IPB-HaH 2332/2334, IPB-HaH 2400); four indeterminate elements (IPB-HaH 2308, IPB-HaH 2315, IPB-HaH 2328, IPB-HaH 2398). Hambach 11: 29 maxillae (IPB-HaR 2044/2070, IPB-HaR 2177/2178); one angular (IPB-HaR 2114); two atlases (IPB-HaR 2025, IPB-HaR 2035); five trunk vertebrae (IPB-HaR 2024; IPB-HaR 2027/2029; IPB-HaR 2037); two sacral vertebrae (IPB-HaR 2026, IPB-HaR 2036); three urostyles (IPB-HaR 2038/2040); two coracoids (IPB-HaR 2125/2126); two scapulae (IPB-HaR 2072/2073); 10 humeri (IPB-HaR 2089/2095, IPB-HaR 2108/2109, IPB-HaR 2153); 16 radioulnae (IPB-HaR 2074/2079, IPB-HaR 2107, IPB-HaR 2123/2124, IPB-HaR 2128, IPB-HaR 2155/2157, IPB-HaR 2180/2182); four ilia (IPB-HaR 2085/2086, IPB-HaR 2104/2105); one

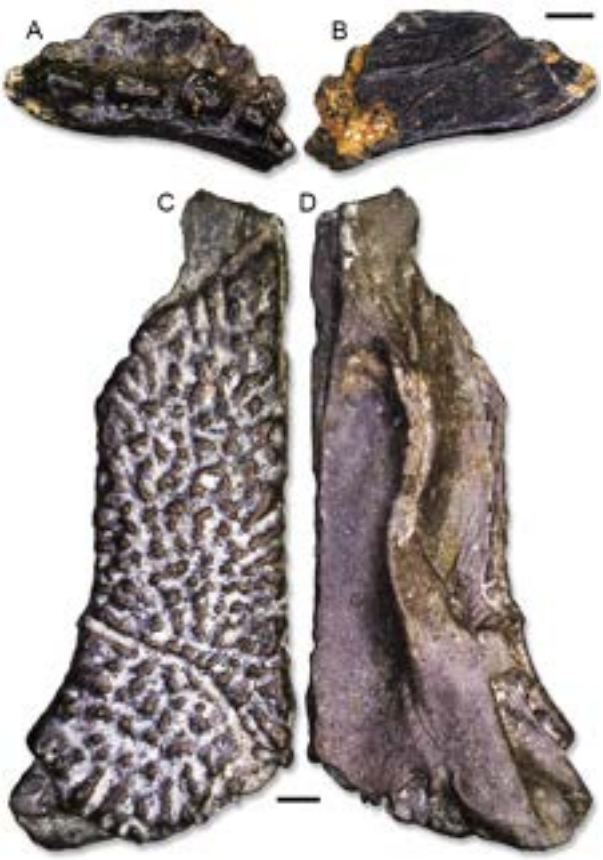

FIGURE 23. Reptiles from Hambach: right squamosal (IPB-HaH 2340) of *Chamaeleo* aff. *andrusovi* in lateral (A) and medial (B) views; left frontal (IPB-HaR 2171) of *Pseudopus* cf. *pannonicus* in dorsal (C) and ventral (D) views. Scale bars equal 1 mm.

ischium (IPB-HaR 2106); three femurs (IPB-HaR 2133/2134, IPB-HaR 2141); 25 tibiofibulae (IPB-HaR 2080/2082, IPB-HaR 2118/2122, IPB-HaR 2135/2140, IPB-HaR 2158/2168); one indeterminate element (IPB-HaR 2169). Hambach 11C: three maxillae (IPB-HaR 2422/2424); one ornamented bone fragment (IPB-HaR 2430); four tibiofibulae (IPB-HaR 2410/2413); one indeterminate element (IPB-HaR 2409).

Remarks. Numerous fossil elements can be assigned to anurans, but are either too poorly preserved or not taxonomically significant enough for a more refined identification.

Reptiles

While studying the amphibian material, we chanced upon a few remains of reptiles that were accidentally not included in Čerňanský et al.'s (2017) work. Most of these are fragments of poorly diagnostic bones, but at least two specimens are worth mentioning and figuring. IPB-HaH 2340 (Figure 23A-B), from Hambach 6C, is probably a fragment of the posterodorsal process of a right jugal. The ornamentation recalls *Chamaeleo andrusovi* Čerňanský, 2010, even though the topotypic jugals of this species show two rows of protuberances instead of just one as in the case of the specimen from Hambach. It is here attributed to *Chamaeleo* aff. *andrusovi*, similar to the squamosal fragment described by Čerňanský et al. (2017) from the same site. IPB-HaR 2171 (Figure 23C-D), from Hambach 11, can be associated to the same taxon as the nasal assigned by Čerňanský et al. (2017) to *Pseudopus* cf. *pannonicus* (Kormos, 1911), because they share a similar dermal sculpturing.

DISCUSSION

The Middle Miocene and Late Pliocene Amphibians from Hambach Compared

Deposition of the two fossiliferous levels in Hambach, stratum 6C (with site Hambach 6C) and stratum 11 (with sites Hambach 11 and 11C), is separated by about a dozen Myr and happened in very different global climatic contexts (the MCO vs a period of climate deterioration preceding the onset of Quaternary glacial cycles). This is clearly reflected in the faunal composition, with a far higher diversity in the Middle Miocene association compared to the Late Pliocene one and the presence of several taxa linked with subtropical conditions in the former (e.g., among amphibians and reptiles: cryptobranchids, *Chelydropsis, Diplocynodon* Pomel, 1847, cobras). Based on our observations and identifications (Table 1), the amphibian component of the Hambach faunas matches with this pattern, all in all. The Middle Miocene fossil assemblage from Hambach 6C includes at least six different urodeles and six anurans. The Hambach 11 and 11C combined assemblage, on the other hand, listed only half the number of urodeles, even though the total of recognized anurans amounts to the same value. The remains attributed to the indeterminate cryptobranchid and to *Chelotriton* stand as evidence of the already-mentioned "tropical" elements present during the Middle Miocene. In agreement with crocodylians (Mörs et al., 2000; Mörs, 2002) and cobras (Čerňanský et al., 2017), but in contrast with what happens with *Chelydropsis* turtles (which possibly persisted in the Upper Pliocene deposits; Mörs, 2002), the two urodeles are absent in younger sites at Hambach, hinting towards a likely extirpation between MN 5 and MN 16a. Other urodeles sharing the same pat-

TABLE 1. Distribution of amphibian taxa identified in the fossiliferous localities within the Hambach mine.

	Middle Miocene	Late Pliocene	
	Hambach 6C	Hambach 11	Hambach 11C
Cryptobranchidae indet.	x		
Palaeoproteus cf. *miocenicus*	x	x	x
?*Palaeoproteus* cf. *miocenicus*	x		
Euronecturus grogu	x		
Mioproteus cf. *wezei*		x	x
Chelotriton sp.	x		
?*Chelotriton* sp.	x		
Lissotriton sp.	x	x	
Triturus sp.	x		
Urodela indet.	x		
Latonia sp.	x	x	x
Palaeobatrachus eurydices		x	x
?Palaeobatrachidae indet.	x		
cf. *Eopelobates* sp.		x	
?*Eopelobates* sp.			x
Pelobatidae indet.	x		
Hyla sp.	x	x	
Bufo gr. *bufo*		x	
Pelophylax sp.	x		
Rana sp.	x		
Ranidae indet.	x	x	
Anura indet.	x	x	x

tern of a Miocene presence and Pliocene absence in Hambach include *Euronecturus grogu* and *Triturus* sp. It is interesting to note that the proteid *E. grogu,* of which Hambach 6C is the only occurrence known worldwide at the moment, seems to be replaced by *Mioproteus*, a member of a different "modern" lineage of Eurasian proteids (Macaluso et al., 2022b). The ranid frogs *Pelophylax* sp. and *Rana* sp. are also recognized in Hambach 6C only, but the presence of ranids in the Upper Pliocene as well is attested by few remains from Hambach 11. At least one of these remains, the ilium IPB-HaR 2087, may even display green frog features, and thus the absence of either one or the two ranids from the younger assemblage may be artifactual.

Nevertheless, there are also amphibians clearly persisting in Hambach in both Middle Miocene and Late Pliocene times. These include at least two urodeles, *Palaeoproteus* cf. *miocenicus* and *Lissotriton* sp., and two anurans, *Latonia* sp. and *Hyla* sp. As mentioned, ranids can also be added to this list, even though detailed identification of the Pliocene remains at specific rank is prevented. Among frogs, palaeobatrachids and pelobatids show the reverse situation, with Late Pliocene remains that can be identified at species *(P. eurydices)* or, possibly, genus (cf. *Eopelobates* sp. and ?*Eopelobates* sp.) ranks respectively, whereas only the general presence of the families can be reported for the Middle Miocene (even in a tentative way in the case of palaeobatrachids). On the opposed side, the toad *Bufo* gr. *bufo* is the only anuran whose presence is certified just for the Late Pliocene in Hambach. Therefore, considering the uncertainty surrounding the possible persistence of some taxa from the Middle Miocene, the composition of the Late Pliocene Hambach 11 and 11C amphibian assemblage is certainly impoverished compared to the older one from Hambach 6C, apparently mainly as far as the urodele component is concerned, but it appears to exhibit an overall similarity and continuity. This differs from other tetrapod groups, which are sporadically represented by the same or related taxa in both Miocene and Pliocene levels (e.g., some petauristid rodents and possibly the already-mentioned *Chelydropsis* turtles; Mörs et al., 2000; Mörs, 2002; Van Laere and Mörs, 2023).

In terms of abundance, the highest numbers of remains identified per taxon in the Miocene assemblage are those referred to *Chelotriton* sp. (57 remains) and *Latonia* sp. (37 remains). These are, therefore, the taxa dominating the oldest Hambach oryctocenosis. *Latonia* persisted as dominant also in the Pliocene with 22 remains (18 from Hambach 11 and six from Hambach 11C), following *P. eurydices* represented by 27 remains (23 and four from Hambach 11 and 11C, respectively). As already mentioned, *Chelotriton* is not present in the Pliocene 11 and 11C sites, in agreement with a general European trend of extinction of this newt. The only Pliocene remains referred to this genus come in fact from the Upper Pliocene of southern France (Bailon, 1989; Macaluso et al., 2022a). The most-represented urodele in the Upper Pliocene of Hambach is *Mioproteus* cf. *wezei*, represented by 15 remains (nine and six, respectively, from Hambach 11 and 11C). Other taxa from both the Miocene and Pliocene assemblages are only represented by very few, less than 10 remains each (except for *Triturus* sp., with 12). Thus, these represent only very minor components of the fossil associations.

Palaeobiogeographical Significance of the Hambach Amphibian Assemblages

The amphibian fossil record from Hambach already proved to host unexpected surprises with the discovery of *Euronecturus grogu*, an enigmatic proteid (see Macaluso et al., 2022b) that is only known from its type locality of Hambach 6C at the moment. The extended study of the whole amphibian record revealed that this is not the only noteworthy taxon preserved in the site, and that significant findings were hidden in both the Miocene and Pliocene assemblages.

Cryptobranchids are in general poorly represented in the fossil record, even though a particular concentration of Neogene cryptobranchid-bearing sites is found in central Europe, and more specifically in Southern Germany (Böhme et al., 2012). Still, they are almost unknown from the European early Middle Miocene, even though their presence in Lower, upper Middle and Upper Miocene sites (Westphal, 1958, 1970; Böttcher, 1987; Miklas, 2002; Böhme, 2003; Kvaček et al., 2004; Tempfer, 2004; Böhme et al., 2012; Vasilyan et al., 2013; Sach, 2016; Georgalis et al., 2019b; Szentesi et al., 2020) suggests their continuous persistence in the continent. As a matter of fact, Hambach 6C is currently the only known occurrence of a cryptobranchid from the early Middle Miocene time frame in Europe, and even adds to a limited Eurasian Langhian record that further includes only few localities in Kazakhstan (Chkhikvadze, 1982; Böhme et al., 2012). Cryptobranchids later declined in Europe during the Pliocene, with their last occurrence at Willershausen, in central Germany (Westphal, 1967; Böhme et al., 2012). The age of Willershausen was reported as Zanclean by Böhme et al. (2012, table 1), but it is now considered as Piacenzian (Kolibáč et al., 2016, and reference therein). Adding to being the only data currently available on European early Middle Miocene cryptobranchids, Hambach 6C represents also the westernmost point ever reached by these urodeles in Eurasia, based on our current knowledge. Only the late Oligocene occurrence at Rott (Westphal, 1958; Mörs, 2002; Böhme et al., 2012), close but located slightly eastward to Hambach, further supports the past existence of cryptobranchid populations west of the Rhine Graben.

One of the most unexpected findings from Hambach is the batrachosauroidid *Palaeoproteus*. Batrachosauroidids are enigmatic urodeles, which are mainly known from the Cretaceous and Palaeogene of North America (Gardner and DeMar, 2013, and reference therein). They persisted in the USA throughout the Miocene, with a handful of occurrences in California (Naylor, 1981), Delaware (Weems and George, 2013), Florida (Estes, 1963; Bryant, 1991), Louisiana (Williams, 2009), and Texas (Taylor and Hesse, 1943; Auffenberg, 1958; Hinderstein and Boyce, 1977; Holman, 1977; Albright, 1994). They are also known from Europe, even though their record on this continent is far poorer. They were possibly present already during the Cretaceous (Duffaud, 1995; Evans and Milner, 1996; Evans and McGowan, 2002), and then are seldomly recovered in the Palaeocene (Estes et al., 1967; Groessens-Van Dyck, 1981), Eocene (Herre, 1935), and Upper Miocene (Vasilyan and Yanenko, 2020). A single record from the Lower Miocene is also reported (Böhme, 2003; Kvaček et al., 2004), but detailed descriptions and identification of these fossils remain unpublished so far. Similar to the cryptobranchids, the Hambach 6C *Palaeoproteus* remains are the only batrachosauroidid fossils currently known from the Middle Miocene in Europe. Adding to this, those coming from Hambach 11 and 11C further stand out as the youngest occurrence of this clade worldwide, as well as the only one postdating the Miocene/Pliocene transition. Moreover, Hambach lists among the northernmost sites reached by these urodeles in post-Palaeogene times, being located even

slightly more northward than Hrytsiv in Ukraine (Vasilyan and Yanenko, 2020) and Ahníkov/Merkur North in Czech Republic (where the presence of these amphibians can be seen as unconfirmed, for the time being; Böhme, 2003; Kvaček et al., 2004). Both the Miocene and Pliocene Hambach material is here referred to the European genus *Palaeoproteus*, and even to a taxon related to the species *P. miocenicus.* Even though a confident identification of the fossils with this Late Miocene species is currently prevented, Hambach is evidence that either one or two morphologically similar forms (depending on whether occurrences from Hambach 6C and Hambach 11 and 11C are conspecific or not) were already present in Europe several Myr before the oldest occurrence reported by Vasilyan and Yanenko (2020) and successively persisted at least up to slightly before the Plio-Pleistocene boundary.

Euronecturus is not the only proteid found in Hambach: *Mioproteus*, a possible representative of a modern European clade including also the extant *Proteus* (Macaluso et al., 2022b), actually replaced it in the youngest level. Several other occurrences of *Mioproteus* are known from Germany throughout the Miocene (Schleich, 1985; Böhme, 2003; Böttcher et al., 2009; Prieto et al., 2009; Abdul Aziz et al., 2010; Sach, 2016; Macaluso et al., 2022a, 2022b), including fossils referred to both *M. caucasicus* and indeterminate species (even though most of these were never properly published). Its absence in Hambach 6C, thus, appears puzzling per se, especially when paired with the presence of *Euronecturus*. Some sort of competitive exclusion cannot be discounted, even though only treated as speculative at the moment due to the very poor information we have about the latter. Later on, *Mioproteus* survived up to the late Early Pleistocene (Młynarski and Szyndlar, 1989; Averianov, 2001; Ivanov, 2007), but all findings postdating the Miocene/Pliocene transition are either unassigned to species (Averianov, 2001; Ratnikov, 2010; Vasilyan et al., 2017) or referred to *M. wezei* (Młynarski et al., 1984; Młynarski and Szyndlar, 1989; Bailon, 1995; Averianov, 2001; Ivanov, 2007; Syromyatnikova et al., 2021, Macaluso et al., 2022a). If our identification is correct, the Upper Pliocene occurrence of *Mioproteus* cf. *wezei* in Hambach would agree with this pattern. Furthermore, this is currently one of the westernmost records of *Mioproteus*, with only *M. wezei* from Balaruc II, in France (Bailon, 1995), located in an even more western position (even though in a far more southern, Mediterranean area).

Among salamandrids, *Chelotriton* is the most represented in Hambach 6C and also very common in Europe, and even in Germany, during the Miocene. Hambach lists among the northernmost Miocene occurrences reached by the genus on the continent, together with the slightly more southern remains from Echzell (Vasilyan et al., 2022). These large salamandrids apparently decreased after the Messinian Salinity Crisis. They are reported from the post-evaporitic succession of Moncucco Torinese in Italy (Colombero et al., 2017), and subsequently the only published occurrence is from the Upper Pliocene of Balaruc II in France (Bailon, 1989). Their absence in Hambach 11 and 11C agrees with this observed pattern of extirpation from northern Europe possibly somewhen in the Late Miocene, and in any case before the Late Pliocene (Macaluso et al., 2022a). *Triturus* newts also are represented in Hambach 6C only in our material, even though, in contrast with *Chelotriton*, their presence as far north as central Germany (Holman, 1998; Böhme, 2000, 2020) and The Netherlands (Villa et al., 2018c) in northwestern Europe is known up to the Quaternary. The genus still persists nowadays in the area of Hambach with the species *T. cristatus* (Sillero et al., 2014; Speybroeck et al., 2016). Few published *Triturus* dated back to MN 5 are also reported in Europe only from southern Germany (Böttcher et al., 2009), but other occurrences from Czech Republic and Germany were mentioned by Böhme (2003) without figures or detailed descriptions. The Hambach specimens add, thus, to the rather poor knowledge of these newts at the Early/Middle Miocene transition. Further significance can be given to the Miocene *Lissotriton* remains from Hambach 6C, given that these stand out among the oldest occurrences of the genus. Older remains were found in two upper Oligocene sites in southern France (Macaluso et al., 2022a) and southern Germany (Böhme 2008), as well as in the Lower Miocene of southern France (two sites; Rage and Hossini, 2000; Rage and Bailon, 2005), western Germany (one site; Vasilyan et al., 2022), and southern Germany (two sites; Böttcher et al., 2009; Böhme, 2010). Macaluso et al. (2022a) further mentioned possible *Lissotriton* identity for lower Eocene vertebrae from France (Augé et al., 1997), but this has yet to be confirmed. Several other localities yielding Early and Middle Miocene *Lissotriton* remains in Germany (possibly going back even to the Oligocene/Miocene transition) were listed by Böhme (2003), but these fossils still await proper publication. On the other hand, the very few vertebrae from Ham-

bach 11 represent the first Pliocene *Lissotriton* remains found in Germany, where otherwise occurrences in the country date to either Miocene or Quaternary. Very few further Late Pliocene remains come from Poland (Sanchiz and Młynarski, 1979b; Młynarski and Szyndlar, 1989) and Spain (Gómez de Soler et al., 2012).

Anurans from Hambach also include very common taxa in Europe during corresponding time frames, as well as unexpected occurrences. The most abundant anuran in Hambach, *Latonia*, is very common all over Europe, including Germany, during most of the Neogene (Roček, 1994b, 2013, and reference therein). It is far less distributed on the continent during the Late Pliocene, when only few occurrences in southern France (Bailon, 1991), central Germany (Böhme, 2000), northern Italy (Vergnaud-Grazzini, 1970), and southern Ukraine (Ratnikov, 2001) are known. In the Pleistocene, relict occurrences of this alytid genus in Europe are only reported from northern Hungary (Szentesi, 2019) and central Italy (Sorbelli et al., 2021). Early Pleistocene *Latonia* remains were also found in Turkey (Vasilyan et al., 2014), but late Quaternary occurrences are limited to Israel (Biton et al., 2016), where the last survivors of these frogs were recently rediscovered (Biton et al., 2013; Perl et al., 2017). After the Miocene/Pliocene boundary, the German site of Kaltensundheim is the only place where *Latonia* was reported (Böhme 2000) that reaches comparable northern latitudes with Hambach. However, Böhme (2002) found no trace of *Latonia* among the fossil material from this Thuringian site and recommended its removal from the taxon list of the assemblage. Thus, Hambach currently stands as the northernmost confirmed occurrence of *Latonia* from the late Neogene onwards.

Palaeobatrachids are almost completely absent from western Europe following the Miocene/Pliocene transition (Wuttke et al., 2012; Roček, 2013; Roček et al., 2021), with the only notable exceptions being Tegelen, in The Netherlands (Villa et al., 2016), and Hambach 11 and 11C. These localities share the same palaeobatrachid species, which is currently not known elsewhere, and are geographically close, even though the Dutch site is younger, being Lower Pleistocene (Gelasian) in age. Other Pliocene and Quaternary occurrences of palaeobatrachids are all located far eastward. The closest one in geographical terms to Tegelen and Hambach, and only other post-Miocene site with palaeobatrachids in Germany, is possibly Voigtstedt, a Chibanian locality in Thuringia, from which *Palaeobatrachus langhae* (Fejérváry, 1917) was reported by Kretzoi (1965) and later mentioned as a tentative occurrence by Holman (1998), Sanchiz (1998), and Böhme (2000). There is no other Miocene occurrence of palaeobatrachids in the northwestern part of continental Europe surrounding Hambach and Tegelen (Wuttke et al., 2012), and the estimated closest relatives to the Plio-Pleistocene species *P. eurydices* are to be found in the Lower Miocene of southern France and central Germany (*Palaeobatrachus robustus* Hossini and Rage, 2000; Hossini and Rage, 2000; Roček, 2013; Villa et al., 2016; Roček et al., 2021; Vasilyan et al., 2022). In this context, the fragmentary maxilla from Hambach 6C testifies that these water-dwelling frogs likely inhabited the area during the early Neogene as well, even though the preservational status prevents both a confident attribution at family rank and even more any inference on the possible persistence of the lineage leading to *P. eurydices.* More Neogene palaeobatrachid fossils from countries such as Belgium, The Netherlands, and (northwestern) Germany are needed to shed light on the early evolution of this possibly relictual lineage.

A situation similar to that of palaeobatrachids arises for pelobatids from Hambach as well. Several pelobatids are reported from the Palaeogene and Neogene of Europe (e.g., Sanchiz, 1998; Roček, 2013; Vergilov and Tzankov, 2021; and reference therein), but only few of them come from the northwestern part of the continent, where Hambach is located. Miocene pelobatids found in the area come from only three localities placed slightly eastward to the latter site: an Aquitanian indeterminate member of the family from Budenheim, near Mainz, mentioned, but neither described nor figured, by Schleich (1988); several Burdigalian remains of *Pelobates sanchizi* Venczel, 2004 from Echzell (Vasilyan et al., 2022); and a Middle Miocene premetamorphic tadpole from Climbach, near Allendorf, attributed to *Eopelobates* sp. (originally referred to *Palaeobatrachus goldfussi* Tschudi, 1838 by von Meyer, 1860, but later reidentified by Špinar, 1972; see Gardner, 2016). The two fossil bones from Hambach 6C are evidence that the range of pelobatids extended further west in this part of Europe in the Middle Miocene, but it is currently impossible to figure out whether or not they were related to either the taxa living in nearby areas in Palaeogene times (e.g., *Eopelobates bayeri* Špinar, 1952 from Belgium, *Eopelobates wagneri* (Weitzel, 1938) from western Germany; Roček, 2013; Roček et al., 2014; Smith et al.,

2018), the Early/Middle Miocene above-mentioned ones from western Germany, or even those from the youngest level in Hambach. If correctly identified, the Late Pliocene *Eopelobates* from Hambach 11 and 11C, on the other hand, shares potentially no relations with other pelobatids identified at genus rank in close-by post-Miocene sites. Known congeneric occurrences postdating the Miocene/Pliocene transition are all located in Eastern Europe (Młynarski 1962; Sanchiz and Młynarski, 1979a; Młynarski and Szyndlar, 1989; Ratnikov, 2001; Venczel, 2001; Roček, 2013; Roček et al., 2014; Vergilov and Tzankov, 2021), even though Rage and Roček (2003), Roček (2013), and Vergilov and Tzankov (2021) recommended caution on these occurrences due to the absence of the most diagnostic cranial elements in the respective material. Nevertheless, only *Pelobates* is recorded in the western part of the continent in the last 5 Myr. Apart from the fossils from Hambach, the other youngest published records of *Eopelobates* in western Europe are Middle Miocene in age (Špinar, 1972; Böhme, 2010; Roček et al., 2014; Gardner, 2016). If our identification is correct, the possible Late Pliocene Hambach *Eopelobates* is, thus, another unexpected late survivor from the site. Available published evidence suggest that *Eopelobates* went extinct before the beginning of the Pleistocene (but see Rage and Roček, 2003, and Vergilov and Tzankov, 2021, for an older extinction date), which agrees with the fact that Quaternary sites in the area close to Hambach only yielded *Pelobates* (Böttcher, 1991; Holman, 1998; Sanchiz, 1998; Schouten, 2016; Villa et al., 2018c).

Taking into account their rather fragile skeleton, tree frogs of the genus *Hyla* are rather common in European sites from the Miocene onwards, especially during the Quaternary. Earliest European representatives of the genus possibly entered the continent in the Early Miocene (Sanchiz and Roček, 1996; Rage and Roček, 2003; Roček, 2013), together with several other amphibians and reptiles (Szyndlar and Schleich, 1993; Ivanov, 2000; Delfino et al., 2003; Rage and Roček, 2003; Rage, 2013; Georgalis et al., 2016; Ivanov et al., 2018; Villa et al., 2018a; Villa and Delfino, 2019; Macaluso et al., 2022a). In this context, tree frogs from Hambach represent one of the oldest occurrences in Germany, together with Oggenhausen 2 in Baden-Württemberg (Böttcher et al., 2009), but also the westernmost location reached in Europe by these frogs during the Neogene based on the current published knowledge (even though, again, bones of tree frogs are very fragile and maybe subject to a strong preservation bias). Hambach is also the first German site yielding Pliocene tree frog remains. Subsequently, tree frogs persisted in the area, as testified at least by the members of the *H. arborea* group found in Tegelen (Villa et al., 2018c). They are widespread throughout northwestern Europe nowadays (Sillero et al., 2014; Speybroeck et al., 2016).

Bufonids and ranids are also inhabitants of modern northwestern Europe, as well as common findings in Neogene and Quaternary fossil assemblages in the continent. Hambach stands out as one of the northernmost known occurrences of the common toad in Pliocene times, together with Kaltensundheim in Germany (Böhme, 2002) and at least Węże 2 in Poland (Młynarski et al., 1984). Both the common toad and the two ranids were found also in the Lower Pleistocene of the nearby Tegelen locality (Villa et al., 2018c).

Palaeoenvironmental Insights and the Role of Northwestern Europe as a Late Neogene Refugial Area for Amphibians

The Hambach palaeofaunas, and especially their amphibian components, appear rather significant for their composition, with representatives of enigmatic and poorly known taxa and unexpected occurrences both in chronological and geographical terms. The palaeoenvironments in which these palaeofaunas lived were certainly humid ones. In addition to sedimentological and palaeobotanical evidence (see Geological setting), these humid conditions are testified by the rather high diversity of amphibians and the presence of other water-related animals (e.g., fish, pond turtles, *Natrix* Laurenti, 1768 snakes, dominant aquatic/semiaquatic forms among the insectivores, beavers; Mörs, 2002; Čerňanský et al., 2017). As far as amphibians are concerned, permanent water bodies are indicated by the occurrences of *Palaeoproteus* (Herre, 1935; Vasilyan and Yanenko, 2020), palaeobatrachids, and, at least in the Pliocene level, *Mioproteus* (a fully aquatic taxon according to Venczel and Codrea, 2018). The extant *Latonia nigriventer* inhabits marshy areas in the Hula Valley, in Israel (Biton et al., 2013, 2016; Perl et al., 2017), and the abundance of *Latonia* in both the Miocene and Pliocene of Hambach hints towards persistent preference for similar swampy environments in past members of the clade as well. Pelobatids are fossorial anurans that suggest the availability of sandy soils in Hambach. Forested areas nearby are supported by the rare tree frogs, as well as *Pliopithecus* Gervais, 1849, and flying

squirrel remains (Mörs, 2002; Van Laere and Mörs, 2023) for the Miocene and Pliocene, respectively.

Humidity in Hambach was particularly high during the Middle Miocene, when cryptobranchids were living in the area. As a matter of fact, these urodeles are tied to high humidity and pluviometry according to Böhme et al. (2012). A certain influx of marine conditions in an estuarine setting is highlighted by the abundant marine fish and rare cetacean remains in Hambach 6C (Mörs, 2002). This changed at the end of the Middle Miocene (Schäfer et al., 2004), long before the deposition of remains found in Hambach 11 and 11C, which only include freshwater fish and is devoid of other marine animals. Fish remains in Hambach also mark another change from slow currents and larger channels in Hambach 6C to more oxygenated waters with higher energy in Hambach 11 and 11C (Mörs, 2002). Moreover, another palaeoenvironmental differences highlighted by the faunal composition in the two Hambach levels lies in the temperature: the Miocene fauna is rich in thermophilic vertebrates, such as giant tortoises, crocodylians, chameleons, "Oriental vipers", and possibly cobras (Mörs, 2002; Čerňanský et al., 2017), whereas these are absent in the Pliocene one. This agrees with the climate reconstruction performed for Hambach 6C based on palaeobotanical data (Utescher et al., 2000, 2002), and makes further sense when considering that the Middle Miocene fauna deposited in a greenhouse interval (the Miocene Climatic Optimum; Steinthorsdottir et al. 2021), whereas the Late Pliocene one in a period of climate deterioration.

The faunal change between Hambach 6C on one side and Hambach 11 and 11C on the other is, thus, evident in several of its components, but it seems to affect the amphibians to a lower extent. Some amphibian taxa indeed disappeared between the Middle Miocene and the Late Pliocene (i.e., cryptobranchids, the *Euronecturus* lineage, *Chelotriton*), but others persisted to even be among the last known representatives of their clades in northern/northwestern Europe (*Latonia*, palaeobatrachids) or worldwide (*Palaeoproteus*). The case of cryptobranchids is particularly interesting because their last reported occurrence in Europe is in Willershausen, an Upper Pliocene locality in Lower Saxony, central Germany. This makes it and Hambach 11 and 11C close or comparable in terms of both geographical position and age, leading to the question on why these urodeles are absent from the Upper Pliocene level in Hambach. The depositional environment in Willershausen was that of a large and deep lake in a sinkhole, surrounded by a hilly mesophytic woodland (Kolibáč et al., 2016, and reference therein). The reconstructed palaeoclimate was cooler than what suggested for the Miocene Hambach, but with similar precipitations (Thiel et al., 2012). Unlike other taxa present in Hambach 6C and absent in Hambach 11 and 11C, then, extirpation of cryptobranchids from there is likely not tied to a decrease in temperature, given their survival in the colder Willershausen. An alternative potential explanation may be the altitudinal distribution model proposed by Böhme et al. (2012): cryptobranchids appear generally limited to higher elevations in drier periods with low basinal relief and colonize lowland environments in hyperhumid moments with high basinal relief. Giant salamanders may have disappeared from the Lower Rhine Embayment in one of such drier periods after the Middle Miocene, whereas the more elevated area near the Willershausen lake (i.e., the Harz Mountains) was able to sustain populations of these amphibians up to at least the late Neogene.

Another locality that is worth comparing with Hambach is Tegelen, in The Netherlands (Table 2). Sediments at Tegelen were also deposited by the Rhine-Meuse river system, even though in a slightly younger, Early Pleistocene, time (van den Hoek Ostende, 2004; van den Hoek Ostende and de Vos, 2006). The Russel-Tiglia-Egypte pit at Tegelen is notable for being the type locality of *P. eurydices,* the palaeobatrachid species found in the Upper Pliocene level at Hambach, and for having yielded a rather diverse assemblage of amphibians and reptiles (Villa et al., 2016, 2018c). Urodeles are much more diverse in Hambach, especially in the Miocene layers. Tegelen only yielded salamandrids (*Triturus* and *Lissotriton*), whereas Hambach has salamandrids, proteids, batrachosauroidids (both Miocene and Pliocene) and cryptobranchids (only Miocene). Among salamandrids, the presence of *Chelotriton* in the Miocene level of Hambach expands the ecomorphological adaptations represented by a member of this clade in this assemblage compared to Tegelen. As already mentioned, *Triturus* is missing in the Pliocene of Hambach, but it is present in the Pleistocene of Tegelen. Given the scarcity of the remains, it is not clear whether the absence of this newt may just be artifactual or not, though. For anurans, significant is the persistence of palaeobatrachids in all levels at Hambach and then in the Russel-Tiglia-Egypte pit at Tegelen, and especially the same species being shared between the Upper

TABLE 2. Comparison between the palaeoherpetofaunas of Hambach and Tegelen. Pliocene sites in Hambach are considered together. Data for Hambach are from: Mörs et al., 2000; Mörs, 2002; Joyce, 2016; Čerňanský et al., 2017; Georgalis and Joyce, 2017; this work. *Mauremys* cf. *sophiae* (reported as *Ocadia* cf. *sophiae* by Mörs, 2002) is here considered as part of *Mauremys* following Hervet (2004). The Tegelen herpetofauna is mainly based on the Russel-Tiglia-Egypte pit assemblage (Villa et al., 2018c), but it also includes the *Emys* occurrences reported by Schreuder (1946) and Villa et al. (2018c). Abbreviation: Croc., Crocodylia.

		Hambach 6C (Middle Miocene)	Hambach 11 & 11C (Upper Pliocene)	Tegelen (Lower Pleistocene)
Urodela	Cryptobranchidae indet.	x		
	Palaeoproteus cf. *miocenicus*	x	x	
	Euronecturus grogu	x		
	Mioproteus cf. *wezei*		x	
	Chelotriton sp.	x		
	Lissotriton sp.	x	x	x
	Triturus gr. *cristatus*			x
	Triturus sp.	x		
Anura	*Latonia* sp.	x	x	
	Palaeobatrachus eurydices		x	x
	?Palaeobatrachidae indet.	x		
	cf. *Eopelobates* sp.		x	
	Pelobates fuscus			x
	Pelobatidae indet.	x		
	Pelodytes sp.			x
	Hyla gr. *arborea*			x
	Hyla sp.	x	x	
	Bufo gr. *bufo*		x	x
	Bombina sp.			x
	Pelophylax sp.	x		x
	Rana sp.	x		x
	Ranidae indet.	x	x	x
Testudines	*Chelydropsis murchisoni*	x		
	Chelydropsis sp.		x	
	Trionychinae indet.	x		
	Emys orbicularis			x
	Emys sp.		x	
	Clemmydopsis sp.	x		
	Mauremys cf. *sophiae*	x		
	Mauremys sp.			x
	Testudo sp. vel *Geochelone* sp.	x		
Croc.	*Diplocynodon* sp.	x		

Pliocene of the former and the Lower Pleistocene of the latter. In general, the overall diversity of frog and toads appears comparable, but there are strong differences in composition of the assemblages. *Latonia* is the most abundant anuran in Hambach, but it is absent in Tegelen. Pelobatids are possibly represented by *Eopelobates* at least in the Pliocene of Hambach, whereas *Pelobates* is identified at Tegelen. On the other hand, the Hambach assemblages lack *Bombina* Oken, 1816, and *Pelodytes* Bonaparte, 1838, taxa otherwise present at Tegelen. *Hyla*, the common toad, and the ranids are shared by both the German and Dutch localities, even though less common in Hambach and

TABLE 2 (continued).

Squamata	*Chamaeleo* aff. *andrusovi*	x			
	Lacerta sp.				x
	Lacertidae indet.	x			x
	Anguis gr. *fragilis*				x
	Pseudopus cf. *ahnikoviensis*	x			
	Pseudopus cf. *pannonicus*			x	
	cf. *Pseudopus* sp.				x
	Eoanilius sp.	x			
	Bavarioboa sp.	x			
	cf. *Falseryx* sp.	x			
	"*Coluber*" sp.	x			
	Texasophis sp.	x			
	Telescopus sp.	x			
	"Colubrinae"/"Colubrines" indet.			x	x
	Natrix natrix				x
	Natrix sp.	x		x	
	cf. *Naja* sp.	x			
	Vipera sp. ("Oriental viper")	x			
	Vipera sp. ("*aspis* complex")	x			
	Vipera sp. (small viper)				x

restricted to specific levels as far as the toad and the ranids are concerned.

When looking at reptiles, crocodylians are absent in both the Pliocene of Hambach and at Tegelen, whereas several cranial and postcranial remains attributed to *Diplocynodon* were recovered in the Miocene level of the former (Mörs et al., 2000; Mörs, 2002). Turtles from Tegelen only include *Emys* Duméril, 1806, and *Mauremys*, moreover never found together in the same pit (Schreuder, 1946; van den Hoek Ostende and de Vos, 2006; Villa et al., 2018c). Hambach displays a higher diversity in the Miocene, with several distinct lineages and both aquatic/semiaquatic and terrestrial animals, but only two taxa in the Pliocene (Mörs, 2002; Klein and Mörs, 2003). *Emys* is shared between the Pliocene of Hambach (even though this occurrence still lacks a detailed publication, with description and figures of the remains, and should be treated with caution) and the Pleistocene of Tegelen, but Hambach misses *Mauremys* and Tegelen misses *Chelydropsis* (again, if its presence in Pliocene Hambach is confirmed). Squamate faunas from Hambach 6C and Tegelen are very different, with the former being far more diverse (especially in the snake component) and including several Palaeogene/Neogene lineages missing in Tegelen (i.e., chameleons, *Eoanilius* Rage, 1974, *Bavarioboa* Szyndlar and Schleich, 1993, cf. *Falseryx* Szyndlar and Rage, 2003, cf. *Naja* Laurenti, 1768, and the "Oriental vipers"; Čerňanský et al., 2017). A small viper is present in both, even though it is not clear if they may represent the same viper group. "Colubrine" snakes and *Natrix* are also shared between Tegelen and both Miocene and Pliocene levels in Hambach. However, Pleistocene and Pliocene "colubrines" remain unidentified at lower taxonomic ranks, whereas the Miocene ones include at least three different taxa ("*Coluber*" Linnaeus, 1758, *Texasophis* Holman, 1977, and *Telescopus* Wagler, 1830). Not a lot can be said about lacertids, except for them being recovered both in the Middle Miocene of Hambach (Čerňanský et al., 2017) and the Pleistocene of Tegelen (Villa et al., 2018c). Diversity seems to be comparable (two taxa), but there seems to be no evidence in Hambach of a possible green lizard as in Tegelen. *Pseudopus* is present in all Hambach levels (Čerňanský et al., 2017; this work) and tentatively even in Tegelen. However, Miocene and Pliocene assemblages in Hambach bear two different *Pseudopus* species, and it is not clear if the Tegelen one may be related to either one of the two.

It seems, thus, that a major change in the reptilian palaeofauna happened already at some point in the Middle Miocene-Late Pliocene interval, with less significant differences between the Upper Pliocene assemblage of Hambach 11 and 11C and the Lower Pleistocene ones of the Tegelen pits (and in particular the Russel-Tiglia-Egypte pit). On the other hand, differences in the batrachofauna are more marked between Hambach 11 and 11C and Tegelen compared to the two levels in Hambach. Whilst the faunal change affecting reptiles agrees with the well-recognized pattern of extirpation of thermophilic taxa from northern Europe characterizing the late Neogene and Quaternary (e.g., Delfino et al., 2007; Rage, 2013; Blain et al., 2016; Villa and Delfino, 2019), amphibians here appear to be less affected by this trend. The differences between Hambach and Tegelen in the amphibian palaeocommunity may be simply explained by different palaeoenvironments (swamp vs floodplain, respectively), but the peculiarity of the batrachofauna in Hambach 11 and 11C (with several taxa otherwise unknown from northwestern Europe in contemporary times) and its similarities with the Hambach 6C one suggest that other factors may be also at play. Reconstructed palaeoclimate at Tegelen based on the herpetofaunistic association recovered from the Russel-Tiglia-Egypte pit (Villa et al., 2018c) indicate a humid subtropical climate, but with MAT and MAP significantly lower than those at Hambach during the Middle Miocene (quantitative climate reconstructions are not available for the Upper Pliocene Hambach sites). A light degree of aridity was also suggested by the same reconstruction. No evidence of a similar dryness is available for the Upper Pliocene level in Hambach. Increased aridization was proposed as a possible cause for the disappearance of some amphibians (i.e., palaeobatrachids; Wuttke et al., 2012) from Western Europe in the late Neogene, but it is evident that areas suitable for these animals persisted at least in the northwestern part of the continent (i.e., in the Lower Rhine Embayment and the Rhine-Meuse delta system) up to the Late Pliocene and, maybe to a lower extent, the Early Pleistocene. High humidity may have allowed the Lower Rhine Embayment to act as a refuge for amphibians during this time, while they were disappearing from other parts of Western Europe. Later, a combination of increasing aridity and potentially the onset of the Quaternary glaciation may have led to the ultimate loss of the refugial conditions and to a faunistic change towards the early Quaternary and subsequent modern batrachofauna of the area. As a matter of fact, various evidence points out to different trends shown by temperatures and precipitations in the Lower Rhine Embayment during the late Neogene, with MATs showing a clear decreasing trend after the early Middle Miocene and MAPs maintaining high values (>1000 mm) well into the Pliocene (Utescher et al., 2000, 2009, 2012; van Dam, 2006; Crampton-Flood et al., 2018). Utescher et al. (2012) further observed that cool events in the Zanclean of northwestern Europe are related to, or start with, wetter conditions, in contrast with the correlation of warmer and wetter periods in the Miocene. This may have favoured the survival of amphibians in this area. In a somehow similar way, a persistent humid climate allowed the Italian Peninsula to act as a preferential refuge for amphibians during the Quaternary glacial cycles, versus the role of reptile refuges that was played by the more arid Balkan and Iberian peninsulae (Macaluso et al., 2021, 2023a). A comparable role may be advocated for the Lower Rhine Embayment as well during the late Neogene and maybe the Early Pleistocene.

CONCLUSIONS

The amphibians identified in the Hambach mine include at least 12 taxa (Cryptobranchidae indet., *Palaeoproteus* cf. *miocenicus, Euronecturus grogu, Chelotriton* sp., *Lissotriton* sp., *Triturus* sp., *Latonia* sp., ?Palaeobatrachidae indet., Pelobatidae indet., *Hyla* sp., *Pelophylax* sp., and *Rana* sp.) from the Middle Miocene Hambach 6C and nine taxa (*Palaeoproteus* cf. *miocenicus*, *Mioproteus* cf. *wezei*, *Lissotriton* sp., *Latonia* sp., *Palaeobatrachus eurydices*, cf. *Eopelobates* sp., *Hyla* sp., *Bufo* gr. *bufo*, and Ranidae indet.) from the Upper Pliocene of Hambach 11 and 11C. Our study revealed the presence of several unexpected or otherwise significant occurrences in these sites, such as:

- The westernmost occurrence ever reached by cryptobranchid salamanders;
- The worldwide youngest occurrence of batrachosauroidid urodeles currently known;
- The second westernmost occurrence of *Mioproteus*;
- The northernmost occurrence of *Latonia* frogs in the late Neogene;
- An additional occurrence of the palaeobatrachid *P. eurydices,* otherwise only known from its type locality in The Netherlands;
- A potential late Neogene survival of the pelobatid *Eopelobates*;

- One of the oldest occurrences of *Hyla* tree frogs, which is also their westernmost Neogene report to date.

This adds to Hambach further being the type locality of the enigmatic proteid *E. grogu,* recently described by Macaluso et al. (2022b). *Latonia* persisted as a dominant component of the batrachofauna from Hambach both in the Miocene and Pliocene, together with the salamandrid urodele *Chelotriton* in the former and *P. eurydices* in the latter.

Our study supports the highly-humid climate suggested by previous authors for both the Middle Miocene and Upper Pliocene levels in the Hambach mine, as well as the presence of permanent water bodies, sandy soils, marshy environments, and forested areas in the nearby. The presence of cryptobranchids in Hambach 6C highlights that the early Middle Miocene was particularly humid, a fact that agrees with the site correlating with the Miocene Climatic Optimum. The high level of persistent humidity in Hambach throughout the Neogene possibly allowed the survival of several amphibian taxa in the area, while thermophilic reptiles were being extirpated by the decreasing temperatures. This hints towards a refugial role played by the area of the Lower Rhine Embayment, and more generally the Rhine-Meuse river system in northwestern Europe, for amphibians during the late Neogene. Comparisons with the younger Dutch locality of Tegelen reveal that this role may have been lowered by the beginning of the Pleistocene, and ultimately lost possibly due to the onset of the Quaternary glaciations. New investigations in other Neogene and Quaternary sites in northwestern European countries, especially focused on amphibians and reptiles, are anticipated in order to further explore this possibility and its implications for the evolution of the modern European fauna.

ACKNOWLEDGEMENTS

We gratefully acknowledge the continuous support of the mining company RWE POWER AG (Cologne) during fieldwork in the Hambach mine. Special thanks go to former employees F. von der Hocht (Kerpen) and B. Wutzler (Bornheim), who generously donated Hambach specimens for this investigation. We thank M.D. Scherz (Copenhagen), G. Carnevale, and M. Delfino (both Turin) for discussions on identifications, K.A. Vega-Pagán and À.H. Luján (both Barcelona) for taxonomic discussions, M. Calvo (Madrid) and O. Rauhut (Munich) for collection access and loan of comparative material, as well as J. Fortuny (Barcelona), R. Rozzi (Halle), and D. Vasilyan (Porrentruy) for providing literature. We thank the staff of Palaeontologia Electronica for their editorial work, as well as two reviewers, G.L. Georgalis (Kraków) and an anonymous one, for their comments on a previous version of this paper. We further acknowledge the staff and contributors of MorphoSource, for their effort in making digitally available specimens to other scholars around the world. L.M. received support from the SYNTHESYS Project (FR-TAF 2486 and HU-TAF 2724) and is funded by the Alexander von Humboldt Foundation through a Humboldt Research Fellowship. A.V. was funded by a Humboldt Research Fellowship from the Alexander von Humboldt Foundation and by the Agencia Estatal de Investigación through a Juan de la Cierva-Formación grant (FCI2019-039443-I/AEI/10.13039/501100011033) during part of the development of this work. He is now supported by the Secretaria d'Universitats i Recerca of the Departament de Recerca i Universitats, Generalitat de Catalunya, through a Beatriu de Pinós postdoctoral grant (2021 BP 00038). This paper is part of R+D+I project PID2020-117289GB-100, funded by the Agencia Estatal de Investigación of the Spanish Ministerio de Ciencia e Innovación (MCIN/AEI/10.13039/501100011033/). A.V. further acknowledges support by the CERCA Programme/Generalitat de Catalunya and the Agència de Gestió d'Ajuts Universitaris i de Recerca of the Generalitat de Catalunya (2021 SGR 00620). T.M. was funded by the Deutsche Forschungsgemeinschaft (DFG) Special Research Project SFB 350.

REFERENCES

Abdul Aziz, H., Böhme, M., Rocholl, A., Prieto, J., Wijbrans, J.R., Bachtadse, V., and Ulbig, A. 2010. Integrated stratigraphy and $^{40}Ar/^{39}Ar$ chronology of the early to middle Miocene Upper Freshwater Molasse in western Bavaria (Germany). International Journal of Earth Sciences, 99:1859–1886. https://doi.org/10.1007/s00531-009-0475-8

Albright, L.B. 1994. Lower vertebrates from an Arikareean (earliest Miocene) fauna near the Toledo Bend Dam, Newton County, Texas. Journal of Paleontology, 68:1131–1145. https://doi.org/10.1017/S002233600002672X

Auffenberg, W. 1958. A new family of Miocene salamanders from the Texas coastal plain. Quarterly Journal of the Florida Academy of Sciences, 21:169–176.

Augé, M., Duffaud, S., Lapparent De Broin, F., Rage, J.-C., and Vasse, D. 1997. Les amphibiens et les reptiles de Prémontré (Cuisien, Bassin parisien): une herpétofaune de référence pour l'Eocène inférieur. Géologie de la France, 1:23–33.

Averianov, A.O. 2001. New records of proteid salamanders (Amphibia, Caudata) from the Pliocene of Ukraine and lower Pleistocene of Moldavia. Vestnik Zoologii, 35:43–46.

Bailon, S. 1989. Les amphibiens et les reptiles du Pliocene Superieur de Balaruc II (Herault, France). Palaeovertebrata, 19:7–28.

Bailon, S. 1991. Amphibiens et reptiles du Pliocène et du Quaternaire de France et d'Espagne: mise en place et evolution des faunes. Unpublished PhD Thesis, Université Paris VII, Paris, France.

Bailon, S. 1995. Présence de *Mioproteus wezei (*Amphibia, Proteidae) dans le Pliocène supérieur (MN 16) d'Europe de l'Ouest. Neues Jahrbuch für Geologie und Paläontologie, Monatshefte, 1995:1–8. https://doi.org/10.1127/njgpm/1995/1995/1

Bailon, S. 1999. Différenciation ostéologique des anoures (Amphibia, Anura) de France, p. 1–41. In Desse, J. and Desse-Berset, N. (eds.), Fiches d'ostéologie animale pour l'Archéologie, Série C: Varia, 1. APDCA, Antibes.

Batsch, A.J.G.K. 1796. Umriß der gesammten Naturgeschichte: ein Auszug aus den frühern Handbüchern des Verfassers für seine Vorlesungen. Christian Ernst Gabler, Jena and Leipzig.

Bell, T. 1839. A History of British Reptiles. John van Voorst, London.

Biton, R., Geffen, E., Vences, M., Cohen, O., Bailon, S., Rabinovich, R., Malka, Y., Oron, T., Boistel, R., Brumfeld, V., and Gafny, S. 2013. The rediscovered Hula painted frog is a living fossil. Nature Communications, 4:1959. https://doi.org/10.1038/ncomms2959

Biton, R., Boistel, R., Rabinovich, R., Gafny, S., Brumfeld, V., and Bailon, S. 2016. Osteological observations on the alytid Anura *Latonia nigriventer* with comments on functional morphology, biogeography, and evolutionary history. Journal of Morphology, 277:1131–1145. https://doi.org/10.1002/jmor.20562

Blain, H.-A., Lózano-Fernández, I., and Böhme, G. 2015. Variation in the ilium of central European water frogs *Pelophylax* (Amphibia, Ranidae) and its implications for species-level identification of fragmentary anuran fossils. Zoological Studies, 54:5. https://doi.org/10.1186/s40555-014-0094-3

Blain, H.-A., Bailon, S., and Agustí, J. 2016. The geographical and chronological pattern of herpetofaunal Pleistocene extinctions on the Iberian Peninsula. Comptes Rendus Palevol, 15:731–744. https://doi.org/10.1016/j.crpv.2015.05.008

Blondel, J., Aronson, J., Bodiou, J.Y., and Boeuf, G. 2010. The Mediterranean region: biological diversity in space and time. Oxford University Press, Oxford.

Boenigk, W. 2002. The Pleistocene drainage pattern in the Lower Rhine Basin. Netherlands Journal of Geosciences – Geologie en Mijnbouw, 81:201–209. https://doi.org/10.1017/S0016774600022447

Böhme, G. 2000. Fossile Amphibien und Reptilien im Quartär Thüringens. Veröffentlichungen Naturkundemuseum Erfurt, 19/2000:79–97.

Böhme, G. 2002. Amphibienreste aus dem Oberpliozän von Kaltensundheim (Rhön, Thüringen). Mitteilungen des Museum für Naturkunde, Berlin, Geowissenschaftliche Reihe, 5:231–238.
Böhme, M. 2003. Miocene Climatic Optimum: evidence from lower vertebrates of central Europe. Palaeogeography, Palaeoclimatology, Palaeoecology, 195:389–401. https://doi.org/10.1016/S0031-0182(03)00367-5
Böhme, M. 2008. Ectothermic vertebrates (Teleostei, Allocaudata, Urodela, Anura, Testudines, Choristodera, Crocodylia, Squamata) from the Upper Oligocene of Oberleichtersbach (Northern Bavaria, Germany). Courier Forschungsinstitut Senckenberg, 260:161–183.
Böhme, M. 2010. Ectothermic vertebrates (Actinopterygii, Allocaudata, Urodela, Anura, Crocodylia, Squamata) from the Miocene of Sandelzhausen (Germany, Bavaria) and their implications for environment reconstruction and palaeoclimate. Paläontologische Zeitschrift, 84:3–41. https://doi.org/10.1007/s12542-010-0050-4
Böhme, M. 2020. New results on amphibians and reptiles from the Early Pleistocene site of Untermassfeld - bioclimatic analysis of the herpetofauna. Monographien des RGZM, 40:1141–1158
Böhme, M., Vasilyan, D., and Winklhofer, M. 2012. Habitat tracking, range dynamics and palaeoclimatic significance of Eurasian giant salamanders (Cryptobranchidae) – indications for elevated Central Asian humidity during Cenozoic global warm periods. Palaeogeography, Palaeoclimatology, Palaeoecology, 342-343:64–72. https://doi.org/10.1016/j.palaeo.2012.04.032
Bonaparte, C.L.J.L. 1831. Saggio d'una distribuzione metodica degli animali vertebrati. Giornale Arcadico di Scienze Lettere ed Arti. Roma, 49:1-86.
Bonaparte, C.L.J.L. 1838. Iconographia della fauna italica per le quattro classi degli animali vertebrati. Tomo II. Amphibi. Fascicolo 23. Salviucci, Roma.
Bonaparte, C.L.J.L. 1850. Conspectus Systematum. Herpetologiae et Amphibiologiae. Editio altera reformata. E.J. Brill, Leiden.
Böttcher, R. 1987. Neue Funde von *Andrias scheuchzeri* (Cryptobranchidae, Amphibia) aus der süddeutschen Molasse. Stuttgarter Beiträge zur Naturkunde B, 131:1–38.
Böttcher, R. 1991. Vertebraten. Stuttgarter Beiträge zur Naturkunde Serie B (Geologie und Paläontologie), 170:25–56.
Böttcher, R., Heizmann, E.P.J., Rasser, M.W., and Ziegler, R. 2009. Biostratigraphy and palaeoecology of a Middle Miocene (Karpathian, MN 5) fauna from the northern margin of the North Alpine Foreland Basin (Oggenhausen 2, SW' Germany). Neues Jahrbuch für Geologie und Paläontologie, 254:237–260. https://doi.org/10.1127/0077-7749/2009/0011
Bryant, D.J. 1991. New early Barstovian (middle Miocene) vertebrates from the upper Torreya Formation, eastern Florida panhandle. Journal of Vertebrate Paleontology, 11:472–489. https://doi.org/10.1080/02724634.1991.10011416
Čerňanský, A. 2010. A revision of chamaeleonids from the Lower Miocene of the Czech Republic with description of a new species of *Chamaeleo* (Squamata, Chamaeleonidae). Geobios, 43:605–613. https://doi.org/10.1016/j.geobios.2010.04.001
Čerňanský, A., Szyndlar, Z., and Mörs, T. 2017. Fossil squamate faunas from the Neogene of Hambach (northwestern Germany). Palaeobiodiversity and Palaeoenvironments, 97:329–354. https://doi.org/10.1007/s12549-016-0252-1
Chkhikvadze, V.M. 1982. On the findings of fossil Cryptobranchidae in the USSR and Mongolia. Vertebrata Hungarica, 21:63–67.
Colombero, S., Alba, D.M., D'Amico, C., Delfino, M., Esu, D., Giuntelli, P., Harzhauser, M., Mazza, P.P.A., Mosca, M., Neubauer, T.A., Pavia, G., Pavia, M., Villa, A., and Carnevale, G. 2017. Late Messinian mollusks and vertebrates from Moncucco Torinese, north-western Italy. Paleoecological and paleoclimatological implications. Palaeontologia Electronica, 20.1.10A:1–66. https://doi.org/10.26879/658
Cope, E.D. 1865. Sketch of the primary groups of Batrachia Salientia. Natural History Review, 5:97–120.

Crampton-Flood, E.D., Peterse, F., Munsterman, D., and Sinninghe Damsté, J.D. 2018. Using tetraether lipids archived in North Sea Basin sediments to extract North Western European Pliocene continental air temperatures. Earth and Planetary Science Letters, 490:193–205. https://doi.org/10.1016/j.epsl.2018.03.030

Dalsätt, J., Mörs, T., and Ericson, P.G.P. 2006. Fossil birds from the Miocene and Pliocene of Hambach (NW Germany). Palaeontographica A, 277: 113–121. https://doi.org/10.1127/pala/277/2006/113

Delfino, M. and Sala, B. 2007. Late Pliocene Albanerpetontidae (Lissamphibia) from Italy. Journal of Vertebrate Paleontology, 27:716–719. https://doi.org/10.1671/0272-4634(2007)27[716:LPALFI]2.0.CO;2

Delfino, M., Rage, J.-C., and Rook, L. 2003. Tertiary mammal turnover phenomena: What happened to the herpetofauna? Deinsea, 10:153–161.

Delfino, M., Böhme, M., and Rook, L. 2007. First European evidence for transcontinental dispersal of *Crocodylus* (late Neogene of southern Italy). Zoological Journal of the Linnean Society, 149:293–307. https://doi.org/10.1111/j.1096-3642.2007.00248.x

Duffaud, S. 1995. A Batrachosauroididae (Amphibia, Caudata) from the late Cretaceous of Champ-Garimond (Southern France). DGF Online Series, available at https://www.2dgf.dk/dgf-online-series

Duméril, A.M.C. 1806. Zoologie Analytique, ou Méthode Naturelle de Classification des Animaux, Rendue plus Facile à l'Aide de Tableaux Synoptiques. Allais, Paris. https://doi.org/10.5962/bhl.title.44835

Estes, R. 1963. Early Miocene salamanders and lizards from Florida. Quarterly Journal of the Florida Academy of Sciences, 26:234–256.

Estes, R. 1981. Handbuch der Paläoherpetologie 2. Gymnophiona, Caudata. Gustav Fischer Verlag, Stuttgart.

Estes, R. and Darevsky, I. 1977. Fossil amphibians from the Miocene of the North Caucasus, U.S.S.R. Journal of the Palaeontological Society of India, 20:164–169.

Estes, R., Hecht, M., and Hoffstetter, R. 1967. Paleocene amphibians from Cernay, France. American Museum Novitates, 2295:1–25.

Evans, S.E. and McGowan, G.J. 2002. Lissamphibian remains from the Purbeck Limestone Group, Southern England. Special Papers in Palaeontology, 68:103–119.

Evans, S.E. and Milner, A.R. 1996. A metamorphosed salamander from the early Cretaceous of Las Hoyas, Spain. Philosophical Transactions of The Royal Society B Biological Sciences, 351:627–646.

Faivovich, J., Haddad, C.F.B., Garcia, P.C.A., Frost, D.R., Campbell, J.A., and Wheeler, W.C. 2005. Systematic review of the frog family Hylidae, with special reference to Hylinae: phylogenetic analysis and taxonomic revision. Bulletin of the American Museum of Natural History, 294:1–240. https://doi.org/10.1206/0003-0090(2005)294[0001:SROTFF]2.0.CO;2

Fejérváry, G. J. 1917. Anoures fossiles des couches préglaciaires de Püspökfürdő en Hongrie. Földtani Közlöny, 47:141–199.

Fischer, G. 1813. Zoognosia. Tabulis Synopticis Illustrata, in Usum Prælectionum Academiæ Imperialis Medico-Chirurgicæ Mosquensis Edita. Editio tertia, volumen primum. Nicolai Sergeidis Vsevolozsky, Moscow. https://doi.org/10.5962/bhl.title.42225

Fitzinger, L.J.F.J. 1826. Neue Classification der Reptilien nach ihren natürlichen Verwandtschaften nebst einer Verwandschafts-Tafel und einem Verzeichnisse der Reptilien-Sammlung des K. K. Zoologischen Museums zu Wien. J.G. Heubner, Wien.

Fitzinger, L.J.F.J. 1843. Systema Reptilium. Fasciculus Primus. Braumüller et Seidel, Wien.

Friant, M. 1944. Caractères anatomiques d'un batracien oligocène de la Limagne, le *Prodiscoglossus vertaizoni* nov. gen. nov. spec. Comptes rendus hebdomadaires des séances de l'Académie des sciences, 219:561–562.

Gardner, J.D. 2016. The fossil record of tadpoles. Fossil Imprint, 72:17–44. https://doi.org/10.14446/FI.2016.17

Gardner, J.D. and DeMar, D.G., Jr. 2013. Mesozoic and Palaeocene lissamphibian assemblages of North America: a comprehensive review. Palaeobiodiversity and Palaeoenvironments, 93:459–515. https://doi.org/10.1007/s12549-013-0130-z

Georgalis, G.L. and Joyce, W.G. 2017. A review of the fossil record of Old World turtles of the clade Pan-Trionychidae. Bulletin of the Peabody Museum of Natural History, 58:115–208. https://doi.org/10.3374/014.058.0106

Georgalis, G.L., Villa, A., and Delfino, M. 2016. First description of a fossil chamaeleonid from Greece and its relevance for the European biogeographic history of the group. The Science of Nature, 103:12. https://doi.org/10.1007/s00114-016-1336-5

Georgalis, G.L., Villa, A., and Delfino, M. 2017. The last European varanid: demise and extinction of monitor lizards (Squamata, Varanidae) from Europe. Journal of Vertebrate Paleontology, 37:e1301946. https://doi.org/10.1080/02724634.2017.1301946

Georgalis, G.L., Villa, A., Ivanov, M., Roussiakis, S., Skandalos, P., and Delfino, M. 2019a. Early Miocene herpetofaunas from the Greek localities of Aliveri and Karydia – bridging a gap in the knowledge of amphibians and reptiles from the early Neogene of southeastern Europe. Historical Biology, 31:1045–1064. https://doi.org/10.1080/08912963.2017.1417404

Georgalis, G.L., Villa, A., Ivanov, M., Vasilyan, D., and Delfino, M. 2019b. Fossil amphibians and reptiles from the Neogene locality of Maramena (Greece), the most diverse European herpetofauna at the Miocene/Pliocene transition boundary. Palaeontologia Electronica, 22.3.68:1–99. https://doi.org/10.26879/908

Gervais, P. 1849. Note sur une nouvelle espèce de singe fossile. Comptes Rendus hebdomadaires des seances de l'Academie des sciences, 28:699–700.

Gleed-Owen, C.P. 1998. Quaternary herpetofaunas of the British Isles: taxonomic descriptions, palaeoenvironmental reconstructions, and biostratigraphic implications. Unpublished PhD Thesis, Coventry University, Coventry, UK.

Goldfuss, G.A. 1820. Handbuch der Zoologie. J. L. Schrag, Nürnberg.

Gómez, R.O. and Turazzini, G.F. 2016. An overview of the ilium of anurans (Lissamphibia, Salientia), with a critical appraisal of the terminology and primary homology of main ilial features. Journal of Vertebrate Paleontology, 36:e1030023. https://doi.org/10.1080/02724634.2015.1030023

Gómez de Soler, B., Campeny Vall-Llosera, G., Van der Made, J., Oms, O., Agustí, J., Sala, R., Blain, H.A., Burjachs, F., Claude, J., García Catalán, S., Riba, D., and Rosillo, R. 2012. A new key locality for the Pliocene vertebrate record of Europe: the Camp dels Ninots maar (NE Spain). Geologica Acta, 10:1–17. https://doi.org/10.1344/105.000001702

Gray, J.E. 1825. A synopsis of the genera of reptiles and Amphibia, with a description of some new species. Annals of Philosophy, 10:193–217.

Gray, J.E. 1869. Description of *Mauremys laniaria*, a new freshwater tortoise. Proceedings of the Zoological Society of London, 37:499–500.

Groessens-Van Dyck, M.C. 1981. Etude des amphibiens du Montien continental de Hainin. Bulletin de la Societe Belge de Geologie/Bulletin van de Belgische Vereniging voor Geologie, 90:87–100.

Herre, W. 1935. Die Schwanzlurche der mitteleocänen (oberlutetischen) Braunkohle des Geiseltales und die Phylogenie der Urodelen unter Einschluß der fossilen Formen. Zoologica - Original-Abhandlungen aus dem Gesamtgebiete der Zoologie, 87:1–85.

Hervet, S. 2004. Systématique du groupe «*Palaeochelys* sensu lato – *Mauremys*» (Chelonii, Testudinoidea) du Tertiaire d'Europe occidentale: principaux résultats. Annales de Paléontologie, 90:13–78. https://doi.org/10.1016/j.annpal.2003.12.002

Heumann, G. and Litt, T. 2002. Stratigraphy and paleoecology of the Late Pliocene and Early Pleistocene in the open-cast mine Hambach (Lower Rhine Basin). Netherlands Journal of Geosciences – Geologie en Mijnbouw, 81:193–199. https://doi.org/10.1017/S0016774600022435

Hierholzer, E. and Mörs, T. 2003. Cypriniden-Schlundzähne (Osteichthyes: Teleostei) aus dem Tertiär von Hambach (Niederrheinische Bucht, NW-Deutschland). Palaeontographica A, 269:1–38. https://doi.org/10.1127/pala/269/2003/1

Hinderstein, B. and Boyce, J. 1977. The Miocene salamander *Batrachosauroides dissimulans* (Amphibia, Urodela) from East Texas. Journal of Herpetology, 11:369–372.
Holman, J.A. 1977. Amphibians and reptiles from the Gulf Coast Miocene of Texas. Herpetologica, 33:391–403.
Holman, J.A. 1998. Pleistocene amphibians and reptiles in Britain and Europe. Oxford monographs on geology and geophysics, 38:1–254.
Hossini, S. 1993. A new species of *Latonia* (Anura, Discoglossidae) from the lower Miocene of France. Amphibia-Reptilia, 14:237–245. https://doi.org/10.1163/156853893X00435
Hossini, S. and Rage, J.-C. 2000. Palaeobatrachid frogs from the earliest Miocene (Agenian) of France, with description of a new species. Geobios, 33:223–231. https://doi.org/10.1016/S0016-6995(00)80019-4
Ivanov, M. 2000. Snakes of the lower/middle Miocene transition at Vieux Collonges (Rhône, France), with comments on the colonisation of western Europe by colubroids. Geodiversitas, 22:559–588.
Ivanov, M. 2007. Herpetological assemblages from the Pliocene to middle Pleistocene in Central Europe: palaeoecological significance. Geodiversitas, 29:297–320.
Ivanov, M., Ruta, M., Klembara, J., and Böhme, M. 2018. A new species of *Varanus* (Anguimorpha: Varanidae) from the early Miocene of the Czech Republic, and its relationships and palaeoecology. Journal of Systematic Palaeontology, 16:767–797. https://doi.org/10.1080/14772019.2017.1355338
Joyce, W.G. 2016. A review of the fossil record of turtles of the clade Pan-Chelydridae. Bulletin of the Peabody Museum of Natural History, 57:21–56. https://doi.org/10.3374/014.057.0103
Joyce, W.G., Klein, N., and Mörs, T. 2004. Carettochelyine turtle from the Neogene of Europe. Copeia, 2004: 406–411. https://doi.org/10.1643/CH-03-172R
Kemna, H.A. 2005. Pliocene and lower Pleistocene stratigraphy in the lower Rhine Embayment, Germany. Kölner Forum für Geologie und Paläontologie 15:1–121.
Kiritzescu, C. 1903. Contributions à la faune des batraciens de Roumanie. Buletinul Societatii de Sciinte din Bucuresci, România, 12:243–265.
Klein, N. and Mörs, T. 2003. Die Schildkröten (Reptilia: Testudines) aus dem Mittel-Miozän von Hambach (Niederrheinische Bucht, NW-Deutschland). Palaeontographica A, 268:1–48. https://doi.org/10.1127/pala/268/2003/1
Kolibáč, J., Adroit, B., Gröning, E., Brauckmann, C., and Wappler, T. 2016. First record of the family Trogossitidae (Insecta, Coleoptera) in the Late Pliocene deposits of Willershausen (Germany). PalZ, 90:681–689. https://doi.org/10.1007/s12542-016-0316-6
Kormos, T. 1911. A Polgárdi pliocén csontlelet. Földtani Közlöny, 41:48–64.
Kretzoi, M. 1965. Die Amphibien aus der altpleistozänen Fundstelle Voigtstedt in Thüringen. Paläontologische Abhandlungen Abteilung A, 2:325–333.
Kvaček, Z., Böhme, M., Dvořák, Z., Konzalová, M., Mach, K., Prokop, J., and Rajchl, M. 2004. Early Miocene freshwater and swamp ecosystems of the Most Basin (northern Bohemia) with particular reference to the Bilina Mine section. Journal of the Czech Geological Society, 49:1–40.
Lacombat, F. and Mörs, T. 2008. The northernmost occurrence of the rare Late Pliocene rhinoceros *Stephanorhinus jeanvireti* (Mammalia, Perissodactyla). Neues Jahrbuch für Geologie und Paläontologie Abhandlungen, 249:157–166. https://doi.org/10.1127/0077-7749/2008/0249-0157
Lartet, E. 1851. Notice sur la Colline de Sansan, suivie d'une récapitulation des diverses espèces d'animaux vertébrés fossil, trouvés soit à Sansan, soit dans d'autres gisements du terrain tertiaire miocène dans le bassin Sous-Pyrenéen. J.A. Portes, Auch.
Latreille, P.A. 1800. Histoire naturelle des Salamandres de France, Précédée d'un Tableau Méthodique des Autres Reptiles Indigènes. Imprimerie de Crapelet, Paris.
Laurenti, J.N. 1768. Austriaci Viennensis specimen medicum, exhibens synopsin reptilium emendatam cum experimentis circa Venena et antidota reptilium Austriacorum quod authoritate et consensu. Joannis Thomae de Trattnern, Caes. Reg. Maj. Aulae Typographi et Bibliopolae, Wien. https://doi.org/10.5962/bhl.title.5108

Linnaeus, C. 1758. Systema naturæ per regna tria naturae, secundum classes, ordines, genera, species cum characteribus, differentiis, synonymis, locis. Tomus 1, Pars 1. Laurentii Salvii, Stockholm.
https://doi.org/10.5962/bhl.title.542

Macaluso, L., Villa, A., Pitruzzella, G., Rook, L., Pogoda, P., Kupfer, A., and Delfino, M. 2020. Osteology of the Italian endemic spectacled salamanders, *Salamandrina* spp. (Amphibia, Urodela, Salamandridae): selected skeletal elements for palaeontological investigations. Journal of Morphology, 281:1391–1410.
https://doi.org/10.1002/jmor.21254

Macaluso, L., Villa, A., Carnevale, G., and Delfino, M. 2021. Past, present, and future climate space of the only endemic vertebrate genus of the Italian peninsula. Scientific Reports, 11:22139.
https://doi.org/10.1038/s41598-021-01492-z

Macaluso, L., Mannion, P.D., Evans, S.E., Carnevale, G., Monti, S., Marchitelli, D., and Delfino, M. 2022a. Biogeographic history of Palearctic caudates revealed by a critical appraisal of their fossil record quality and spatio-temporal distribution. Royal Society Open Science, 9:220935.
https://doi.org/10.1098/rsos.220935

Macaluso, L., Villa, A., and Mörs, T. 2022b. A new proteid salamander (Urodela; Proteidae) from the middle Miocene of Hambach (Germany) and implications for the evolution of the family. Palaeontology, 65:e12585.
https://doi.org/10.1111/pala.12585

Macaluso, L., Bertini, A., Carnevale, G. Eronen, J.T., Martinetto, E., Saarinen, J., Villa, A., Capasso, F., and Delfino, M. 2023a. A combined palaeomodelling approach reveals the selective role as refugia of the Mediterranean peninsulas. Palaeogeography, Palaeoclimatology, Palaeoecology, 625:111699.
https://doi.org/10.1016/j.palaeo.2023.111699

Macaluso, L., Wencker, L.C.M., Castrovilli, M., Carnevale, G., and Delfino, M. 2023b. A comparative atlas of selected skeletal elements of European urodeles (Amphibia: Urodela) for palaeontological investigations. Zoological Journal of the Linnean Society, 197:569–619.
https://doi.org/10.1093/zoolinnean/zlac063

Médail, F. and Diadema, K. 2009. Glacial refugia influence plant diversity patterns in the Mediterranean Basin. Journal of biogeography, 36:1333–1345.
https://doi.org/10.1111/j.1365-2699.2008.02051.x

Mendelssohn, H. and Steinitz, H. 1943. A new frog from Palestine. Copeia, 1943:231–233.
https://doi.org/10.2307/1438135

Merrem, B. 1820. Versuch eines Systems der Amphibien I (Tentamen Systematis Amphibiorum). J.C. Krieger, Marburg.

Miklas, P.M. 2002. Die Amphibienfauna (Amphibia: Caudata, Anura) der obermiozänen Fundstelle Götzendorf an der Leitha (südliches Wiener Becken, Niederösterreich). Annalen des Naturhistorischen Museums in Wien, 103A:161–211.

Młynarski, M. 1962. Notes on the amphibian and reptilian fauna of the Polish Pliocene and early Pleistocene. Acta Zoologica Cracoviensis, 7:177–194.

Młynarski, M. and Szyndlar, Z. 1989. Płazy i gady. Folia Quaternaria, 59-60:69–88.

Młynarski, M., Szyndlar, Z., Estes, R., and Sanchíz B. 1984. Amphibians and reptiles from the Pliocene locality of Węże II near Działoszyn (Poland). Acta Palaeontologica Polonica, 29:209–229.

Mörs, T. 2002. Biostratigraphy and paleoecology of continental Tertiary vertebrate faunas in the Lower Rhine Embayment (NW-Germany). Netherlands Journal of Geosciences – Geologie en Mijnbouw, 81:177–183.
https://doi.org/10.1017/S0016774600022411

Mörs, T. and Kalthoff, D.C. 2004. A new species of *Karydomys* (Rodentia, Mammalia) and a systematic re-evaluation of this rare Eurasian Miocene hamster. Palaeontology, 47:1387–1405.
https://doi.org/10.1111/j.0031-0239.2004.00413.x

Mörs, T. and Stefen, C. 2010. The castorid *Steneofiber* from NW Germany and its implications for the taxonomy of Miocene beavers. Acta Palaeontologica Polonica, 55:189–198.
https://doi.org/10.4202/app.2009.0013

Mörs, T., von Koenigswald, W., and von der Hocht, F. 1998. Rodents (Mammalia) from the late Pliocene Reuver Clay of Hambach (Lower Rhine Embayment, Germany). Mededelingen Nederlands Instituut voor Toegepaste Geowetenschappen TNO, 60:135–160.
Mörs, T, von der Hocht, F., and Wutzler, B. 2000. Die erste Wirbeltierfauna aus der miozänen Braunkohle der Niederrheinischen Bucht (Ville-Schichten, Tagebau Hambach). Paläontologische Zeitschrift, 74:145–170. https://doi.org/10.1007/BF02987958
Naylor, B.G. 1981. A new salamander of the family Batrachosauroididae from the Late Miocene of North America, with notes on other batrachosauroidids. PaleoBios, 39:1–14.
Oken, L. 1816. Lehrbuch der Naturgeschichte, vol. 3. Zoologie. Abtheilung 2. Atlas. C.H. Reclam, Leipzig.
Parker, H.W. 1929. Two fossil frogs of the lower Miocene of Europe. Annals and Magazine of Natural History, 4:270–281. https://doi.org/10.1080/00222932908673051
Peracca, M.G. 1898. Descrizione di una nuova specie di tritone italiano. Bollettino dei Musei di Zoologia e Anatomia Comparata della R. Università di Torino, 13:1–6.
Perl, R.G.B., Gafny, S., Malka, Y., Renan, S., Woodhams, D.C., Rollins-Smith, L., Pask, J.D., Bletz, M.C., Geffen, E., and Vences, M. 2017. Natural history and conservation of the rediscovered Hula painted frog, *Latonia nigriventer*. Contributions to Zoology, 86:11–37. https://doi.org/10.1163/18759866-08601002
Peters, K.F. 1868. Zur Kenntnis der Wirbelthiere aus den Miocenschichten von Eibiswald in Steiermark. I. Die Schildkrötenreste. Sitzungsberichte der Kaiserlichen Akademie der Wissenschaften, mathematisch-naturwissenschaftliche Classe, 57:72–74.
Pomel, A. 1847. Note sur des animaux fossiles découverts dans le département de l'Allier. Bulletin de la Societé géologique de France, 4:378–385.
Pomel, M. 1853. Catalogue méthodique et descriptif des vertébrés fossiles découverts dans le bassin hydrogeographique supérieur de la Loire, et surtout dans la vallée de son affluent principal, l´Allier. J.-B. Baillière, Paris.
Prieto, J., Böhme, M., Maurer, H., Heissig, K., and Abdul Aziz, H. 2009. Biostratigraphy and sedimentology of the Fluviatile Untere Serie (Early and Middle Miocene) in the central part of the North Alpine Foreland Basin: implications for palaeoenvironment and climate. International Journal of Earth Sciences, 98:1767–1791. https://doi.org/10.1007/s00531-008-0331-2
Rafinesque, C.S. 1815. Analyse de la Nature ou Tableau de l'Univers et des Corps Organisés. Jean Barravecchia, Palermo. https://doi.org/10.5962/bhl.title.106607
Rage, J.-C. 1974. Les serpents des Phosphorites du Quercy. Palaeovertebrata, 6:274–303.
Rage, J.-C. 2013. Mesozoic and Cenozoic squamates of Europe. Palaeobiodiversity and Palaeoenvironments, 93:517–534. https://doi.org/10.1007/s12549-013-0124-x
Rage, J.-C. and Bailon, S. 2005. Amphibians and squamate reptiles from the late early Miocene (MN 4) of Béon 1 (Montréal-du-Gers, southwestern France). Geodiversitas, 27:413–441.
Rage, J.-C. and Hossini, S. 2000. Les amphibiens du Miocène moyen de Sansan. Mémoires du Muséum national d'Histoire naturelle, 183:177–217.
Rage, J.-C. and Roček, Z. 2003. Evolution of anuran assemblages in the Tertiary and Quaternary of Europe, in the context of palaeoclimate and palaeogeography. Amphibia-Reptilia, 24:133–167.
Ratnikov, V.Yu. 2001. Pliocene anurans of east-European platform. Russian Journal of Herpetology, 8:171–178. https://doi.org/10.30906/1026-2296-2001-8-3-171-178
Ratnikov, V.Yu. 2010. A review of tailed amphibian remains from late Cenozoic sediments of the East European Plain. Russian Journal of Herpetology, 17:59–66. https://doi.org/10.30906/1026-2296-2010-17-1-59-66
Ratnikov, V.Yu. and Litvinchuk, S.N. 2007. Comparative morphology of trunk and sacral vertebrae of tailed amphibians of Russia and adjacent countries. Russian Journal of Herpetology, 14:177–190. https://doi.org/10.30906/1026-2296-2007-14-3-177-190

Ratnikov, V.Yu. and Litvinchuk, S.N. 2009. Atlantal vertebrae of tailed amphibians of Russia and adjacent countries. Russian Journal of Herpetology, 16:57–68. https://doi.org/10.30906/1026-2296-2009-16-1-57-68

Reilly, S.M. and Jorgensen, M.E. 2011. The evolution of jumping in frogs: morphological evidence for the basal anuran locomotor condition and the radiation of locomotor systems in crown group anurans. Journal of Morphology, 272:149–168. https://doi.org/10.1002/jmor.10902

Roček, Z. 1994a. A review of the fossil Caudata of Europe. Abhandlungen und Berichte für Naturkunde, 17:51–56.

Roček, Z. 1994b. Taxonomy and distribution of tertiary discoglossids (Anura) of the genus *Latonia* v. Meyer, 1843. Geobios, 27:717–751. https://doi.org/10.1016/S0016-6995(94)80058-8

Roček, Z. 2003. Larval development and evolutionary origin of the anuran skull, p. 1877–1995. In Heatwole, H. and Davies, M. (eds.), Amphibian Biology 4, Osteology. Surrey Beatty & Sons, Chipping Norton, New South Wales, Australia.

Roček, Z. 2013. Mesozoic and Tertiary Anura of Laurasia. Palaeobiodiversity and Palaeoenvironments, 93:397–439. https://doi.org/10.1007/s12549-013-0131-y

Roček, Z., Wuttke, M., Gardner, J.D., and Bhullar, B.-A.S. 2014. The Euro-American genus *Eopelobates*, and a re-definition of the family Pelobatidae (Amphibia, Anura). Palaeobiodiversity and Palaeoenvironments, 94:529–567. https://doi.org/10.1007/s12549-014-0169-5

Roček, Z., Rage, J.-C., and Venczel, M. 2021. Fossil frogs of the genus *Palaeobatrachus* (Amphibia: Anura). Abhandlungen der Senckenberg Gesellschaft für Naturforschung, 575:1–151.

Sach, V.J. 2016. Fossilienkatalog der Miozän-Molasse in Südwestdeutschland (Obere Süßwassermolasse, Brackwassermolasse, Obere Meeresmolasse, Untere Süßwassermolasse). Documenta Naturae, SB 70:1–115.

Sanchiz, B. 1981. Registro fosil y antiguedad de la familia Hylidae (Amphibia, Anura) en Europa. Anais do Congreso Latino-americano de Paleontología, 22:757–764.

Sanchiz, B. 1998. Handbuch der Paläoherpetologie. 4 – Salientia. Friedrich Pfeil, München.

Sanchiz, B. and Młynarski, M. 1979a. Remarks on the fossil anurans from the Polish Neogene. Acta Zoologica Cracoviensia, 24:153–174.

Sanchiz, B., and Młynarski, M. 1979b. Pliocene salamandrids (Amphibia, Caudata) from Poland. Acta Zoologica Cracoviensia, 24:175–188.

Sanchiz, B. and Roček, Z. 1996. An overview of the anuran fossil record, p. 317–328. In Tinsley, R.C. and Kobel, H.R. (eds.), The Biology of *Xenopus*. Clarendon Press, Oxford, UK.

Sanchiz, B. and Sanz, J.L. 1980. Los anfibios del Pleistoceno medio de Aridos-1 (Arganda, Madrid), p. 105–126. In López Martínez, N., Pérez González, A., and Santonja Gómez, M. (eds.), Ocupaciones achelenses en el valle del Jarama. Diputación Provincial, Servicios de Extensión Cultural y Divulgación, Madrid.

Schäfer, A., Utescher, T., and Mörs, T. 2004. Stratigraphy of the Cenozoic Lower Rhine Basin, northwestern Germany. Newsletters on Stratigraphy, 40:73–110. https://doi.org/10.1127/0078-0421/2004/0040-0073

Schleich, H.H. 1985. Zur Verbreitung tertiärer und quartärer Reptilien und Amphibien. I. Süddeutschland. Münchner Geowissenschaftliche Abhandlungen Reihe A, 4:67–149.

Schleich, H.H. 1988. Paläoherpetologische Materialien und Faunenspektren aus dem Kalktertiär des Mainzer Beckens (Oberoligozän – Untermiozän). Geologisches Jahrbuch, A110:289–306.

Schoch, R.R., Poschmann, M., and Kupfer, A. 2015. The salamandrid *Chelotriton paradoxus* from Enspel and Randeck Maars (Oligocene–Miocene, Germany). Palaeobiodiversity and Palaeoenvironments, 95:77–86. https://doi.org/10.1007/s12549-014-0182-8

Schouten, S. 2016. Een overzicht van de Pleistocene en Holocene herpetofauna (reptielen en amfibieën) van Nederland. Met aandacht voor vondsten langs de nederlandse kust. Cranium, 33:11–24.

Schouten, S. 2019. Schildpadden gezocht: de eerste melding van een fossiele beekschildpad (*Mauremys* sp.) uit de Noordzee, gevonden op het strand van Hoek van Holland. Cranium, 36:44–48.

Schouten, S. 2020. De eerste vondsten van echte hagedissen (Lacertidae) en hazelwormen (Anguidae) op Maasvlakte 2. Cranium, 37:74–80.
Schreuder, A. 1946. De moerasschildpad, *Emys orbicularis* (L.), fossiel en levend in Nederland. Natuurhistorisch maandblad, 25:72–75.
Sillero, N., Campos, J., Bonardi, A., Corti, C., Creemers, R., Crochet, P.-A., Crnobrnja Isailović, J., Denoël, M., Ficetola, G.F., Gonçalves, J., Kuzmin, S., Lymberakis, P., de Pous, P., Rodríguez, A., Sindaco, R., Speybroeck, J., Toxopeus, B., Vieites, D.R., and Vences, M. 2014. Updated distribution and biogeography of amphibians and reptiles of Europe. Amphibia-Reptilia, 35:1–31. https://doi.org/10.1163/15685381-00002935
Smith, K.T., Schaal, S.F.K., and Habersetzer, J. 2018. Messel. An ancient greenhouse ecosystem. Senckenberg Gesellschaft für Naturforschung, Frankfurt am Main.
Sonnini de Manoncourt, C.S. and Latreille, P.A. 1801. Histoire naturelle des reptiles, avec figures dissinées d'après nature. Volume 4. Deterville, Paris.
Sorbelli, L., Villa, A., Gentili, S., Cherin, M., Carnevale, G., Tschopp, E., and Delfino, M. 2021. The Early Pleistocene ectothermic vertebrates of Pietrafitta (Italy) and the last Western European occurrence of *Latonia* Meyer, 1843. Comptes Rendus Palevol, 20:555–583. https://doi.org/10.5852/cr-palevol2021v20a26
Speybroeck, J., Beukema, W., Bok, B., and Van der Voort, J. 2016. Field guide to the amphibians and reptiles of Britain and Europe. Bloomsbury Publishing, London.
Špinar, Z.V. 1952. *Eopelobates bayeri*—a new frog from the Tertiary of Bohemia. Sborník Ústředního ústavu geologického, 19:457–488.
Špinar, Z.V. 1972. Tertiary frogs from Central Europe. Academia, Prague.
Stefen, C. and Mörs, T. 2008. The beaver *Anchitheriomys* from the Miocene of Central Europe. Journal of Paleontology, 82:1009–1020. https://doi.org/10.1666/06-049.1
Steinthorsdottir, M., Coxall, H., de Boer, A., Huber, M., Barbolini, N., Bradshaw, C.D., Burls, N.J., Feakins, S.J., Gasson, E., Henderiks, J., Holbourn, A.E., Kiel, S., Kohn, M.J., Knorr, G., Kürschner, W.M., Lear, C.H., Liebrand, D., Lunt, D.J., Mörs, T., Pearson, P.N., Pound, M.J., Stoll, H., and Strömberg, C.A.E. 2021. The Miocene: the Future of the Past. Paleoceanography and Paleoclimatology, 36:e2020PA004037. https://doi.org/10.1029/2020PA004037
Stejneger, L. 1899. Description of a new genus and species of discoglossoid toad from North America. Proceedings of the United States National Museum, 21:899–901.
Stöck, M., Dubey, S., Klütsch, C., Litvinchuk, S.N., Scheidt, U., and Perrin, N. 2008. Mitochondrial and nuclear phylogeny of circum-Mediterranean tree frogs from the *Hyla arborea* group. Molecular Phylogenetics and Evolution, 49:1019–1024. https://doi.org/10.1016/j.ympev.2008.08.029
Strauch, A. 1870. Revision der Salamandriden-Gattungen nebst Beschreibung einiger neuen und weniger bekannten Arten dieser Familie. Mémoires de l'Académie Impériale des Sciences de St. Pétersbourg. Série 7, 16:1–110.
Syromyatnikova, E.V. 2017. Two pelobatid frogs from the late Miocene of Caucasus (Russia). Palaeontologia Electronica, 20.2.36A:1–12. https://doi.org/10.26879/772
Syromyatnikova, E.V. 2019. Redescription of *Pelobates praefuscus* Khosatzky, 1985 and new records of *Pelobates* from the late Miocene–Pleistocene of Eastern Europe. Historical Biology, 31:888–897. https://doi.org/10.1080/08912963.2017.1402015
Syromyatnikova, E. and Roček, Z. 2019. New *Latonia* (Amphibia: Alytidae) from the late Miocene of northern Caucasus (Russia). Palaeobiodiversity and Palaeoenvironments, 99:495–509. https://doi.org/10.1007/s12549-018-0350-3
Syromyatnikova, E., Roček, Z., and van de Velde, S. 2019. New discoveries in the frog *Latonia seyfriedi* (Anura: Alytidae) and their impact on taxonomy of the genus *Latonia*. PalZ, 93:669–677. https://doi.org/10.1007/s12542-019-00477-8
Syromyatnikova, E., Tesakov, A., Frolov, P., and Titov, V. 2021. A Pliocene *Mioproteus* (Urodela: Proteidae) from the Taman Peninsula (Russia). Russian Journal of Herpetology, 28:125–128. https://doi.org/10.30906/1026-2296-2021-28-2-125-128

Szentesi, Z. 2019. *Latonia gigantea* (Lartet, 1851) remains and other herpetological observations from the middle Pleistocene Esztramos 6 locality (Aggtelek–Rudabánya Mountains, North Hungary). Fragmenta Palaeontologica Hungarica, 36:141–158. http://doi.org/10.17111/FragmPalHung.2019.36.14

Szentesi, Z., Sebe, K., and Szabó, M. 2020. Giant salamander from the Miocene of the Mecsek mountains (Pécs-Danitzpuszta, southwestern Hungary). PalZ, 94:353–366. https://doi.org/10.1007/s12542-019-00499-2

Szyndlar, Z. and Rage, J.-C. 2003. Non-erycine Booidea from the Oligocene and Miocene of Europe. Institute of Systematics and Evolution of Animals, Polish Academy of Sciences, Kraków.

Szyndlar, Z. and Schleich, H.H. 1993. Description of Miocene snakes from Petersbuch 2 with comments on the lower and middle Miocene ophidian faunas of Southern Germany. Stuttgarter Beiträge zur Naturkunde, Serie B (Geologie und Paläontologie), 192:1–47.

Taylor, E.H. and Hesse, C.J. 1943. A new salamander from the upper Miocene beds of San Jacinto County, Texas. The American Journal of Science, 241:185–193.

Tempfer, P.M. 2004. *Andrias scheuchzeri* (Caudata: Cryptobranchidae) from the Upper Miocene (MN7/8) locality Mataschen/Styria. Joannea Geologie & Paläontologie, 5:257–268.

Thiel, C., Klotz, S., and Uhl, D. 2012. Palaeoclimate estimates for selected leaf floras from the Late Pliocene (Reuverian) of Central Europe based on different palaeobotanical techniques. Turkish Journal of Earth Sciences, 21:263–287. https://doi.org/10.3906/yer-1007-41

Tourneville, A. 1879. Description d'une nouvelle espece de batracien urodèle d'espagne (*Pelonectes boscai* Lataste). Bulletin de la Société Zoologique de France, 4:69–87.

Tschudi, J.J. 1838. Classification der Batrachier, mit Berücksichtigung der fossilen Thiere dieser Abteilung der Reptilien. Petitpierre, Neuchatel.

Utescher, T., Mosbrugger, V., and Ashraf, A.R. 2000. Terrestrial climate evolution in northwest Germany over the last 25 million years. Palaios, 15:430–449. https://doi.org/10.2307/3515514

Utescher, T., Mosbrugger, V., and Ashraf, A.R. 2002. Facies and paleogeography of the Tertiary of the Lower Rhine Basin – sedimentary versus climatic control. Netherlands Journal of Geosciences – Geologie en Mijnbouw, 81:185–191. https://doi.org/10.1017/S0016774600022423

Utescher, T., Mosbrugger, V., Ivanov, D., and Dilcher, D.L. 2009. Present-day climatic equivalents of European Cenozoic climates. Earth and Planetary Science Letters, 284:544–552. https://doi.org/10.1016/j.epsl.2009.05.021

Utescher, T., Ashraf, A.R., Dreist, A., Dybkjaer, K., and Mosbrugger, V. 2012. Variability of Neogene continental climates in northwest Europe – A detailed study based on microfloras. Turkish Journal of Earth Sciences, 21:289–314. https://doi.org/10.3906/yer-1005-3

van Dam, J.A. 2006. Geographic and temporal patterns in the late Neogene (12–3 Ma) aridification of Europe: The use of small mammals as paleoprecipitation proxies. Palaeogeography, Palaeoclimatology, Palaeoecology, 238:190–218. https://doi.org(10.1016/j.palaeo.2006.03.025

Van den Hoek Ostende, L.W. 2004. The Tegelen clay-pits: a hundred year old classical locality. Scripta Geologica, Special Issue 4:127–141.

Van den Hoek Ostende, L.W. and de Vos, J. 2006. A century of research on the classical locality of Tegelen (province of Limburg, The Netherlands). Courier Forschungsinstitut Senckenberg, 256:291–304.

Van Laere, G. and Mörs, T. 2023. Beavers and flying squirrels (Rodentia: Castoridae, Pteromyini) from the Late Pliocene of Hambach 11C, Germany. Geodiversitas, 45:223–241. https://doi.org/10.5252/geodiversitas2023v45a7

Vasilyan, D. and Yanenko, V. 2020. The last *Palaeoproteus* (Urodela: Batrachosauroididae) of Europe. Scientific Reports, 10:2733. https://doi.org/10.1038/s41598-020-59255-1

Vasilyan, D., Böhme, M., Chkhikvadze, V.M., Semenov, Y.A., and Joyce, W.G. 2013. A new giant salamander (Urodela, Pancryptobrancha) from the Miocene of eastern Europe (Grytsiv, Ukraine). Journal of Vertebrate Paleontology, 33:301–318. https://doi.org/10.1080/02724634.2013.722151

Vasilyan, D., Schneider, S., Bayraktutan, M.S., and Şen, Ş. 2014. Early Pleistocene freshwater communities and rodents from the Pasinler Basin (Erzurum Province, north-eastern Turkey). Turkish Journal of Earth Sciences, 23:293–307. https://doi.org/10.3906/yer-1307-16

Vasilyan, D., Zazhigin, V.S., and Böhme, M. 2017. Neogene amphibians and reptiles (Caudata, Anura, Gekkota, Lacertilia, and Testudines) from the south of Western Siberia, Russia, and Northeastern Kazakhstan. PeerJ, 5:e3025. https://doi.org/10.7717/peerj.3025

Vasilyan, D., Čerňanský, A., Szyndlar, Z., and Mörs, T. 2022. Amphibian and reptilian fauna from the early Miocene of Echzell, Germany. Fossil Record, 25:99–145. https://doi.org/10.3897/fr.25.83781

Vater, M. 2003. Anatómia kostrovej sústavy mloka vrchovského (*Triturus alpestris*) a jej ontogenéza. Unpublished PhD Thesis, Prague University, Prague, Czech Republic.

Venczel, M. 2001. Anurans and squamates from the Lower Pliocene (MN14) Osztramos 1 locality (Northern Hungary). Fragmenta Palaeontologica Hungarica, 19:79–90.

Venczel, M. 2004. Middle Miocene anurans from the Carpathian Basin. Palaeontographica Abt. A, 271:151–174. https://doi.org/10.1127/pala/271/2004/151

Venczel, M. and Codrea, V.A. 2018. A new proteid salamander from the early Oligocene of Romania with notes on the paleobiogeography of Eurasian proteids. Journal of Vertebrate Paleontology, 38:e1508027. https://doi.org/10.1080/02724634.2018.1508027

Vergilov, V. and Tzankov, N. 2021. Giant pelobatid fossil larva from the middle Miocene of Bulgaria. Historia Naturalis Bulgarica, 43:29–42. https://doi.org/10.48027/hnb.43.031

Vergnaud-Grazzini, C. 1970. Les amphibiens fossiles du gisement d'Arondelli. Palaeontographica Italica, 66:47–65.

Villa, A. and Delfino, M. 2019. Fossil lizards and worm lizards (Reptilia, Squamata) from the Neogene and Quaternary of Europe: an overview. Swiss Journal of Palaeontology, 138:177–211. https://doi.org/10.1007/s13358-018-0172-y

Villa, A., Andreone, F., Boistel, R., and Delfino, M. 2014. Skull and lower jaw osteology of the Lanza's salamander, *Salamandra lanzai* (Amphibia, Caudata), p. 171–200. In Capula, M. and Corti, C. (eds.), Scripta Herpetologica. Studies on Amphibians and Reptiles in honour of Benedetto Lanza. Edizioni Belvedere, Latina.

Villa, A., Roček, Z., Tschopp, E., van den Hoek Ostende, L.W., and Delfino, M. 2016. *Palaeobatrachus eurydices*, sp. nov. (Amphibia, Anura), the last western European palaeobatrachid. Journal of Vertebrate Paleontology, 36:e1211664. https://doi.org/10.1080/02724634.2016.1211664

Villa, A., Abella, J., Alba, D.M., Almécija, S., Bolet, A., Koufos, G.D., Knoll, F., Luján, À.H., Morales, J., Robles, J.M., Sánchez, I.M., and Delfino, M. 2018a. Revision of *Varanus marathonensis* (Squamata, Varanidae) based on historical and new material: morphology, systematics, and paleobiogeography of the European monitor lizards. PLoS ONE, 13:e0207719. https://doi.org/10.1371/journal.pone.0207719

Villa, A., Blain, H.-A., and Delfino, M. 2018b. The Early Pleistocene herpetofauna of Rivoli Veronese (Northern Italy) as evidence for humid and forested glacial phases in the Gelasian of Southern Alps. Palaeogeography, Palaeoclimatology, Palaeoecology, 490:393–403. https://doi.org/10.1016/j.palaeo.2017.11.016

Villa, A., Blain, H.-A., van den Hoek Ostende, L.W., and Delfino, M. 2018c. Fossil amphibians and reptiles from Tegelen (Province of Limburg) and the early Pleistocene palaeoclimate of The Netherlands. Quaternary Science Reviews, 187:203–219. https://doi.org/10.1016/j.quascirev.2018.03.020

Viosca, P. Jr. 1937. A tentative revision of the genus *Necturus* with descriptions of three new species from the southern Gulf drainage area Copeia, 1937:120–138. https://doi.org/10.2307/1436953

von Meyer, H. 1843. Mittheilungen an Professor Bronn gerichtet. Neues Jahrbuch für Geologie und Paläontologie, Geognosie, Geologie und Petrefactenkunde, 1843:579–590.

von Meyer, H. 1860. Frösche aus den Tertiär-Gebilden Deutschlands. Palaeontographica, 7:123–182.
Wagler, J. 1830. Natürliches System der Amphibien, mit vorangehender Classification der Säugthiere und Vögel. Ein Beitrag zur vergleichenden Zoologie. J.G. Cotta, München, Stuttgart and Tübingen.
Weems, R.E. and George, R.A. 2013. Amphibians and nonmarine turtles from the Miocene Calvert Formation of Delaware, Maryland, and Virginia (USA). Journal of Paleontology, 87:570–588.
https://doi.org/10.1666/12-071
Weitzel, K. 1938. *Propelodytes wagneri* n. g. n. sp., ein Frosch aus dem Mittel-Eozän von Messel. Notizblatt der Hessischen Geologischen Landes-Anstalt, 19:42–46.
Westphal, F. 1958. Die Tertiären und rezenten Eurasiatischen Riesensalamander. Palaeontolographica Abteilung A, 110:20–92.
Westphal, F. 1967. Erster Nachweis des Riesensalamanders (*Andrias*, Urodela, Amphibia) im europäischen Jungpliozän. Neues Jahrbuch für Geologie und Paläontologie – Monatshefte, 1967:67–73.
Westphal, F. 1970. Neue Riesensalamander-Funde (*Andrias*, Amphibia) aus der Oberen Süßwassermolasse von Wartenberg in Bayern. Mitteilungen der Bayerischen Staatssammlung für Paläontologie und historische Geologie, 10:253–260.
Williams, M.J. 2009. Miocene herpetofaunas from the central Gulf Coast USA: their paleoecology, biogeography, and biostratigraphy. Unpublished PhD Thesis, Louisiana State University and Agricultural and Mechanical College, Baton Rouge, Lousiana, U.S.A.
Wuttke, M., Přikryl, T., Ratnikov, V.Yu., Dvořak, Z., and Roček, Z. 2012. Generic diversity and distributional dynamics of the Palaeobatrachidae (Amphibia: Anura). Palaeobiodiversity and Palaeoenvironments, 92:367–395.
https://doi.org/10.1007/s12549-012-0071-y
Ziegler, R. and Mörs, T. 2000. Marsupialia, Lipotyphla und Chiroptera (Mammalia) aus dem Miozän des Braunkohlentagebaus Hambach (Niederrheinische Bucht, NW-Deutschland). Palaeontographica A, 257:1–26.
Zweifel, R.G. 1956. Two pelobatid frogs from the Tertiary of North America and their relationships to fossil and recent forms. American Museum Novitates, 1762:1–45.